IN VITRO FUNCTIONAL PROPERTIES AND *IN VIVO* LOCAL EFFECTS OF TRANSPLANTED HUMAN PROGENITOR CELLS IN ISCHEMIC TISSUES

Yan Zhang

This thesis is submitted to the Faculty of Graduate and Postdoctoral Studies
in partial fulfillment of the requirements for the Degree of

DOCTOR OF PHILOSOPHY
IN CELLULAR AND MOLECULAR MEDICINE
UNIVERSITY OF OTTAWA

Department of Cellular and Molecular Medicine
Faculty of Medicine
University of Ottawa
Division of Cardiac Surgery
University of Ottawa Heart Institute

© Yan Zhang, Ottawa, Canada, 2011

Authorization has been granted for the use of figures and tables that have been published in scientific journals

Abstract

Growing evidence from animal and clinical studies suggests that cardiac cell therapy can restore perfusion and improve function in the ischemic/infarcted myocardium. However, cell therapy is hindered by insufficient cell numbers, inefficient cell homing and engraftment, and inadequate cellular interactions. Furthermore, the biological mechanisms and local effects of transplanted cells have not been well-elucidated. The research presented herein attempts to address some of these issues.

In manuscript #1, a new subpopulation of circulating progenitor cells (CPCs), termed derived $CD133^+$ cells, was generated from the $CD133^-$ fraction of human peripheral blood. The derived $CD133^+$ progenitors appeared to have superior vasculogenic potential *in vitro*, which may prove to be beneficial in inducing vasculogenesis in ischemic tissues.

Positron emission tomography (PET) with direct cell labeling and reporter gene techniques were employed to assess the fate of transplanted human CPCs *in vivo* at different subjects of investigation, and different stages of cell transplantation. In manuscript #2, PET imaging with 2-[^{18}F]fluoro-2-deoxy-D-glucose (^{18}F-FDG) direct cell labeling was used to demonstrate that collagen-based matrices improve the early homing and retention of delivered CPCs in a rat ischemic hindlimb model. This mechanism conferred by the matrix may have implications on cell therapy at the early stages after transplantation.

In manuscript #3, a more efficient, stable and accurate labeling method, hexadecyl-4-[^{18}F]fluorobenzoate (^{18}F-HFB) direct cell labeling, was developed to quantify cell distribution of transplanted CPCs in a rat myocardial infarction model. PET

imaging of ^{18}F-HFB-CPCs revealed significant cell washout from the myocardium immediately after intramyocardial injection, with only a small proportion of transplanted CPCs remaining in the target area in the first 4 hours after delivery.

In manuscript #4, human CPCs transduced with lentiviral vectors showed stable expression of PET reporter genes. This reporter gene based-cell labeling technique can be developed for noninvasive tracking cells within a bioengineered matrix by PET, while preserving cell phenotype, viability and function.

These studies contribute important insights into the biology and physiology of transplanted stem cells and the ability of delivery matrices to improve transplanted cell engraftment, survival, and function. I believe with further refinement, cell expansion, tissue engineering and PET imaging could facilitate the clinical applications of cell therapies in years to come.

Table of Contents

CHAPTER 1: GENERAL INTRODUCTION 1

1.1 Cardiac Cell Therapy 2

1.1.1 Cell Sources and Cell Types 2

1.1.2 Potential Mechanisms Underlying the Benefits of Cardiac Cell Therapy 7

1.1.3 Clinical Application of Cardiac Cell Therapy 14

1.1.4 Challenges of Cardiac Cell Therapy 18

1.2 Tissue-engineered Biomaterials for Cell Delivery 19

1.3 Cell Labeling and Cell Tracking 21

1.3.1 Molecular Imaging Modalities 21

1.3.2 Positron Emission Tomography 24

1.3.3 Labeling Methods for PET Imaging of Cells 25

1.4 Research plan 31

1.4.1 Aims 31

1.4.2 Hypotheses 32

CHAPTER 2: MANUSCRIPT #1 33

Introduction to Manuscript #1 33

Contributions of Authors 35

Abstract 36

Introduction 38

Materials and Methods 41
Results 45
Discussion 58
Supplemental Materials and Methods 63
CHAPTER 3: MANUSCRIPT #2 65
Introduction to Manuscript #2 65
Contributions of Authors 67
Abstract 68
Introduction 70
Methods 72
Results 76
Discussion 87
Clinical Perspective 93
CHAPTER 4: MANUSCRIPT #3 94
Introduction to Manuscript #3 94
Abstract 97
Introduction 99
Materials and Methods 101
Results 106
Discussion 122

Conclusions 127

CHAPTER 5: MANUSCRIPT #4 129

Introduction to Manuscript #4 129

Contributions of Authors 131

Abstract 132

Introduction 134

Methods 136

Results 140

Discussion 149

Conclusion 154

CHAPTER 6: GENERAL DISCUSSION 155

6.1 Successful Expansion and Characterization of Human $CD133^{+}$ cells 156

6.2 Homing and Engraftment of CPCs within or without Collagen Matrices 158

6.3 Clinical Perspective and Future Directions 162

6.4 Conclusions 164

REFERENCES 166

APPENDICES 204

Structure of Radioisotopes 204

Curriculum Vitae 205

List of Tables

Table 1-1 Selected clinical trials ofcardiac cell therapy 17

Table 1-2 Molecular imaging for stem cell tracking 23

Table 2-1 Patients' characteristics 42

Table 3-1 Retention of ^{18}F-FDG in CPCs 77

Table 4-1 Cell phenotypes and function at 24 hours post-labeling 112

List of Figures

Figure 1-1: Proposed processes mechanisms involved in cell therapy for heart disease.. 13

Figure 1-2: Direct cell labeling with a radioisotope. 27

Figure 1-3: Reporter gene-based cell labeling. 30

Figure 2-1: Hurdles in cardiac cell therapy. 40

Figure 2-2: $CD133^{+}$ generation. 48

Figure 2-3: Cell migration. 53

Figure 2-4: Cell vasulogenesis. 57

Figure 3-1: The effect of CPC concentration on cell labeling efficiency. 78

Figure 3-2: The effect of ^{18}F-FDG labeling on cell viability. 80

Figure 3-3: The effect of matrices on the retention of ^{18}F-FDG radioactivity. 81

Figure 3-4: Small animal PET whole-body images at 150 minutes postinjection. 83

Figure 3-5: Biodistribution of ^{18}F-FDG accumulation in different organs 180 minutes after injection. 85

Figure 3-6: Identification of the transplanted cells. 86

Figure 4-1: Cell labeling efficiency of ^{18}F-HFB and ^{18}F-FDG. 108

Figure 4-2: Stability of radiolabeling in ^{18}F-HFB-CPCs and ^{18}F-FDG-CPCs. 110

Figure 4-3: The effect of radiolabeling on cell phenotype and function. 111

Figure 4-4: ^{18}F-HFB retention in matrices. 114

Figure 4-5: Dynamic PET imaging of labeled-CPCs after intramyocardial injection. 115

Figure 4-6: The dynamic distribution of transplanted CPCs. 118

Figure 4-7: Biodistribution of radioactivity in different organs at 5 hours post-injection. 119

Figure 4-8: Immunofluorescence identification of transplanted cells in the border zone of infarcted myocardium. 121
Figure 5-1: Expression of reporter proteins in transduced human circulating progenitor cells. 142
Figure 5-2: Morphology and viability of transduced circulating progenitor cells. 144
Figure 5-3: Cell function of transduced circulating progenitor cells. 145
Figure 5-4: The maintenance of GFP expression in transduced circulating progenitor cells. 147
Figure 5-5: Representative images of GFP expression in the transduced CPCs. 148
Figure 8-1: Structures of PET radiotracers for direct cell labeling. 204

List of Abbreviations

^{18}F-FDG	2-[^{18}F]fluoro-2-deoxy-D-glucose
^{18}F-FDG-6P	fructose-6 phosphate analogue
^{18}F-FHBG	9-(4-[^{18}F]fluoro-3-hydroxymethylbutyl) guanine
^{18}F-HFB	hexadecyl-4-[^{18}F]fluorobenzoate
^{18}F-SFB	N-succimidyl-4-[^{18}F]fluorobenzoate
^{99m}Tc-HMPAO	^{99m}Tc-hexamethylpropyleneamine oxime
AMI	acute myocardial infarction
BDNF	brain-derived neurotrophic factor
BLC	B-lymphocyte chemoattractant
BLI	bioluminescence imaging
BM	bone marrow
CAD	coronary artery disease
CHF	congestive heart failure
CPCs	circulating progenitor cells
CSCs	cardiac stem cells
DAPI	4'6-diamidino-2'-phenylindole
EBM-2	endothelial basal medium 2
ECM	extracellular matrix
EGF	epidermal growth factor
ENA-78	epithelial cell-derived neutrophil-activating protein-78
EPCs	endothelial progenitor cells

ER-LBD	estrogen receptor ligand binding domain
FACS	fluorescence activated cell sorting
FGF	fibroblast growth factor
FIAU	2’ fluoro-β-D-arabinofuranosyluracil
Fluc	firefly luciferase
FOV	field of view
GCP	granulocyte chemotactic protein
G-CSF	granulocyte colony-stimulating factor
Gd-DTPA	gadolinium-diethylene triamine penta-acetic acid
GDNF	glial cell line-derived neurotrophic factor
GFP	green fluorescence protein
GM-CSF	granulocyte-macrophage colony-stimulating factor
GRO	growth-related oncogene
HGF	hepatocyte growth factor
HPFs	high powered fields
HSCs	hematopoietic stem cells
HSV1-sr39tk	herpes simplex virus type 1 truncated thymidine kinase
HSV1-tk	herpes simplex virus type 1 thymidine kinase
hTK2	human mitochondrial thymidine kinase type 2
HUVECs	human umbilical vein endothelial cells
ID	injected dose
IFN	interferon

IGF	insulin-like growth factor
IGFBP	insulin-like growth factor-binding protein
IL	interleukin
IP-10	interferon-inducible protein 10
iPS cells	induced pluripotent stem cells
Isl1	islet-1
Klf4	kruppel like family of transcription factor 4
LIF	leukemia inhibitory factor
LIGHT	lymphotoxin-related inducible ligand that competes for glycoprotein D binding to herpes virus entry mediator on T-cells
MACS	magnetically activated cell sorter
MCP	monocyte chemoattractant protein
MCSF	macrophage colony-stimulating factor
MDC	macrophage-derived chemokine
MI	myocardial infarction
MIF	macrophage migration inhibitory factor
MIG	monokine induced by gamma interferon
MIP	macrophage inflammatory protein
MNCs	mononuclear cells
MOI	multiplicity of infection
MRI	magnetic resonance imaging
MSCs	mesenchymal stem cells

NAP	neutrophil-activating protein
NIRF	near-infrared fluorophores
NT	neurotrophic factor
Oct3/4	octamer-binding transcription factor
PARC	pulmonary and activation-regulated chemokine
PB	peripheral blood
PDGF	platelet-derived growth factor
PET	positron emission tomography
PIGF	placental growth factor
RANTES	regulated upon activation normal T-cell expressed and secreted
RFP	red fluorescence protein
ROIs	regions of interest
Sca1	stem cell antigen-1
SCF	stem cell factor
SD	standard deviation
SDF	stromal cell-derived factor
SEM	standard error of the mean
Sox2	sex determining region Y- box2
SPECT	single-photon emission computed tomography
SPIO	superparamagnetic iron oxide particles
SSEA-1	stage specific embryonic antigen-1
TARC	thymus and activation-regulated chemokine

TFR	triple-fusion reporter
TGF	transforming growth factor
TIMP	tissue inhibitor of metalloproteinases
TNF	tumor necrosis factor
VE-cadherin	vascular endothelial-cadherin
VEGF	vascular endothelial growth factor
VEGFR-2	vascular endothelial growth factor receptor 2

Acknowledgements

First and foremost, I would like to express my sincere gratitude to my supervisor Dr. Marc Ruel for his exemplary mentorship and constant support throughout my research. I have learned a great deal from him, and medical research is only the beginning. I also would like to thank my co-supervisor Dr. Erik Suuronen, and my other advisory committee members: Drs. Jean DaSilva, Rob Beanlands and Patrick Burgon. Their patience, advice and thoughtful comments were essential to this research.

Throughout my time at University of Ottawa Heart Institute, I have met numerous individuals that have helped me develop not only as a scientist but as an individual. In particular, I would like to add a special thanks to the many lab colleagues that trained me in various techniques, added helpful advices, and provided an enjoyable place to work. Special thanks to Drew Kuraitis, Suzanne Crowe, Serena Wong, Branka Vulesevic, Céline Giordano, and Joanne McBane for making this a memorable experience. I would like to take the opportunity one more time to thank my mentors, Drs. Marc Ruel and Erik Suuronen. They provided kindness, encouragement and financial support for me during this research and allowed me the opportunity to freely investigate areas of interest to me.

From the Cardiac PET Centre, I would like to acknowledge Stephanie Thorn and Myra Kordos for their support on the PET imaging acquisition. They not only supported me technically, but were true friends during many long imaging sessions. Dr. Jean DaSilva, Tayebeh Hadizad and Samantha Mason were especially helpful and kindly provided me with variable radiotracers for cell labeling. Dr. Robert deKemp and Jennifer Renaud were supportive of PET imaging analysis. None of the described experiments

would be possible without the contributions of blood donors and the efforts of the Animal Care staff.

This work is dedicated to my husband, Miles Li. Thank you for your years of infinite patience, understanding and love. Your unconditional support is a foundation for all my efforts in the past years. I owe any success in life to you. I would like to also thank my parents for encouraging me to pursue my academic interests. Though I can never replace my time away from them, I know they are proud of me.

CHAPTER 1: GENERAL INTRODUCTION

1.1 Cardiac Cell Therapy

Coronary artery disease (CAD) is a complex disease that is caused by reduced or absent blood flow in one or more of the arteries that encircle and supply the heart (Jaffe et al. 2007). Since the adult myocardium has a limited capacity for self-repair, CAD may result in irreversible tissue loss, ventricular remodeling and progression to heart failure. CAD and its complications are the number one cause of morbidity and mortality in the Western world. Despite considerable advances in cardiovascular therapeutics over the past few decades, our ability to effectively treat CAD and subsequent heart failure remains restricted because the necrotic or scarred myocardium cannot be restored. Since 1994, an experimental treatment called "cardiac cell therapy" has emerged (Soonpaa et al. 1994), in an attempt to mimic the natural processes that occur during growth and development, namely the formation of new blood vessels and new cardiomyocytes (Leor et al. 1997; Mayer et al. 1997). It is hoped that the new cells will replace the damaged ones, thus effectively restoring perfusion and function to the heart (Pittenger et al. 2004; Ruel et al. 2004; Cho et al. 2006). Growing evidence from animal studies and clinical trials has indicated that stem cell or progenitor cell therapy can improve the function of ischemic or infarcted myocardium (Assmus et al. 2002; Wollert et al. 2004). This has led to even greater interest in cardiac cell therapy, with the goal of safely and successfully restoring perfusion and/or improving contractility to the injured myocardium (Ruel et al. 2008).

1.1.1 Cell Sources and Cell Types

An ideal cell population for repairing the damaged heart should be readily available, capable of myogenesis and neovascularization, positively affect regional and global ventricular remodeling, and not lead to unwanted side-effects. Undifferentiated adult

stem or progenitor cells may be a good candidate for cardiac cell therapy due to their high plasticity, their physiologic involvement in vascular and tissue repair (Kawamoto et al. 2001; Edelberg et al. 2002; Balbarini et al. 2007), and their availability for autologous clinical use (Strauer et al. 2002).

Stem cells are defined as precursor cells that possess the capability for proliferation and self-renewal and the ability to regenerate multiple cell types, including cardiac myocytes, endothelial cells and vascular smooth muscle cells (Krause et al. 2001). Like stem cells, progenitor cells also have differentiation potential, but are more restricted than stem cells in their multipotentcy and are programmed to differentiate towards a specific cell lineage (Seaberg et al. 2003). The most important difference between stem cells and progenitor cells is that stem cells can replicate indefinitely (Zeng et al. 2008), whereas progenitor cells can only divide a limited number of times (Islam et al. 2007). Several different types of adult stem or progenitor cells have been identified and used for improving cardiac function after myocardial ischemia and infarction, although it remains unclear which of these cells have the greatest therapeutic potential.

1.1.1.1 Skeletal Myoblasts

Cell-based cardiac repair began with the transplantation of autologous skeletal myoblasts or satellite cells that reside in skeletal muscle. Some clinical case-reports suggest that skeletal myoblast therapy may improve clinical symptoms and ventricular function (Menasche et al. 2001; Herreros et al. 2003; Siminiak et al. 2005); however, the transplanted myoblasts remain committed to a skeletal muscle fate, do not differentiate into cardiomyocytes (Reinecke et al. 2002), and lack the adhesion and gap junction

proteins necessary to electrically couple the cells to the surrounding myocardium, thus posing a risk of arrhythmia (Reinecke et al. 2000).

1.1.1.2 Bone Marrow-derived Stem Cells

At present, adult bone marrow and peripheral blood are the most frequent sources of stem and/or progenitor cells used for clinical cardiac repair due to their autologous nature and simplicity of acquisition (Dimmeler et al. 2005). The bone marrow is a rich reservoir of tissue-specific stem and progenitor cells, and these cells can be released into circulating peripheral blood. A number of papers reported that bone marrow cells may serve as a central repository for the primitive stem cells that can repopulate somatic tissues (Krause 2002; Orlic et al. 2002); therefore, most of the recent studies of cell-based therapy have focused on bone marrow-derived cell populations. Bone marrow-derived stem cells contain a complex assortment of adult stem and progenitor cells, including hematopoietic stem cells (HSCs), endothelial progenitor cells (EPCs), and mesenchymal stem cells (MSCs), which may retain the ability to differentiate into vascular cells, and thus in theory might incorporate directly into the wall of newly formed or remodeled vessels (Kinnaird et al. 2004). Bone marrow-derived cell therapy has thus far proven safe and potentially beneficial (Wollert et al. 2004; Drexler et al. 2006), but the cells' intrinsic regeneration potential is controversial.

Bone marrow-derived progenitor cells from adult peripheral blood are called circulating progenitor cells (CPCs). These cells share characteristics of HSCs, such as expression of CD34. CD133 (also known as AC133, or prominin-1), as a marker for stem and immature progenitor cells, has also been adopted (Yin et al. 1997). Since CPCs contain cells expressing the endothelial markers such as vascular endothelial growth

factor receptor 2 (VEGFR-2) and capable of differentiating into endothelial cells *in vitro* and inducing neovascularization in animal models, they have also been referred to as circulating EPCs in some cases. Circulating EPCs are a specialized subset of hematopoietic cells found in the peripheral circulation (Asahara et al. 1997). With their varied sources of procurement, derivation, and methods of culture, circulating EPCs share expression of cell-surface markers that may or may not include CD31, CD34, CD133, c-kit, and other endothelial markers, including VEGFR-2 and vascular endothelial (VE)-cadherin (Urbich et al. 2004). CD133, VEGFR-2 and CD34 are often used as markers for selection and purification of EPCs because CD133 is not found on mature endothelial cells, and VEGFR-2 and CD34 are not found on the undifferentiated stem cells from which EPCs are derived (Hristov et al. 2003).

1.1.1.3 Adipose-derived Stem Cells

Adipose tissue is an additional source of distinct subsets of stem/progenitor cells potentially useful for cardiac repair and neovascularization (Meliga et al. 2007). Both MSCs and EPCs have been isolated after enzymatic digestion of adipose tissue (Colazzo et al. 2010), and showed beneficial effects in animal and clinical studies (Mazo et al. 2008; Mizuno 2010). The acquisition of adipose tissue can be performed in greater quantities than other source tissues. Although relatively rare at onset, clinically relevant stem cell numbers can be extracted from isolated adipose tissue since it possesses a higher stem cell proliferation rate than bone marrow-derived MSCs (Wagner et al. 2005). Therefore, adipose tissue represents an abundant, practical, and appealing source of donor tissue for autologous cell replacement. The therapeutic benefit of adipose-tissue derived cells is currently being studied in CAD patients (APOLLO trial, NCT00442806;

PRECISE trial, NCT00426868), and the techniques to isolate and purify potent cells will need to be optimized if clinical use is to evolve.

1.1.1.4 Cardiac Stem Cells

It was originally thought that the heart was incapable of regeneration or repair, but recently, it was reported that the mammalian myocardium includes a small proportion of stem cells that express cell-surface markers c-kit, stem cell antigen-1 (Sca1), islet-1 (Isl1) or stage specific embryonic antigen-1 (SSEA-1) (Beltrami et al. 2001; Smith et al. 2008). The discovery of cardiac stem cells (CSCs) offers the potential for *in vivo* induction of proliferation and differentiation of these cells, which are poised to acquire a cardiac phenotype and, therefore, might be optimally suited for cardiac repair. Human CSCs can be isolated and expanded from myocardium obtained by a endovascular biopsy procedure; however, they possess an extremely low rate of myocardial cell turnover (Barile et al. 2007). Recently, several groups have reported that CSCs can generate cardiomyocytes and/or vascular lineages *in vitro* and *in vivo* (Beltrami et al. 2003; Oh et al. 2004). Additionally, after specific culture, CSCs spontaneously organized into spherical multicellular clusters, thus named cardiospheres. The bromodeoxyuridine assessment indicated that c-Kit$^+$ population increased as cellular proliferation occurred within the core of the cardiosphere (Smith et al. 2008). Cardiosphere-derived CSCs as well as c-Kit$^+$ CSCs are capable of long-term self-renewal and can differentiate into the major specialized cell types of the heart, i.e. cardiac myocytes and vascular cells that express either endothelial or smooth muscle cell markers. CSCs can be clonally expanded for autologous use and have minimal risk of immune rejection or teratoma formation, thus CSCs might be a logical cell source to use in the treatment of heart disease. Some

clinical trials are underway (Caduceus trial; NCT00893360), but no published results are available yet.

1.1.1.5 Induced Pluripotent Stem Cells

Induced pluripotent stem cells (iPS cells) are a type of pluripotent stem cell artificially derived from a non-pluripotent cell, typically an adult somatic cell, by inducing "forced" expression of certain genes, including octamer-binding transcription factor (Oct3/4), sex determining region Y- box2 (Sox2), kruppel-like family of transcription factor 4 (Klf4), and c-Myc (Takahashi et al. 2007; Wernig et al. 2007; Lowry et al. 2008; Park et al. 2008; Moretti et al. 2010). Human iPS cells are believed to be identical to natural pluripotent stem cells in many respects, such as morphology, proliferation, surface antigens, gene expression, and telomerase activity (Okita et al. 2007; Yu et al. 2007; Park et al. 2008; Kattman et al. 2011). One study showed that iPS cells generated from human adult somatic cells can differentiate into cardiac myocytes *in vitro* (Duinsbergen et al. 2008). It was also reported that the intramyocardial injection of iPS cells achieved the regeneration in infarcted myocardium and the improvement of cardiac function (Nelson et al. 2009). Therefore, iPS cells may be a cell of choice, offering the additional benefit of individual, patient-specific cells (Smart et al. 2008). However, the full extent of their relation to natural pluripotent stem cells and their preclinical applicability for cardiac regeneration are still being assessed (Yu et al. 2007).

1.1.2 Potential Mechanisms Underlying the Benefits of Cardiac Cell Therapy

A crucial issue in designing more rational approach for cardiac cell therapies is to understand the mechanisms by which stem cells or progenitor cells affect myocardial

performance. The exact mechanism(s) is still incompletely understood, but seem multifactorial. A number of studies have suggested that neovascularization and possible cardiomyogenesis might be involved in the functional benefits observed with cell delivery (Orlic et al. 2001; Oh et al. 2003). Alternatively, several studies have provided evidence that paracrine effects are the principal mechanism responsible for the observed improvements in cardiac function following cell therapy (Maltais et al. 2010).

1.1.2.1 Cell Homing

The "homing" of stem cells to the injured myocardium is essential for cell therapy, as it concentrates the transplanted cells in an environment that may guide their growth and function. Cell homing is a complex cascade of events, including the initial recognition and interaction with microvascular endothelium, transmigration through the endothelium and, finally, migration to and invasion of the target tissue (Smart et al. 2008). The whole process relies on the interaction between cytokines, chemokines, adhesion molecules, and extracellular matrix (ECM)-degrading proteases. The capacity of stem cells to migrate and invade may be pivotal to functional integration even when cells are injected directly into the site of injury (Smart et al. 2008). Additionally, ischemia and hypoxia may facilitate the homing process by increasing vascular permeability, enhancing the release of chemoattractive factors, and promoting the expression of adhesion proteins (Perin et al. 2003).

1.1.2.2 Cell Differentiation and Cell Fusion

Cell differentiation is the process by which stem cells or progenitor cells become a more specialized cell type (e.g. cardiomyocyte, endothelial cell or smooth muscle cell). If stem

cells are indeed transformed into solid-organ-specific cells, the exogenous cell must become an integral morphologic part of the newly acquired tissue (Korbling et al. 2003). However, some studies cast doubt on the potential of cells derived from the hematopoietic lineage to undergo transdifferentiation (Anderson et al. 2001; Balsam et al. 2004). Meanwhile, the results of recent studies on the plasticity of stem cells contradict the dogma that the differentiation and commitment of adult stem cells are restricted to their original tissue (Graf 2002; Korbling et al. 2003). Additionally, others demonstrated that the multipotent stem or progenitor cells appear to have the capability of differentiating into endothelial and smooth muscle phenotypes, but rarely can they adopt a cardiomyocyte phenotype (Alvarez-Dolado et al. 2003; Boodhwani et al. 2006). The fusion of transplanted stem cells with resident cardiomyocytes has been offered as an alternative explanation for previous claims of transdifferentiation (Alvarez-Dolado et al. 2003; Balsam et al. 2004; Murry et al. 2004; Nygren et al. 2004). Cell fusion appears to account for the presence of transplanted cells in the heart that show donor characteristics to some extent, but not completely (Orlic et al. 2002).

1.1.2.3 Paracrine Effects

To maintain engraftment and survival in host myocardium, implanted cells may release bioactive growth factors in a paracrine manner to stimulate neovascularization and cardiomyogenesis. It has been demonstrated that stem cells secrete cytokines and growth factors which may promote angiogenesis, inhibit cardiac apoptosis, modulate interstitial matrix remodeling, and recruit endogenous stem cells (Kamihata et al. 2001; Kinnaird et al. 2004; Meyer et al. 2007). For instance, EPCs showed a marked expression of growth factors such as vascular endothelial growth factor (VEGF), fibroblast growth factor

(FGF), hepatocyte growth factor (HGF), and insulin-like growth factor 1 (IGF-1). The release of growth factors in turn may influence the classical process of angiogenesis, including the proliferation, migration, and survival of mature endothelial cells (Urbich et al. 2004). These cytokines may even recruit circulating stem or progenitor cells and activate resident CSCs, which can then themselves become new blood vessel cells and myocytes (Orlic et al. 2001; Jiang et al. 2002; Fazel et al. 2006). Paracrine factors may also supress the death of resident cardiomyocytes, affect remodeling, or enhance endogenous repair (Dimmeler et al. 2005; Uemura et al. 2006).

1.1.2.4 Neovascularization

Generally, neovascularization relies on either vasculogenesis or angiogenesis in which one mechanism involves the participation of donor stem cells in the formation of new vessels by incorporating into the newly forming vessel wall (Asahara et al. 1997). Neovascularization can be mediated by the physical incorporation of stem or progenitor cells into new capillaries or by perivascular accumulation of stem cells (Kawamoto et al. 2003; Suuronen et al. 2007). Adult circulating EPCs that originate in the bone marrow and circulate in peripheral blood play an important role in angiogenesis and vasculogenesis in the ischemic and infarcted heart (Kawamoto et al. 2003). EPCs can be recruited to injured area, where they differentiate into endothelial cells and proliferate to form vasculature (Urbich et al. 2004). Furthermore, transplanted stem cells may release growth factors (paracrine effects) that promote angiogenesis by acting on mature endothelial cells (Rehman et al. 2003; Urbich et al. 2005). Some studies indicated that the paracrine effects play a major role in neovascularization, which can be sustained by host-

generated cytokines even after the transplanted cells disappear (Burst et al. 2010 ; Cho et al. 2007).

1.1.2.5 Cardiomyogenesis

One aim of cardiac cell therapy is to replenish the injured myocardium with contractile elements. However, cell therapy with adult progenitor cells has only had limited success in generating substantial numbers of nascent cardiomyocytes and their functional integration in the myocardium (Lee et al. 2010). Although CSCs have greater potential for cardiomyogenesis (Beltrami et al. 2003; Hosoda et al. 2011), there is no convincing evidence for the formation of new cardiomyocytes by transdifferentiation of bone marrow-derived cells and other adult progenitors. In addition, most recently, some studies reported that iPS cells can differentiate into functional cardiomyocytes *in vitro* (Quattrocelli et al. 2011), thus the use of iPS cells for myogenesis of injured myocardium is currently under investigation.

1.1.2.6 Modulation of Ventricular Remodeling

Many animal studies and clinical trials indicated that cell therapies can increase wall thickness and prevent ventricular dilation (Taylor et al. 1998; Etzion et al. 2001; Jain et al. 2001; Muller-Ehmsen et al. 2002). Thus, the attenuation of adverse ventricular remodeling may represent a significant component of the benefits conferred by implanted cells. Post-infarct ventricular remodeling involves complex adaptive and maladaptive changes in the ECM (Laflamme et al. 2007), which are thought to contribute to myocardial dysfunction (Lindsey et al. 2003). MSCs were shown to directly attenuate cardiac fibroblast proliferation and collagen synthesis via the release of paracrine factors

in vitro (Ohnishi et al. 2007). However, it is unclear whether the stem cell–mediated decrease in fibrosis is a secondary effect limited to cardiomyocyte apoptosis, or whether stem cells have a direct effect on ECM remodeling.

Regardless of the exact mechanism(s), the delivery of stem/progenitor cells appears to increase tissue perfusion and improve cardiac function (Figure 1-1). When discussing the mechanisms considered for improving functional recovery, it might be essential to distinguish between the target patient populations (e.g. acute infarction versus chronic ischemia), in order to target different pathophysiological processes (Dimmeler et al. 2008).

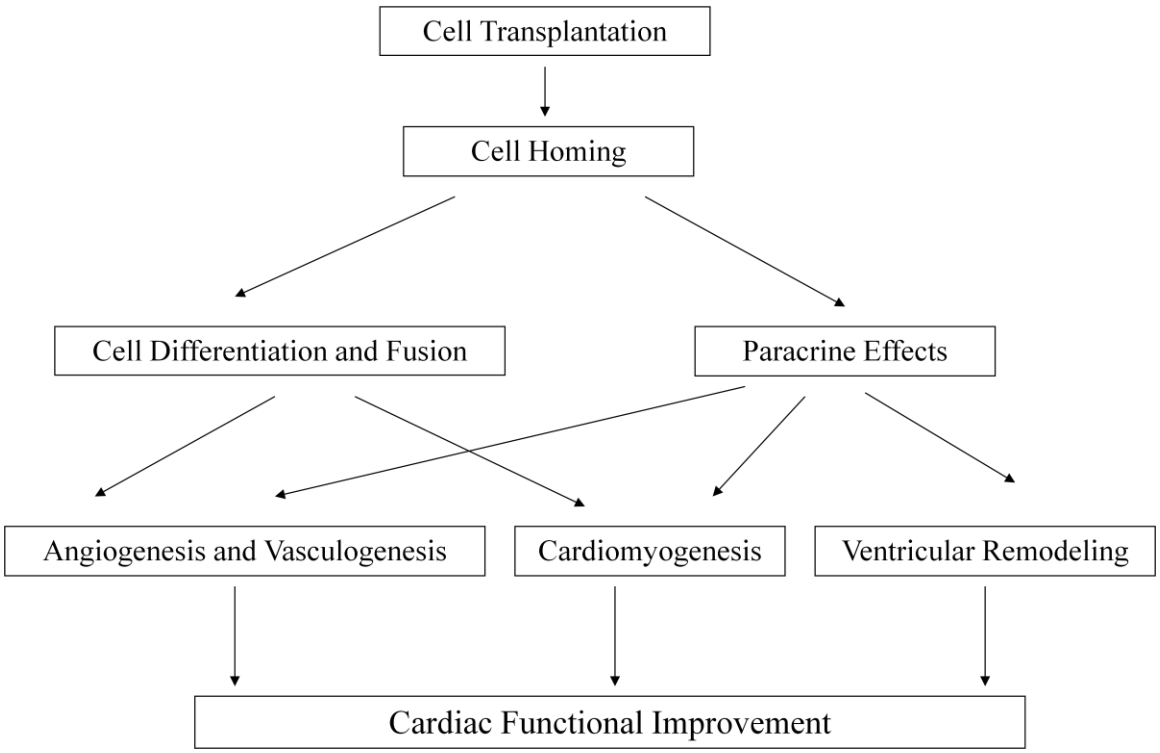

Figure 1-1: Proposed processes mechanisms involved in cell therapy for heart disease.

Stem/progenitor cells may improve cardiac function by various potential mechanisms, including cell homing, cell differentiation, cell fusion, and paracrine effects. Initial cell homing is considered to be the primary mechanism of action of cell therapy. Subsequently, cell differentiation and fusion have been demonstrated to account for many instances of presumed de novo formation of blood vessels (neovascularization) and myocardium (cardiomyogenesis). Many now believe that the paracrine effects of transplanted cells on injured myocardium are the major driver of cardiac functional benefits.

1.1.3 Clinical Application of Cardiac Cell Therapy

Both acute myocardial infarction (AMI) and chronic myocardial ischemia may result in congestive heart failure (CHF). Based on several animal studies, the introduction of stem and/or progenitor cells into the peri-infarct or infarct region provides a means to facilitate revascularization and improve cardiac function. Most clinical trials so far have been performed in patients with CAD (Table 1-1).

1.1.3.1 Acute Myocardial Infarction

Recent randomized clinical trials provide the evidence that cell therapy may work in AMI patients.The Transplantation of Progenitor Cells and Regeneration Enhancement in Acute Myocardial Infarction (TOPCARE-AMI) study indicated improvement in ventricular function and regional wall motion of the infarct zone at 1 year after intracoronary infusion of either bone marrow mononuclear cells (BMMNCs) or CPCs (Assmus et al. 2002; Schachinger et al. 2004). Another randomized trial, the Bone Marrow Transfer to Enhance ST-elevation Infarct Regeneration (BOOST), also demonstrated the recovery of regional left-ventricular ejection fraction (LVEF) in the border zone of patients with AMI after treatment with BMMNCs (Wollert et al. 2004; Meyer et al. 2006). The published report on the mid-term follow-up showed that the cell-treated group maintained improved LVEF at 6 months, but these differences did not persist at 18 months. The REPAIR-AMI trial showed that intracoronary administration of bone marrow-derived cells into patients with AMI improved vascular conductance capacity and microvascular function in the cell-treated coronary territory (Erbs et al. 2007). It will be important to determine whether increased coronary vascular conductance capacity ultimately translates into

improved clinical outcome to establish a cause-and-effect relationship between cell therapy–based improvements in neovascularization and functional cardiac regeneration.

1.1.3.2 Chronic Myocardial Ischemia

By comparison, in patients with chronic ischemic heart disease and old myocardial infarction, initial attempts at cell therapy were more disappointed in outcome, likely owing in part to the more diverse populations treated. The first such trial used skeletal muscle–derived progenitor cells, directly injected into the scarred region of the LV during open heart surgery for coronary artery bypass grafting (Menasche et al. 2001). Global and regional LV function was significantly and persistently improved, although concomitant revascularization complicated the assessment of benefit. Unfortunately, the enthusiasm for injecting myoblasts into scar tissue for cardiac repair has been dampened by the fact that some patients receiving this treatment experienced life-threatening arrhythmias (Menasche et al. 2003). In another nonrandomized trial, Erbs et al showed that intracoronary transplantation of CPCs after recanalization of chronic coronary total occlusion resulted in an improvement of macro- and microvascular function and contributed to the functionalization of hibernating myocardium (Erbs et al. 2005).

1.1.3.3 Congestive Heart Failure

Heart failure ensues when contractile reserve is depleted below a critical threshold. While indispensable to current treatment of end-stage heart failure, more aggressive interventions such as heart transplantation and the use of mechanical LV assist devices are limited by availability and morbidity issue (Reinlib et al. 2003). Cellular therapy might be an alternative treatment of CHF, with enormous therapeutic implications. In the

Myoblast Autologous Grafting in Ischemic Cardiomyopathy (MAGIC) clinical trials, the CHF patients recieved the autologous skeletal myoblasts during the by pass surgery. After 6 months, myoblast transfer did not improve regional or global LV function compared to the placebo, but absolutely increased the LVEF and significantly reduced LV end diastolic volume (Menasche et al. 2008). Petel et al reported a higher EF in patient treated with the $CD34^{+}$ bone marrow-derived cells at the time of off-pump coronary artery bypass grafting (Patel et al. 2005). The 6-month follow-up results indicated that autologous stem cell transplantation led to significant improvement of LVEF. Another clinical trial demonstrated that intramyocardial injection of BMC at the site of ischemia increased blood flow and improved regional and global ventricular function in patients with severe ischemic heart failure (Perin et al. 2003). Heart failure could be reversed or prevented if new myocardium could be grown in diseased hearts. As it is clinically possible to improve the heart's function without myogenesis or neovascularization, other potential mechanisms of action must also be considered. For example, the attenuation of ventricular remodeling may represent a significant component of the benefits conferred by transplanted cells.

Table 1-1 Selected clinical trials ofcardiac cell therapy

Study	Patient	Cell Type	Route	Follow-up	Results
TOPCARE-AMI	AMI (n=29) AMI (n=30)	2.1×10^8 BMCs 1.6×10^7 CPCs	IC	12m	Increased LV perfusion and contractility
BOOST	AMI (n=30)	2.4×10^9 BMCs	IC	18m	No improvements of LV function in infarct region
REPAIR-AMI	AMI (n=102)	BMCs (50 mL BM)	IC	12 m	Improved LVEF; decreased infarct size
ASTAMI	AMI (n=50)	BMCs (50 mL BM)	IC	6 m	No benefit
Strauer et al.	AMI (n=10)	2.8×10^7 BMCs	IC	3m	Decreased infarct size; improved LV perfusion and function
Erbs et al.	CTO (n=13)	6.9×10^7 G-CSF-mobilized cells	IC	3m	Improved wall motion; decreased hibernating myocardium
TOPCARE-CHD	CMI (n=28) CMI (n=24)	2.1×10^8 BMCs 2.2×10^7 CPCs	IC	3m	Improved wall motion in infarct zone
Katritsis et al.	CMI (n=11)	$2\text{-}4\times10^6$ BMC and EPCs	IC	4m	Decreased perfusion defects and infarct size
Stamm et al.	CMI (n=20)	5×10^6 $AC133^+$ BMCs	IM	6m	Improved EF and myocardial perfusion
MAGIC	HF (n=97)	$4\text{-}8\times10^8$ SMB	IM	6m	Improved EF and reduced ESV
Perin et al.	HF (n=14)	3×10^7 BMCs	IM	4m	Improved EF, regional myocardial perfusion and function

TOPCARE-AMI = Transplantation Of Progenitor Cells And Regeneration Enhancement in Acute Myocardial Infarction; BOOST =BOne marrOw transfer to enhance ST-elevation infarct regeneration; ASTAMI = autologous stem cell transplantation in acute myocardial infarction; MAGIC = Myoblast Autologous Grafting in Ischemic Cardiomyopathy; AMI = acute myocardial infarction; CMI = chronic myocardial infarction; AP = angina pectoris; CTO = chronic total occlusion; HF = heart failure; BMC = bone marrow cell; CPC = circulation progenitor cell; G-CSF = Granulocyte Colony-Stimulating Factor; SMB = skeletal myoblast; IC = intracoronary; IM = intramyocardial; LV = left ventricular; EF = ejection fraction; ESV = end-systolic volume.

1.1.4 Challenges of Cardiac Cell Therapy

In the past decade, despite the tremendous benefits of myocardial regenerative therapy in animal studies, clinical trials have demonstrated only modest benefit (Abdel-Latif et al. 2007). One identified limitation is the insufficient number of autologous stem cells. To circumvent this obstacle, a rapid and relative simple purification and expansion procedure is required. Another potential limitation to cell therapy is inadequate cell delivery. Regardless of cell type, multiple studies indicated that most cells delivered to the heart are lost to the circulation or leak back out of the injection site (Hofmann et al. 2005). Transplanted cells may quickly fade from the target tissue and have low survival rates, significantly impacting on their beneficial effects. Therefore, it is needed to develop a sufficient cell graft with appropriate structural and functional properties (Segers et al. 2008). Meanwhile, the optimal cell type, dose, delivery timing and method are still not well known, which also reduces the efficacy of cell therapy.

Despite these hurdles, the outlook for stem cell or progenitor cell therapies for ischemic heart disease and blood vessel repair appears promising. A deeper understanding of the cell biology and a more thorough preclinical evaluation of the therapeutics is necessary prior to clinical trials in order to maximize the chances of successful clinical application. The growing clinical need, the encouraging experimental results, and the existence of advanced molecular technologies, will undoubtedly further stimulate investigational efforts to optimize cell therapies for CAD (Kinnaird et al. 2004).

1.2 Tissue-engineered Biomaterials for Cell Delivery

One challenge of cell therapies is to develop an administration strategy that maintains adequate cell numbers in a desired location for a sufficient amount of time to not only induce the growth of new vessels or new myocytes, but also to allow their maturation and functional integration. Generally, homing and retention of cells within a specific tissue relies on adhesion characteristics of the donor cells and the host. The state of the recipient tissue may be incapable of donor cell retention in sufficient quantity for the desired effect. Cell retention in the infarcted myocardium is only about 1-10% as early as a few hours after transplantation (Hofmann et al. 2005; Kang et al. 2006). With scientific advances in biomaterials and cell biology, opportunities to fabricate tissues in the laboratory from combinations of tissue-engineered materials (patches, scaffolds, matrices and cell sheets) and stem cells may provide unique biomimetic environments for tissue regeneration and/or replacement.

Tissue engineering employs a combination of cells, engineered materials, and suitable biochemical and physiochemical factors to develop biological substitutes that restore, maintain, or improve the function of injured tissues or organs (Langer et al. 1993; MacArthur et al. 2005). So far, many types of biomaterials have been developed and tested, including metals, alloys, polymers, ceramics, composites, and glasses. Of the many biomaterials, collagens are considered as one of the most attractive options.

Collagen is a natural component of ECM, which forms the essential framework of the tissues and organs. Collagen-cell interactions are essential during wound healing and tissue remodeling in adults. Therefore, collagen-based biomaterials may present a stable mechanical support, offer biocompatibility, biodegradability and minimal

immunogenicity, provide a large surface area for cell seeding, and porosity for capillary/arteriole in-growth during direct cell transplantation. An added benefit of collagen-based cell delivery vehicles is that the introduction of ECM components may help alter matrix remodeling, stabilize ischemic tissues and restore function (Kofidis et al. 2005; Mizuno et al. 2005), thus assisting in cell-based tissue regeneration (Cao et al. 2002; Cao et al. 2003; Suuronen et al. 2004; Bauer et al. 2005; Christman et al. 2005; Mi et al. 2006). Purified collagen materials have been used in many clinical studies as implants without significant adverse reactions (Moench et al. 2010).

Several forms of delivery materials have been developed for the support of transplanted cells. Survival and integration of delivered cells can be improved by embedding them in a collagen-based matrix (Suuronen et al. 2004; Suuronen et al. 2006), by seeding them in a fibrin biopolymer patch (Liu et al. 2004), or by implanting cells as monolayer sheets (Miyahara et al. 2006). Synthetic myocardial patches have also been tested experimentally but these materials can be rigid, elicit a foreign body inflammatory response, limit cell mobility and vascularization (Suuronen et al. 2008), and have been inferior to ECM scaffolds that allow regeneration to occur (Robinson et al. 2005). Another potential strategy for cell delivery involves the development of thermo-sensitive injectable materials that are liquid during preparation, and form hydrogels at physiological temperatures (Christman et al. 2004; Christman et al. 2004; Kofidis et al. 2005; Zhang et al. 2006). These materials can facilitate targeted, less invasive tissue renovation after myocardial injury including increased cell survival, restored blood flow and improved cardiac function.

1.3 Cell Labeling and Cell Tracking

The introduction of stem cells and/or progenitor cells into damaged myocardium has promising therapeutic potential in ischemic heart diseases and dilated cardiomyopathy. However, understanding the biological mechanisms and local effects of transplanted cells during cardiac regenerative therapy remains mostly limited to histological assessment. In order to demonstrate cell survival and evaluate the fate of transplanted cells, new quantification techniques and imaging modalities are required to distinguish successful treatments from nonviable options, and to understand the mechanism(s) of repair.

1.3.1 Molecular Imaging Modalities

An ideal imaging method of cell trafficking would ensure that cell viability and functional characteristics are truly depicted in real time. This imaging technology should have single-cell detection capability and allow quantification of cell numbers at any anatomical location and at any given time-point without necessitating sacrifice. Regardless of the level of sensitivity achieved, accurate quantification of cell number can be particularly difficult when certain technical limitations are considered, such as the effects of contrast agent dilution during cell division, or the propensity of some contrast agents to be transferred to other non-specific cells (Frangioni et al. 2004; Beeres et al. 2007). Furthermore, since current cardiac cell therapy uses a relatively small number of stem cells that can be found at any one site after administration, a strong signal is likely to be required for defining the distribution of transplanted stem cells within tissues and organs. In addition, the successful imaging technology should permit cell tracking over a long period of time, both serially and noninvasively, in living subjects. The time frame that the signal remains detectable should be in the range that provides useful clinical

information. Molecular imaging modalities, including positron emission tomography (PET), single-photon emission computed tomography (SPECT), magnetic resonance imaging (MRI), and optical imaging, are powerful tools that allow visual representation and quantification of various biologic processes at the cellular and subcellular levels in a living organism (Blasberg et al. 2003). Therefore, all these techniques have the potential for application in the evaluation of transplanted stem cell survival and function in the heart. Every method has its own advantages and disadvantages (Table 2-1) and can provide relevant and useful information. However, at present, no single imaging modality possesses all the desired qualities for optimal evaluation of stem cell therapy.

Table 1-2 Molecular imaging for stem cell tracking

Modality		Possible labeling agents	Sensitivity (mol/L)	Spatial resolution	Advantages	Disadvantages
Optical	BLI	Luciferase	10^{-15}-10^{-17}	3-5 mm	High sensitivity	Only for small animals
	Fluorescence	NIRF	10^{-9}-10^{-12}	2-3 mm	Uses conventional microscopy	Only for near-surface
MRI		SPIO, Gd-DTPA	10^{-3}-10^{-5}	25-100 μm	High resolution; anatomical imaging	Low sensitivity; not directly reflecting viable cells; contra-indicated with many cardiac devices
Nuclear	SPECT	^{99m}Tc-HMPAO, ^{111}In-oxine	10^{-10}-10^{-11}	0.5-1.5 mm	High labeling efficiency and stability; good resolution; signal is related to cell viability	Radioactive decay; attenuation-associated accuracy limit; lack of anatomical information*
	PET	^{18}F-FDG, ^{18}F-HFB, ^{18}F-SFB	10^{-11}-10^{-12}	1-2 mm	High sensitivity; good resolution; quantification possible; signal directly related to cell viability	Rapid loss of signal due to the short half-life of radioisotopes; lack of anatomical information*

BLI = bioluminescence; MRI = magnetic resonance imaging; SPECT = single-photon emission computed tomography; PET = positron emission tomography; NIRF = near-infrared fluorophores; SPIO = superparamagnetic iron oxide particles; Gd-DTPA = gadolinium-diethylene triamine penta-acetic acid; ^{99m}Tc-HMPAO = ^{99m}Tc-hexamethylpropyleneamine oxime; ^{18}F-FDG = 2-[^{18}F]fluoro-2-deoxy-D-glucose; ^{18}F-HFB = hexadecyl-4-[^{18}F]fluorobenzoate; ^{18}F-SFB = *N*-succimidyl-4-[^{18}F]fluorobenzoate.

* anatomical resolution can be achieved using CT with hybrid human or animal systems, but is associated with increased radiation doses.

1.3.2 Positron Emission Tomography

To study physiological processes, PET uses radioactive molecular probes that are tracers labeled with positron-emitting isotopes. The positron-labeled molecular probe, including receptor ligands or enzyme substrates, binds to a specific target protein or is trapped in cells of interest. The accumulation of the radioactive probe in tissues or cells is then measured by the PET scanner (Herschman 2004).

With the projected rapid growth of cell therapy for heart disease, PET is expected to play a major role in monitoring relevant changes that occur at every stage in cardiac regenerative therapy. As an advanced nuclear imaging technology, PET is one of the best suited modalities to evaluate stem cell therapy since it is readily applicable to measure most end-points, including the cell delivery, local and remote tracking, and therapeutic response (deKemp et al. 2000; Bax et al. 2002; Beanlands et al. 2002; Bengel et al. 2004; Dobert et al. 2004; Yoshinaga et al. 2005; Ruel et al. 2008).

PET cameras allow electronic rather than mechanical collimation of incoming photons by recording the coincidence of simultaneous pairs of annihilation photons at opposite detectors (Blokland et al. 2002). The dose of radioactivity required to produce a signal of PET is very small, and generally does not impact the biological system under study. The sensitivity of PET is at least 7 log order more sensitive than MRI (10^{-4} versus 10^{-11} M) (Shao et al. 1997), 1–2 orders of magnitude better than SPECT (10^{-10} M), thus providing a good potential for accurate quantification of low cell numbers (Gambhir et al. 2000) and then for noninvasive assessment of stem cell retention, survival, and function after transplantation.

1.3.3 Labeling Methods for PET Imaging of Cells

In order to implement a stem cell PET imaging protocol, it is important to develop a rapid and stable labeling method without altering the viability or function of the cells. Two radiolabeling approaches have been explored to achieve this end: 1) direct cell labeling with a radionuclide; and 2) reporter gene-based cell labeling.

1.3.3.1 Direct Cell Labeling

Direct cell labeling with a PET isotope is a proven technique that can provide whole body biodistribution information with high sensitivity. Cells are incubated with the radiotracer, allowing the radioactive molecule to be "trapped" in or on the cell (Figure 1-2). Following incubation, the cells are washed to remove unbound tracer and are then injected into the host. Ideally, the radioactive probe should be rapidly incorporated into the cell and fully retained. However, labeling efficiencies close to 100% are not realistic, and depend intimately on the cell type, radiotracer characteristics, incubation time, and environment (Dewanjee et al. 1991; Welling et al. 1995; Massler et al. 1997; Acton et al. 2005; Doyle et al. 2007). After cell transplantation, unbound tracer diffuses out of the cell and tissue, and then can be cleared from the circulation and excreted.

Direct labeling of cells with a radionuclide has been used for many years to track cells *in vivo* (Pozzilli et al. 1983). Many PET tracers (such as ^{18}F-FDG) are physiologically identical to natural biological substrates. As a result, a PET tracer in the body will follow the same physiological pathways as the non-radioactive natural substrate that it mimics. Current efforts for stem cell tracking are having an increased focus on this approach due to its minimal toxicity and easy accessibility. In general, PET imaging with direct cell labeling studies can supply the evidence of successful target

delivery and allow quantification of the cell distribution to a particular site at early stages of cell transplantation. Tracking stem cells with PET in clinical trials can help understand the effects of cell therapy at various stages, and thus direct therapy.

Cell labeling using a radioisotope displays minimal toxicity and is an established method in clinical nuclear medicine. However, the stability of the labeled cells remains an issue due to the cleavage process leading to incomplete trapping mechanism of the cell-ligand complex, thus producing a signal from the labeled moiety distinct from that of the labeled cell. Moreover, the major limitation of direct cell labeling technique is the short half-life of most available PET tracers (eg. 110 min for ^{18}F), which limits its ability to monitor long-term survival kinetics and cellular trafficking of stem cell therapy. In addition, direct cell labeling cannot provide information regarding cell proliferation because the radiotracers are not passed on from mother to daughter cells. On all accounts, the measurable signal will diminish over time, through radioactive decay, cell division, metabolism or degradation of the labeled agent either by enzymatic action or radiolysis.

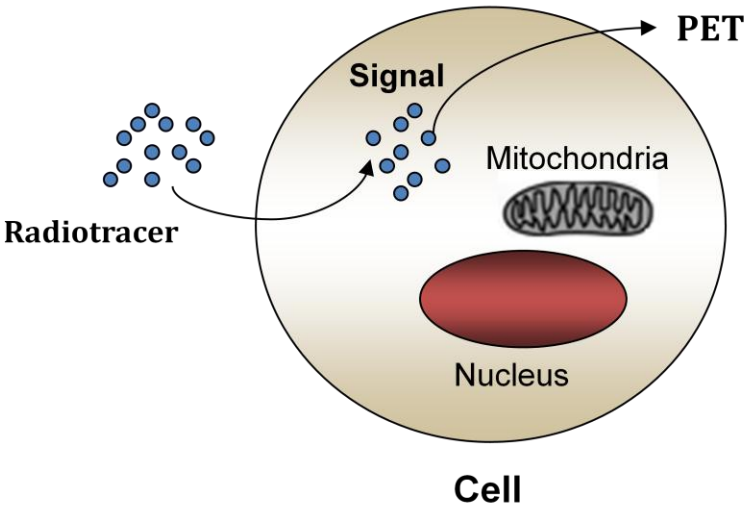

Figure 1-2: Direct cell labeling with a radioisotope.

Cells are incubated with the radiotracer, allowing the radioactive molecules to be "trapped" in the cell. When sufficient radiotracer accumulation occurs within the cell, the signal can be detected by PET.

1.3.3.2 Reporter gene-based cell labeling

Stem cells can also be labeled after transfection with a reporter gene, which can subsequently be visualized by using a PET reporter probe that binds to the enzyme, receptor or transporter produced by reporter genes, therefore allowing serial *in vivo* evaluation of cell viability and proliferation in long-term follow-up studies. Recently, some studies successfully used this method to visualize implanted stem cells by PET imaging in animals (Cao et al. 2006).

In general, PET reporter genes are DNA sequences that encode for a reporter protein, which will form a complex via specific binding with a selected radiotracer. Detection of this ligand or substrate will produce a signal which can then be quantified serially and noninvasively by PET imaging. The implementation of reporter gene imaging techniques to monitor cells is a multi-step process (Figure 1-3). First, the genetically encoded reporter genes must be successfully introduced into cells. Typical reporter genes consist of a chimeric gene linking an endogenous or exogenous promoter. This construct is inserted into a viral or non-viral vector and then delivered into the target cell nucleus by this vector. The reporter gene will be transcribed to mRNA and subsequently translated to the reporter protein within the cell. PET reporter proteins are either receptors/transporters that bind and/or sequester positron-emitting "ligand probes", or enzymes that metabolize positron-emitting "substrate probes". When the corresponding PET reporter probe is injected, cells expressing the reporter gene will sequester the radioprobe (Vassaux et al. 2003) resulting in specific binding and the generation of a signal which can be detected by PET (Herschman 2004; Acton et al. 2005; Kim et al. 2006; Sheikh et al. 2006). Cells not expressing PET reporter genes will

not retain PET reporter probes. Tomographic imaging then demonstrates PET reporter gene-dependent sequestration of the radioactive reporter probe. This technique has made it possible to monitor the viability, function and proliferation of labeled cells administered to host recipients and then to monitor cell migration *in vivo*.

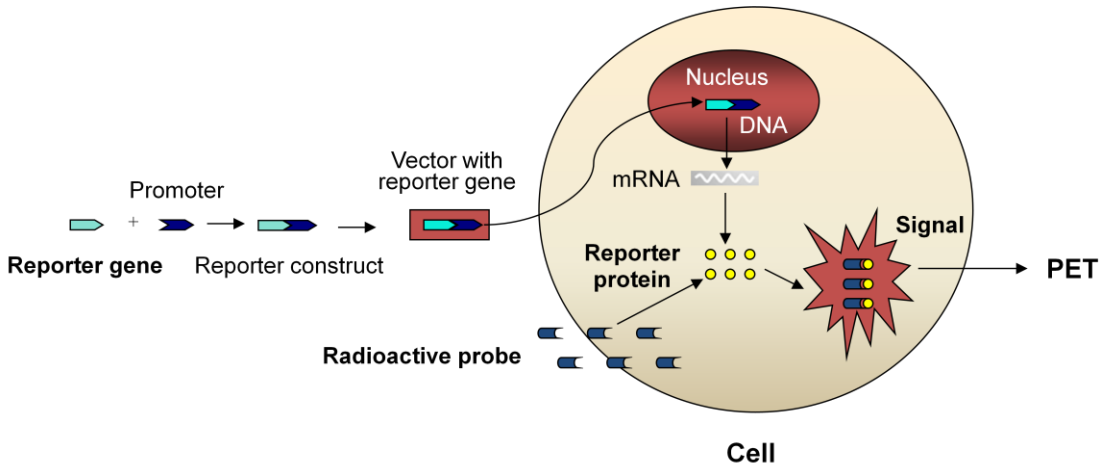

Figure 1-3: Reporter gene-based cell labeling.

The reporter construct contains a promoter region and the reporter gene it drives. This construct is inserted into a vector and then delivered into the target cell nucleus by this vector. The reporter gene is transcribed to mRNA and subsequently translated to the reporter protein within the cell. Finally, the radiolabeled probe interacts with the reporter protein resulting in specific binding and the generation of a signal which can be detected by positron emission tomography.

1.4 Research plan

1.4.1 Aims

The primary goal of my research was to develop techniques for successful transplantation of human stem/progenitor cells for cardiac regeneration.

Specific Aim 1 was focused on developing techniques that will expand human $CD133^+$ cells from adult peripheral blood (Manuscript #1). Previous studies showed that $CD133^+$ cells contributed to restore perfusion and enhance global function in the infarcted myocardium (Agbulut et al. 2004; Suuronen et al. 2006). However, the presence of $CD133^+$ cells in the blood and bone marrow is low. Therefore, expansion and characterization of derived $CD133^+$ cells would not only address challenges in cardiac regeneration, but also contribute to improving cell transplantation in general.

Specific Aim 2 was to develop and utilize stable cell labeling methods for *in vivo* monitoring the transplanted cell fate with a non-invasive PET imaging. Following the transplanted cells is an essential step in assessing their local effects and biological mechanisms. However, it is mostly limited to histological examination. Therefore, the research in my Ph.D. project involved the development of a non-invasive PET imaging with direct cell labeling (Manuscript #2 & #3) and reporter gene-based cell labeling (Manuscript #4) to study the homing and engraftment of transplanted human CPCs.

Specific Aim 3 addressed challenges associated with the successful delivery of stem cells to the target sites. Specifically, my experiments focused on the investigation of collagen I-based matrices to enhance transplanted cell homing and engraftment (Manuscript #2). As discussed, collagen matrices have been shown to improve the functional results of cardiac cell therapy. However, their mechanism(s) and local effects

remain unclear. PET imaging provides the potential for assessing the ability of collagen matrices to improve the efficacy of cell therapy.

1.4.2 Hypotheses

It was hypothesized that 1) human $CD133^+$ cells can be generated from the $CD133^-$ fraction, and derived $CD133^+$ cells might have comparative capacities of migration and angiogenesis to fresh $CD133^+$ cells and other progenitor populations used in cardiac cell therapy. 2) PET imaging with ^{18}F-FDG or ^{18}F-HFB labeling, and reporter gene techniques can be used to assess the fate of transplanted human CPCs *in vivo* at different target sites and different stages after transplantation. 3) PET imaging with ^{18}F-FDG labeling is a feasible approach to understand the role of collagen matrices in delivered CPCs at early stages of cell transplantation. Furthermore, PET imaging with reporter gene techniques can be used to examine the long-term effects of collagen-based matrices on transplanted CPC homing, retention and engraftment.

CHAPTER 2: MANUSCRIPT #1

Introduction to Manuscript #1

Previous studies from our group and others showed that $CD133^+$ cells restored perfusion in the ischemic tissue (Suuronen et al. 2006) and enhanced global function in the infarcted myocardium (Agbulut et al. 2004). However, the presence of $CD133^+$ cells in the blood and bone marrow is low, and their mechanisms and functional role in cell therapy remain unclear. Furthermore, these studies did not directly compare the efficacy of $CD133^+$ cells with other cell populations. In this study, I investigated a method of human $CD133^+$ cell expansion from peripheral blood and evaluated the function of derived $CD133^+$ cells compared to other commonly used progenitors. To obtain sufficient quantities of adult autologous progenitor cells and potentially identify an ideal cell source and type for cardiac cell therapy, manuscript #1 details the *ex vivo* expansion of human peripheral blood $CD133^+$ cells and *in vitro* functional comparison of therapeutically relevant progenitor populations.

The Journal of Thoracic and Cardiovascular Surgery 2010; 140: 216-24

In vitro Functional Comparison of Therapeutically Relevant Human Vasculogenic Progenitor Cells Used for Cardiac Cell Therapy

Yan Zhang, MD, MSc,[a,b,*] Serena Wong, BSc,[a,b,*] Jessica Laflèche, BSc,[a,b] Suzanne Crowe,[a] Thierry G. Mesana, MD, PhD,[a] Erik J. Suuronen, PhD, [a,b] Marc Ruel, MD, MPH[a,b]

From the Division of Cardiac Surgery,[a] University of Ottawa Heart Institute, Department of Cellular and Molecular Medicine,[b] University of Ottawa, Ottawa, Ontario, Canada

Supported by the Canadian Institutes of Health Research (to Drs Ruel and Suuronen, grant MOP-77536), by the Canadian Foundation for Innovation (to Dr Ruel, award 7346), and by the Heart and Stroke Foundation of Canada Doctoral Research Award (to Dr Zhang).

Disclosure: None

* Y. Zhang and S. Wong contributed equally to this work.

Address for reprints: Marc Ruel, MD, MPH, and Erik Suuronen, PhD, Division of Cardiac Surgery, University of Ottawa Heart Institute

Copyright © 2010 by The American Associattion for Thoracic Surgery

Doi:10.1016/j.jtctv.2009.11.016

Contributions of Authors

The design and execution of the experiments in this manuscript were performed jointly by the M.Sc. candidate that initiated the project, Serena Wong and myself, with practical help from M.Sc. candidate Jessica Laflèche. Suzanne Crowe operated the FACSAria for flow cytometry analysis. Dr. Thierry Mesana provided a clinical perspective on the data. I worked on manuscript preparation and submission under the guidance and supervision of Drs. Marc Ruel and Erik Suuronen.

Abstract

Objectives: In cardiac cell therapy, almost every cell type tested experimentally has yielded some benefit. However, there is a lack of studies directly comparing the function of various stem/progenitor cell populations. This study describes the expansion of peripheral blood $CD133^+$ cells, and compares their functional properties with that of other commonly used human progenitor cell populations.

Methods: $CD133^+$ cells were generated from the $CD133^-$ fraction of peripheral blood, either serially (pooled-derived) or after 14 days of culture (derived). Their phenotypic, migratory, and vasculogenic properties were compared with that of 4 commonly used progenitor cell populations *in vitro*.

Results: Serial expansion resulted in an 11-fold increase in the number of $CD133^+$ cells. The proportion of derived $CD133^+$ cells collected between 0 and 8 days also expressing CD34 and VEGFR-2 was similar (approximately 60%; $P = .41$). Adherent, 4-day cultured endothelial progenitor cells demonstrated enhanced migration compared to each of the other 5 cell populations (all $P \leq .002$). The migration of derived $CD133^+$ progenitors was enhanced by co-culture with $CD133^-$ cells or its supernatant ($P < .05$). *In vitro* vasculogenesis assays revealed that derived and pooled-derived $CD133^+$ cells had superior vasculogenic potential compared to other progenitor populations ($P \leq .03$).

Conclusions: A novel source of expandable $CD133^+$ cells can be generated from the $CD133^-$ fraction of peripheral blood. The CD133 phenotypic marker translates into the cell being vasculogenically more potent *in vitro*, which could be beneficial to induce

vasculogenesis in the ischemic heart. Furthermore, intercellular interactions appear important for improving the therapeutic efficacy of cell transplantation.

Key words: Stem cells; Vasculogenesis; Cell therapy; Ischemia; Myocardium

Introduction

Cardiac cell-based therapies, one of the major areas of translational research where heart surgeons play a key role, involve the delivery of stem/progenitor cells to areas of ischemic and/or infarcted myocardium in order to stimulate and accelerate the processes of vasculogenesis, myogenesis, or both (Ruel et al. 2004). A number of different cell types have been transplanted into the hearts of experimental animals or patients with coronary artery disease (CAD), and almost every cell type tested has yielded some degree of benefit experimentally. However, clinical benefits have been modest. Today, there remain major hurdles in cell expansion, delivery, adhesion, local amplification, vascularization, and functional incorporation (Figure 2-1).

One issue that needs to be addressed is the identification of the "ideal" stem/progenitor cell population for optimal vasculogenesis, considering how important the paracrine/humoral mechanism might be (Gnecchi et al. 2008). In clinical use, autologous cells from the blood, bone marrow, or other tissues are favored because they circumvent the potential problems associated with ethics, availability, and immune responses. Several heterogeneous and pre-selected progenitor cell populations derived from bone marrow (BM) or peripheral blood (PB) mononuclear cells (MNCs), such as mesenchymal stem cells (MSCs), endothelial progenitor cells (EPCs) or circulating progenitor cells (CPCs), have been used in various experimental and clinical settings (Stamm et al. 2003; Hofmann et al. 2005; Suuronen et al. 2007; Zhang et al. 2008). One cell population of interest for therapeutic vasculogenesis in the ischemic or infarcted myocardium is the MSC. Transplanting MSCs into the heart has been shown to improve its perfusion and function (Suuronen et al. 2007). Another cell population, the circulating

progenitor cells (CPCs), which include endothelial progenitor cells (EPCs), can home to injured tissues and are important for vascular repair and maintenance (Suuronen et al. 2007; Zhang et al. 2008). A variety of cell sources, isolation methods, and culture conditions have been used to produce mainly heterogeneous populations of EPCs for transplantation. One commonly used ex-vivo expansion technique yields 4-7 day adherent EPCs from the culture of circulating PB-MNCs on fibronectin (Zhang et al. 2008).

Pre-selection to obtain more specific subpopulations of EPCs may be performed, involving an isolation of cells based on markers such as CD34, vascular endothelial growth factor receptor 2 (VEGFR-2) and/or CD133 (Peichev et al. 2000). CD34 and VEGFR-2 are both expressed at lower levels on mature endothelial cells, whereas CD133, also known as prominin or AC133, is expressed on hematopoietic stem cells but is absent on mature endothelial cells and monocytic cells. Although CD133 may be a more specific marker of stem/progenitor cells and may provide a clinical benefit (Stamm et al. 2007), its functional role in cell biology remains uncertain.

Recently, the peripheral blood became a preferred cell source for regenerative therapy considering its non-invasiveness and easy availability. However, the frequency of $CD133^{+}CD34^{+}VEGFR\text{-}2^{+}$ cells in total PB-MNCs is very low (~0.002%) (Masuda et al. 2003). Although some research showed that granulocyte colony-stimulating factor-mobilized blood from patients contains 5- to 100-fold higher levels of MSCs and EPCs, compared with non-mobilized blood (Powell et al. 2005), the ability of these cells to improve cardiac remodeling and function after acute myocardial infarction (AMI) has been disappointing (Hill et al. 2005).

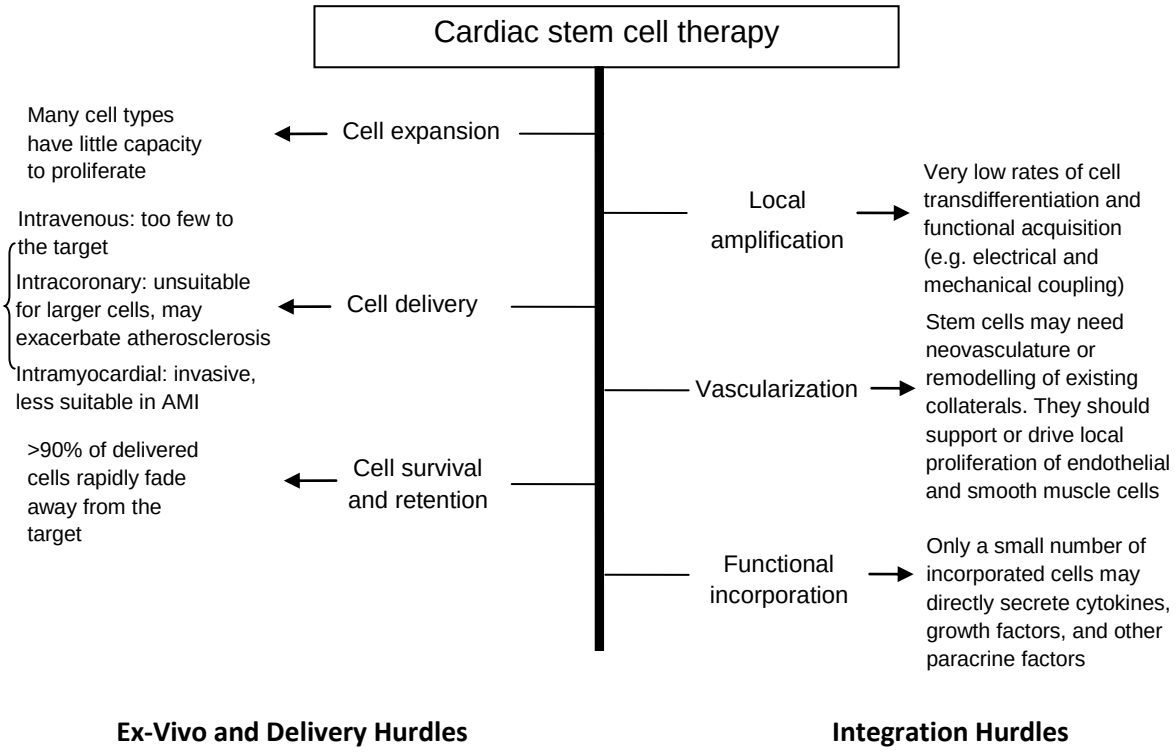

Figure 2-1: Hurdles in cardiac cell therapy.

AMI, Acute myocardial infarction.

Consequently, one first step for clinical stem cell therapy would be to obtain large amounts of homogenous and well-characterized cells, and to study them. In this regard, we identified a new subpopulation of EPCs, termed "derived" $CD133^+$ PB cells (Suuronen et al. 2006). These cells demonstrated improved adhesion and ability to form capillary-like structures *in vitro* compared to freshly isolated $CD133^+$ progenitors from the PB.

Many studies have examined the efficacy of different progenitor cell populations individually; however, direct functional studies that compare several cell populations are lacking. Additionally, intercellular interactions can have a significant impact on the functional activity of progenitor populations both *in vitro* and *in vivo* (Suuronen et al. 2006; Suuronen et al. 2007), and further elucidation of these interactions and cytokine influence may benefit the optimization of cell therapy strategies. Therefore, assessing the vasculogenic properties and interactions of different EPC and BM populations may be invaluable in order to optimize clinical cell-based therapeutic vasculogenesis. This study was designed: 1) to investigate methods of $CD133^+$ PB cell expansion; 2) to characterize derived $CD133^+$ PB cells and the influence of intercellular interactions on their function; and 3) to evaluate their vasculogenic and migratory properties in comparison with other commonly used human progenitor populations from the PB and BM.

Materials and Methods

Cell Isolation and Expansion

This study was approved by the Human Research Ethics Board of the University of Ottawa Heart Institute. After acquiring informed consent from human patient donors

undergoing valve surgery (n=12), without concomitant CAD or diabetes (in order to limit inter-patient variability in progenitor cell function), both PB and sternal BM were harvested immediately after sternotomy. Details of patient characteristics are found in Table 2-1.

Table 2-1 Patients' characteristics

	All patients (n=12)	Aortic valve disease (n=6)	Mitral valve disease (n=5)	Aortic and mitral valve disease (n=1)
Age (y)	64.7±10.7	65.7±8.3	61.0±13.0	79
Male/female (n)	10/2	5/1	5/0	0/1
CAD (n)	0	0	0	0
Diabetes (n)	0	0	0	0
CHF (n)	2 (17%)	1	1	0
Hypertension (n)	5 (42%)	3	1	1
Hypercholesterolemia (n)	5 (42%)	2	2	1
Smoking (n)	4 (33%)	2	2	0

CAD, Coronary artery disease; *CHF*, congestive heart failure.

Overall, 6 different populations of stem/progenitor cells were obtained from PB or BM as described in the Supplemental Material: (1) fresh $CD133^+$ PB cells; (2) derived $CD133^+$ PB cells; (3) pooled-derived $CD133^+$ PB cells; (4) "classical" EPCs; (5) fresh $CD133^+$ BM cells; and (6) MSCs. Cell counts and viability were determined by using a cell counter (Beckman Coulter, Mississauga, Canada).

Briefly, to obtain derived $CD133^+$ PB cells from $CD133^-$ fractions, two different protocols were used. Cells in protocol 1 had fresh media added every 3 days without aspiration of the old media. After 14 days, both adherent and non-adherent cells were collected and separated to obtain derived $CD133^+$ PB cells. In protocol 2, the non-adherent population was removed every 2 days over a period of 8 days, separated to collect the $CD133^+$ cells, and cryopreserved. After 8 days, cryopreserved cells were combined together to constitute the pooled-derived $CD133^+$ population. Cell phenotype was analyzed by flow cytometry (FACSAria cell sorting system; BD Biosciences, San Jose, Calif). Details are provided in the online supplemental Materials and Methods section.

Investigation of $CD133^+$ Cell Generation

Freshly isolated $CD133^-$ PB cells were cultured under conditions: (1) supernatant from whole PB-MNCs; (2) fresh $CD133^+$ PB cells and (3) supplemented endothelial basal medium 2 (EBM-2 [control]; Clonetics, Guelph, Canada). After 48 hours of exposure, the adherent and nonadherent cells from each condition were lifted and separated to obtain the $CD133^+$ cells, and the numbers of derived $CD133^+$ cells were determined.

In Vitro Migration Assay

Each of the 6 cell populations were labeled with CellTracker Orange (Molecular Probes, Eugene, Ore), and then 2 x 10^4 labeled cells of each type were placed separately in the upper chamber with EBM-2 without VEGF (Ruel et al. 2005). The lower chamber contained serum-free media with 50ng/ml vascular endothelial growth factor (VEGF; Sigma, Oakville, Canada). After 24 hours of incubation, cells migrated into the lower chamber were counted manually from 6 random high-powered fields.

Interactions Between $CD133^+$ and $CD133^-$ PB Fractions

The cell groups were as follows: (1) fresh $CD133^+$ PB; (2) derived $CD133^+$ PB; (3) fresh $CD133^+$ PB combined with fresh $CD133^-$ PB; (4) derived $CD133^+$ PB combined with fresh $CD133^-$ PB; (5) fresh $CD133^+$ PB with the $CD133^-$ supernatant; and (6) derived $CD133^+$ PB with the $CD133^-$ supernatant. Cell migratory potential was assessed according to the methods described previously (Suuronen et al. 2006). Before and after culture, flow cytometry analysis was performed to determine the expression of VEGFR-2 on $CD133^+$ cells in the first 4 groups.

Cytokine Antibody Array

We sought to determine the cytokines present in the supernatant of various cell populations after 24 hours of culture with the human cytokine antibody array V (RayBiotech, Norcross, Ga). The cell populations examined were: (1) fresh $CD133^+$ PB; (2) derived $CD133^+$ PB; and (3) fresh $CD133^-$ PB. Supplemented EBM-2 was used as a control and the differences in the level of each growth factor and cytokine were quantified against internal controls within the array and then compared between cell

populations as fold changes. Kodak 1D Imaging software (Kodak, Rochester, NY) was used to determine intensities of cytokine spots on each array.

In Vitro Vasculogenesis Assay

Labeled cells (1 x 10^4) of each population were seeded onto solidified ECMatrix (Chemicon, Temecula, Calif) with 1 x 10^4 human umbilical vein endothelial cells (HUVECs) as supporting cells. HUVECs alone were used as a control. After 24 hours of incubation, six random HPFs were taken for each cell type. The complete area of tubules formed, total tube length and percentage contribution to the total area of capillaries were determined.

Statistics

Data are presented as mean ± standard error of the mean (SEM). Statistical analyses were performed in SigmaStat 3.1.1 (SigmaStat, Richmond, Calif). Comparisons of data between groups were performed with a 1-way analysis of variance, using Bonferroni corrections as appropriate.

Results

Expansion of PB $CD133^+$ Progenitors

The number of $CD133^+$ cells was expanded by culturing the $CD133^-$ PB fraction according to two protocols (Figure 2-2, *A*). With protocol 1, the culture of $CD133^-$ cells for 14 days resulted in derived $CD133^+$ cells (0.32±0.10 x 10^6) equivalent to a 3.09±1.37 fold increase compared to the number of $CD133^+$ cells in the fresh PB-MNC isolate (0.12±0.03 x 10^6; $P < .05$). With protocol 2, after 8 days the number of generated $CD133^+$

cells in the pooled-derived population (1.21±0.22 x 10^6) was 11-fold greater than that obtained from the freshly isolated PB-MNCs (0.14±0.03 x 10^6; $P < .05$). Also, the number of $CD133^+$ cells generated in the pooled-derived group was significantly greater than in the 14-day derived group ($P < .05$). Expression of CD34 and VEGFR-2 on $CD133^+$ cells obtained was examined by flow cytometry (see Figure 2-E1, *A*). On day 0, the proportion of circulating $CD133^+$ cells also expressing CD34 and VEGFR-2 was 39.5±9.3%. For day 2, 4, 6 and 8, the percentages were 67.6±9.5%, 56.2±14.5%, 58.0±8.9% and 69.4±15.1%, respectively (see Figure 2-E1, *B*; $P = .41$), suggesting that similar cell populations were being generated every 2 days.

Potential Mechanisms Involved in $CD133^+$ Generation

Fresh $CD133^-$ PB cells were cultured under 3 conditions to investigate a potential mechanism involved in the generation of $CD133^+$ cells. The results showed that generation of $CD133^+$ cells was significantly inhibited by the presence of $CD133^+$ cells and by whole PB-MNC culture supernatant ($P < .003$; Figure 2-2, *B*). When exposed to $CD133^+$ cells, only 71.7±7.7% derived $CD133^+$ cells were obtained relative to control (100%). Similarly, exposure of $CD133^-$ cells to PB-MNC supernatant resulted in only 49.4±9.2% generation of derived $CD133^+$ cells compared with control numbers.

Migratory Potential of Various Progenitor Cell Populations

The VEGF-induced migration potential of 6 cell populations was tested (see Figure 2-E2, *A*-*F*). The number of migrating cells per field of view (/FOV) were not significantly different between fresh $CD133^+$ PB cells (5.29±0.53) and $CD133^+$ BM cells (7.04±1.06), MSCs (4.23±0.79), derived $CD133^+$ PB cells (3.63±0.46), and pooled-

derived $CD133^+$ PB cells (5.58±0.59; P= .9). However, all populations had significantly lower migration compared with "classical" EPCs (61.09±19.57) from PB ($P \leq$ .002; Figure 2-3, *A*).

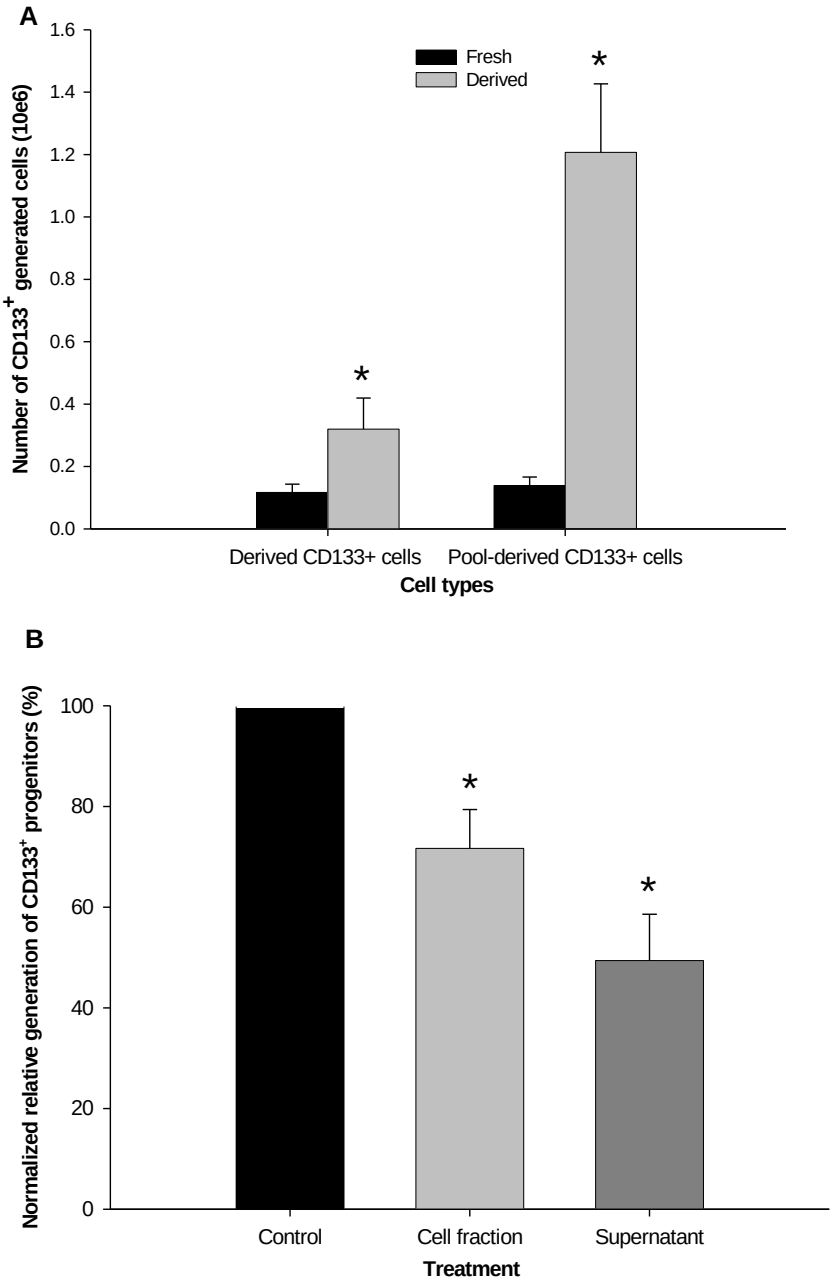

Figure 2-2: CD133$^+$ generation.

A, The number of pooled-derived CD133$^+$ cells (derived serially) was significantly greater than that of derived CD133$^+$ cells (after 14 days of culture). *P< .05 versus fresh CD133$^+$ cells; ^P< .05 versus. derived CD133$^+$ cells. B, The presence of a peripheral blood mononuclear cell (*PB-MNC*) supernatant or CD133$^+$ cells (from whole PB-MNC) inhibited the generation of CD133$^+$ cells from the CD133$^-$ fraction compared with normal expansion conditions (*Control*). *P< .003 versus control.

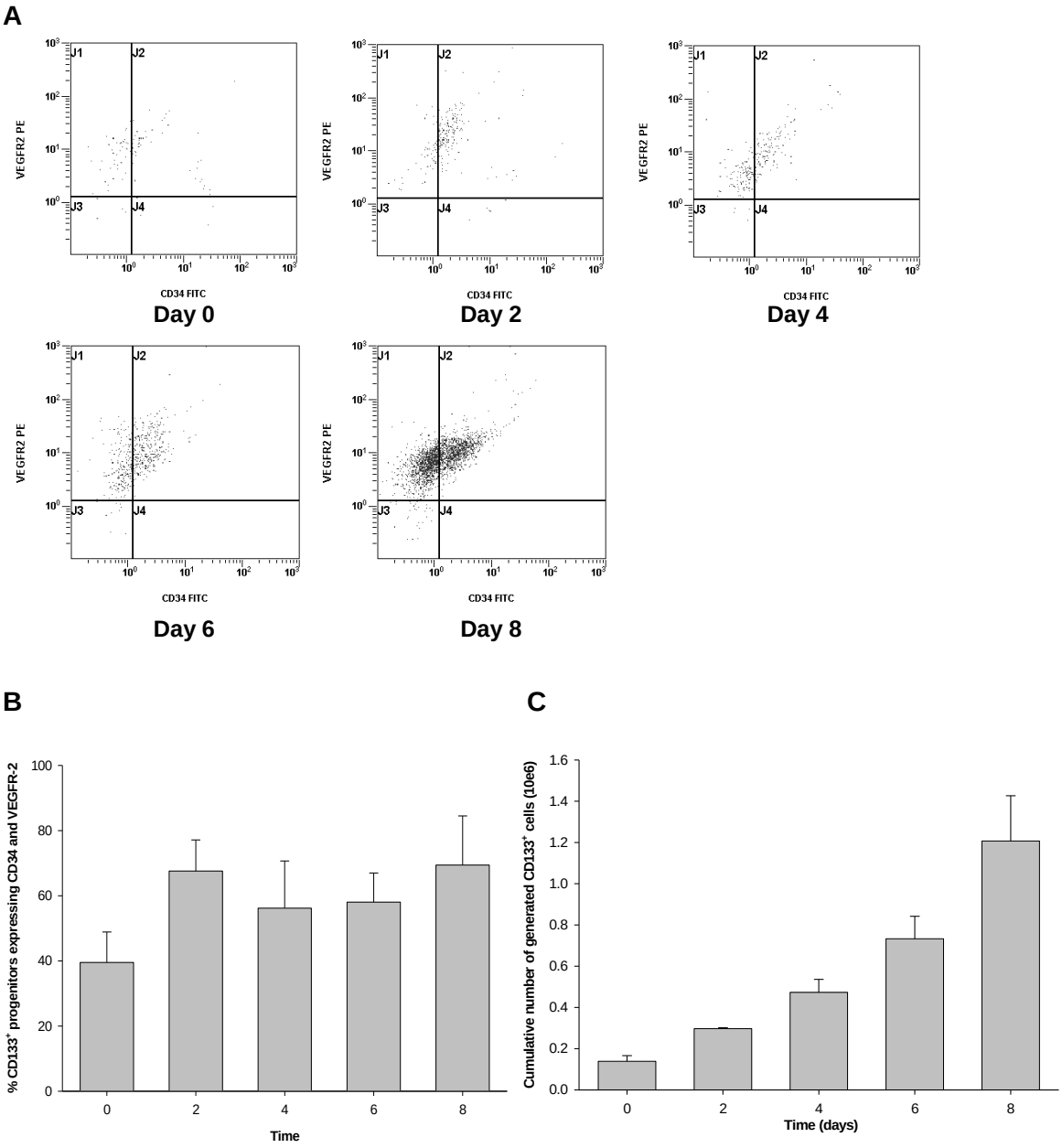

Figure 2-E1: Cell expansion.

(A) Representative flow cytometry analysis for co-expression of CD34 and VEGFR-2 on fresh and serially derived $CD133^+$ cells collected every 2 days for a period of 8 days. (B) Flow cytometry results showing the percentage of $CD133^+$ cells also expressing CD34 and VEGFR-2 over 8 days. (C) Cumulative number of generated $CD133^+$ cells removed every 2 days from the serial culture of the $CD133^-$ fraction of peripheral blood mononuclear cells. ***P*< .001 for day 8 versus other times.

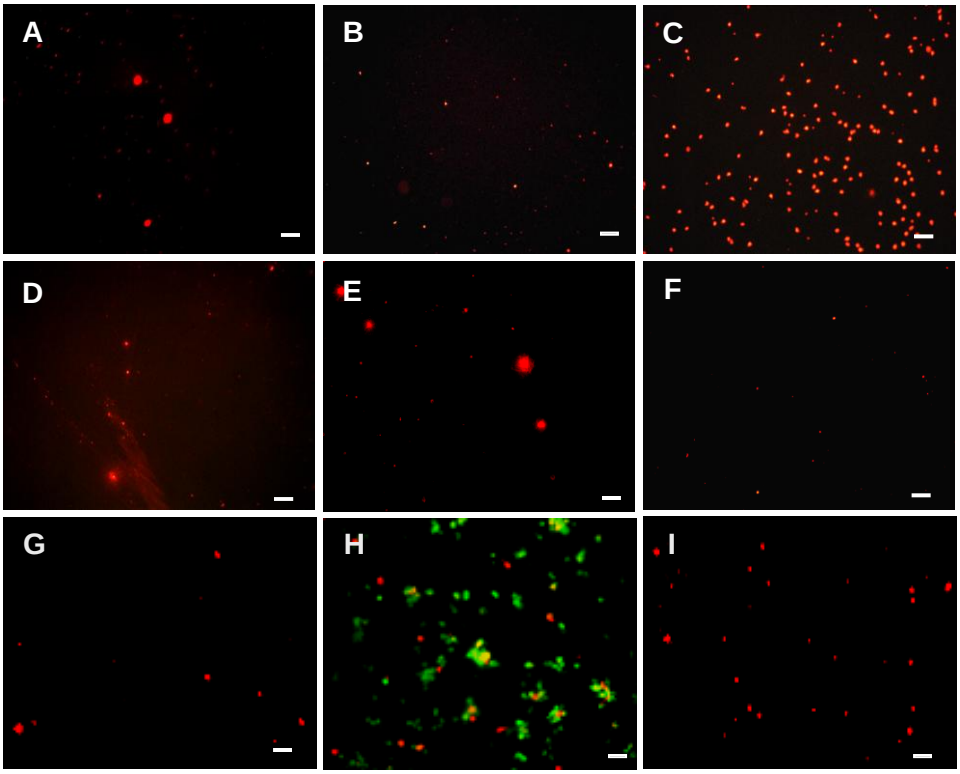

Figure 2-E2: Cell migration.

(A-F) The migration properties of 6 cell populations. Representative migration assay images of (A) fresh $CD133^+$ PB cells; (B) fresh $CD133^+$ BM cells; (C) PB "classical" EPCs; (D) BM MSCs; (E) derived $CD133^+$ PB cells; and (F) pooled-derived $CD133^+$ PB cells. (G-I) Cell interaction effects on $CD133^+$ cell migration. Representative migration assay images of (G) derived $CD133^+$ cells alone; (H) derived $CD133^+$ cells with $CD133^-$ cells; and (I) derived $CD133^+$ cells with $CD133^-$ cell supernatant after 24h of culture. Scale bar = 75 µm.

Cell Interaction Effects on Migration of $CD133^+$ Cells

Fresh and derived $CD133^+$ cells were cultured with $CD133^-$ cells or their supernatant to improve their migratory potential (Figure 2-3, *B* and see Figure 2-E2, *G*-*I*). When combined with $CD133^-$ cells, the number of migrating cells for both fresh (26.87±1.52) and derived (19.67±1.84) $CD133^+$ populations significantly increased when compared to the cells plated alone (5.69±0.31 and 3.66±0.24, respectively; $P< .05$). Similarly, the addition of the supernatant of $CD133^-$ cells also increased the number of migrating fresh $CD133^+$ cells (29.63±2.56). For the derived $CD133^+$ cells, when combined with the supernatant of $CD133^-$ cells, the number of migrating cells (30.33±1.93) was significantly increased compared to derived $CD133^+$ cells combined with the $CD133^-$ cells themselves ($P< .05$).

At the time of isolation, 59.89±6.41% of fresh $CD133^+$ cells expressed VEGFR-2 and after 24 hours of culture alone, expression decreased significantly to 48.72±8.37% ($P= .04$). When the fresh $CD133^+$ cells were cultured with $CD133^-$ cells, VEGFR-2 expression increased significantly to 74.92±4.36% ($P= .04$). However, for derived $CD133^+$ cells, VEGFR-2 expression before culture was 95.88±1.32% and did not significantly change whether cells were cultured alone (98.18±0.74%) or with $CD133^-$ cells (98.20±0.96%; see Figure 2-E3, *A*).

Cytokines and Growth Factors Released by $CD133^-$ Cells

The supernatant of cultured $CD133^-$ cells was shown to have elevated levels of different cytokines and growth factors (see Figure 2-E3, *B*). These included (fold increase vs control given in parentheses) growth-related oncogene (GRO;4.7); interleukin (IL) 1β (2.6); IL-6 (38.0); IL-8 (23.1); IL-10 (8.9); monocyte chemoattractant protein (MCP) -1

(12.4); macrophage inflammatory protein (MIP) 1β (3.5); regulated upon activation, normal T-cell expressed and secreted (RANTES; 3.1); and neutrophil-activating protein (NAP) 2 (3.0). The release of GRO, IL-6, IL-8, IL-10 and MCP-1 by $CD133^-$ cells was also significantly greater than their release from cultured fresh and derived $CD133^+$ PB progenitors after 24 hours (Figure 2-3, *C*).

Comparison of Vasculogenic Potential of Progenitor Populations

In vitro vasculogenesis assays on all 6 cell populations (Figure 2-4, *A*-*H*) revealed that derived $CD133^+$ cells (0.31±0.02 mm^2) and pooled-derived $CD133^+$ cells (0.32±0.04 mm^2) significantly enhanced the complete area of tubules formed compared with control cells ($P < .03$) while MSCs (0.002±0.00 mm^2) significantly decreased capillary formation ($P = .01$; Figure 2-4, *I*). Total tube length was also calculated for each cell type revealing that derived $CD133^+$ cells (9.37±1.15 mm), pooled-derived $CD133^+$ cells (9.89±0.91mm) and fresh $CD133^+$ PB cells (9.04±0.79 mm) had significantly enhanced capillary tube length compared to control ($P < .01$; Figure 2-4, *J*). The presence of MSCs from the BM (0.19±0.06 mm) created an environment that significantly inhibited the ability of HUVECs to form extended capillaries ($P < .001$). The derived $CD133^+$ cells (22.84±3.26%) and the pooled-derived $CD133^+$ cells (18.90±2.53%) had significantly greater physical contribution to the total area of capillaries compared to the other groups ($P < .001$; Figure 2-4, *K*).

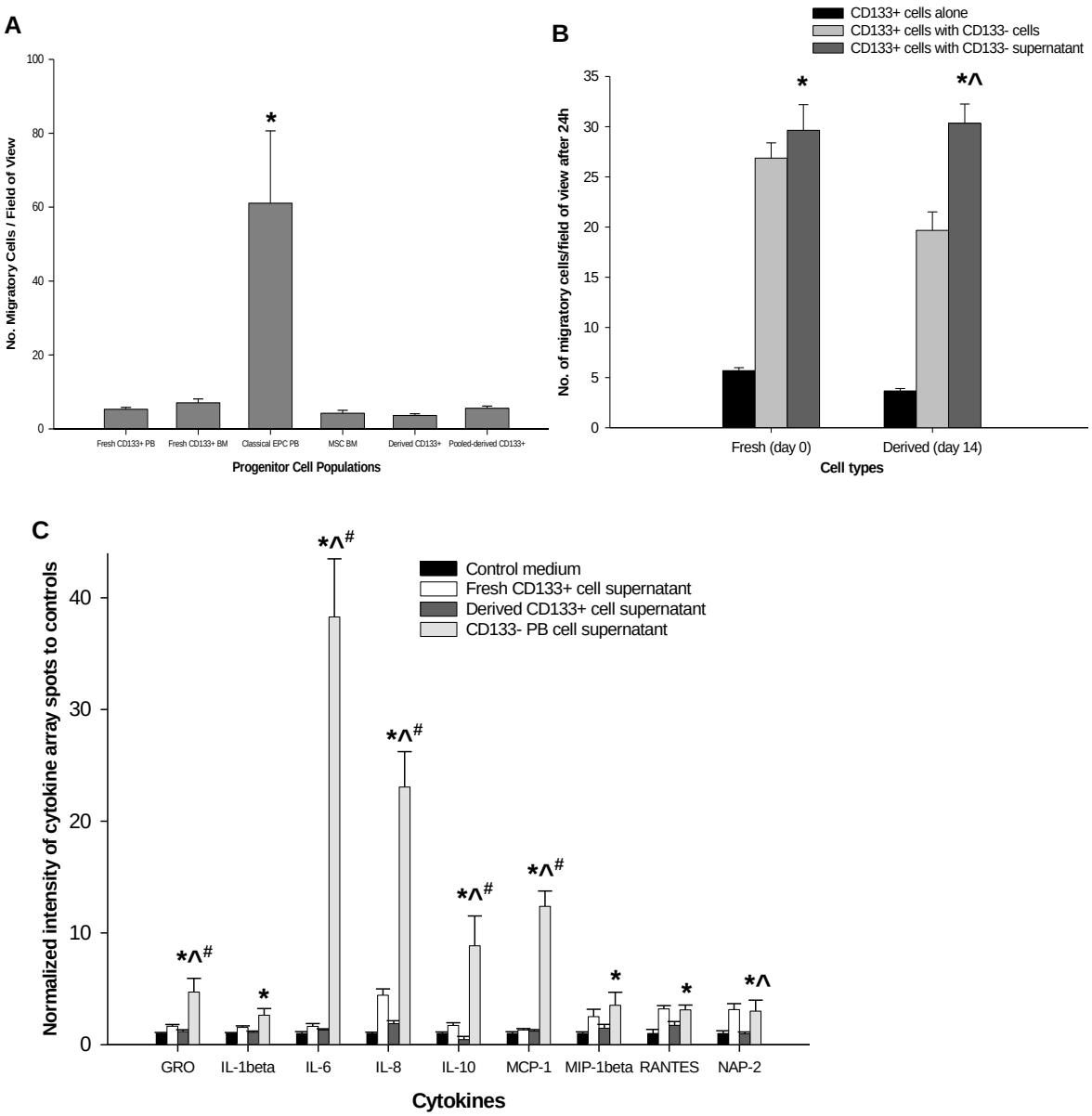

Figure 2-3: Cell migration.

A, The average number per field of view of migrating cells for the 6 progenitor populations. **P*< .001 versus all other cell populations. *PB*, Peripheral blood; *BM*, bone marrow; *EPC*, endothelial progenitor cell; *MSC*, mesenchymal stem cell. B, The number per high powered fields of migrating $CD133^+$ cells (fresh or derived) with $CD133^-$ cells or its supernatant after 24 hours of culture. **P*≤ .005 versus $CD133^+$ alone; ^*P*< .05 versus incubation with $CD133^-$ cells. C, Relative expression of selected cytokines and growth factors (normalized to controls for each cytokine). **P*<.005 versus control media; ^*P*<.05 versus supernatant of fresh $CD133^+$ peripheral blood cells; $^{\#}P$<.05 vs. supernatant of derived $CD133^+$ peripheral blood cells. GRO, Growth-related oncogene; IL, interleukin; MCP-1, monocyte chemoattractant protein 1; MIP-1 beta, macrophage inflammatory protein 1β; RANTES, regulated upon activation normal T cell expressed and secreted; NAP-2, neutrophil-activating protein 2.

A

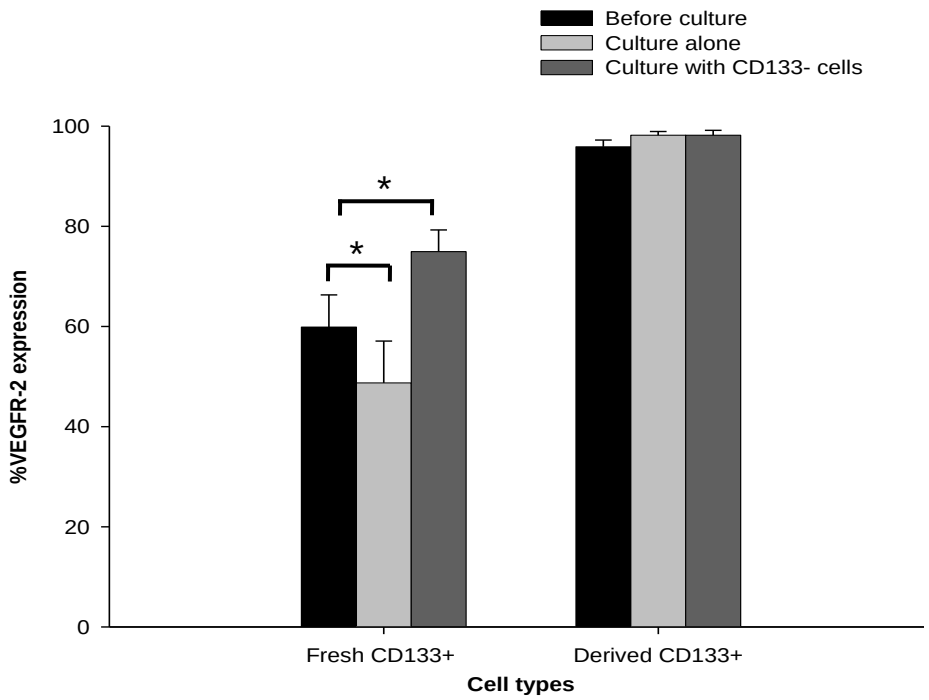

B

	A	B	C	D	E	F	G	H	I	J	K
1	Pos	Pos	Pos	Pos	Neg	Neg	ENA-78	GCSF	GM-CSF	GRO	GRO-α
2	I-309	IL-1α	IL-1 β	IL-2	IL-3	IL-4	IL-5	IL-6	IL-7	IL-8	IL-10
3	IL-12 p40p70	IL-13	IL-15	IFN- γ	MCP-1	MCP-2	MCP-3	MCSF	MDC	MIG	MIP-1β
4	MIP-1δ	RANTES	SCF	SDF-1	TARC	TGF-β1	TNF-α	TNF-β	EGF	IGF-I	Angiogenin
5	Oncostatin M	Thrombopoietin	VEGF	PDGF-BB	Leptin	BDNF	BLC	Ck β 8-1	Eotaxin	Eotaxin-2	Eotaxin-3
6	FGF-4	FGF-6	FGF-7	FGF-9	Flt-3 Ligand	Fractalkine	GCP-2	GDNF	HGF	IGFBP-1	IGFBP-2
7	IGFBP-3	IGFBP-4	IL-16	IP-10	LIF	LIGHT	MCP-4	MIF	MIP-3 α	NAP-2	NT-3
8	NT-4	Osteoprotegerin	PARC	PIGF	TGF- β 2	TGF- β 3	TIMP-1	TIMP-2	Neg	Pos	Pos

C

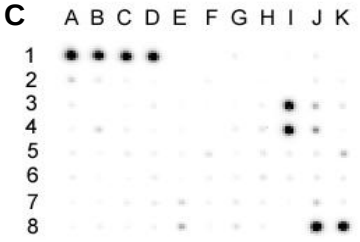

D

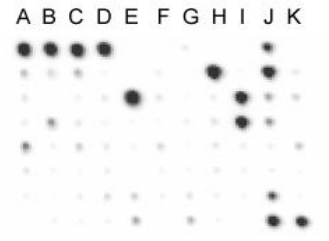

E

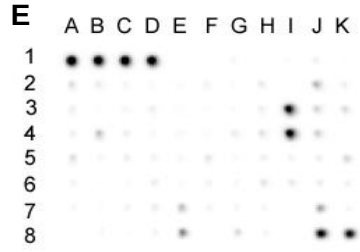

F

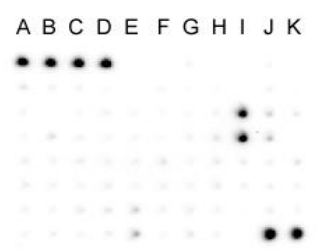

Figure 2-E3: Mechanisms involved in the migration improvement by cell interactions.

A, Expression of VEGFR-2 on fresh or derived $CD133^+$ cells cultured with or without $CD133^-$ cells for 24h. **P*<.05. B-F, Representative cytokine/growth factor array images of cytokine/growth factor map of array membrane (B); culture medium only (C); $CD133^-$ peripheral blood (PB) cell supernatant after 24 hours of incubation (D); fresh $CD133^+$ PB cell supernatant after 24 hours of incubation (E); and derived $CD133^+$ PB cell supernatant (F) after 24 hours of incubation are shown. *Pos*, Positive; *Neg*, negative; *ENA-78*, epithelial cell-derived neutrophil-activating protein-78; *GCSF*, granulocyte colony-stimulating factor; *GM-CSF*, granulocyte-macrophage colony-stimulating factor; *GRO*, growth-related oncogene; *I-309*, a small glycoprotein secreted by activated T-cells; *IL*, interleukin; *IFN*, interferon; *MCP*, monocyte chemoattractant protein; *MCSF*, macrophage colony- stimulating factor; *MDC*, macrophage-derived chemokine; *MIG*, monokine induced by gamma interferon; *MIP*, macrophage inflammatory protein; *RANTES*, regulated upon activation normal T-cell expressed and secreted; *SCF*, stem cell factor; *SDF*, stromal cell-derived factor; *TARC*, thymus and activation-regulated chemokine; *TGF*, transforming growth factor; *TNF*, tumor necrosis factor; *EGF*, epidermal growth factor; *IGF*, insulin-like growth factor; *VEGF*, vascular endothelial growth factor; *PDGF*, platelet-derived growth factor; *BDNF*, brain-derived neurotrophic factor; *BLC*, B-lymphocyte chemoattractant; *FGF*, fibroblast growth factor; *GCP*, granulocyte chemotactic protein; *GDNF*, glial cell line–derived neurotrophic factor; *HGF*, hepatocyte growth factor; *IGFBP*, insulin-like growth factor–binding protein; *IP-10*, interferon-inducible protein 10; *LIF*, leukemia inhibitory factor; *LIGHT*, lymphotoxin-related inducible ligand that competes for glycoprotein D binding to herpes virus entry mediator on T-cells; *MIF*, macrophage migration inhibitory factor; *NAP*, neutrophil-activating protein; *NT*, neurotrophic factor; *PARC*, pulmonary and activation-regulated chemokine; *PIGF*, placental growth factor; *TIMP*, tissue inhibitor of metalloproteinases.

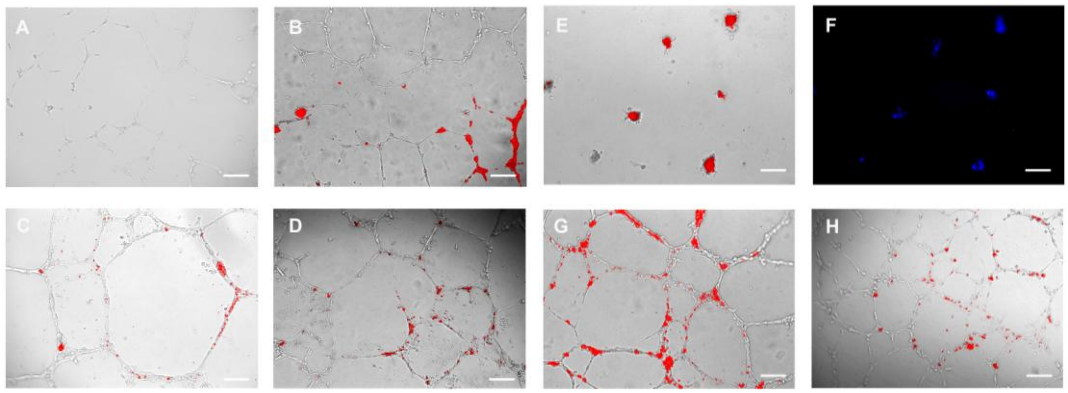
A
B
E
F
C
D
G
H

I

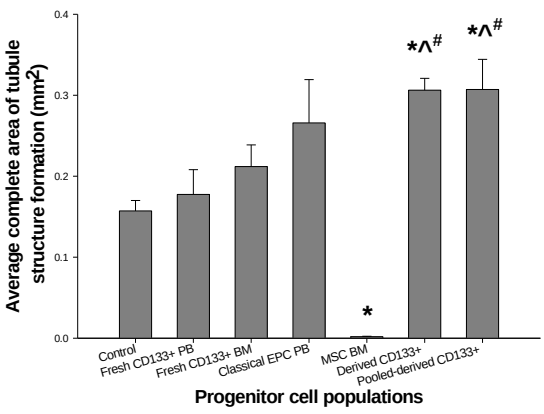
Average complete area of tubule structure formation (mm2)
0.0
0.1
0.2
0.3
0.4
*^#
*^#
*
Control
Fresh CD133+ PB
Fresh CD133+ BM
Classical EPC PB
MSC BM
Derived CD133+
Pooled-derived CD133+
Progenitor cell populations

J

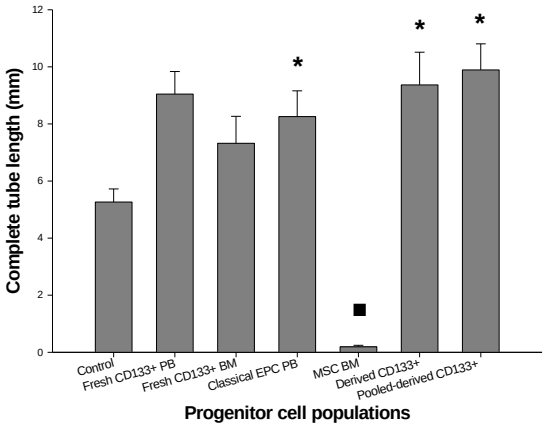
Complete tube length (mm)
0
2
4
6
8
10
12
*
*
*
■
Control
Fresh CD133+ PB
Fresh CD133+ BM
Classical EPC PB
MSC BM
Derived CD133+
Pooled-derived CD133+
Progenitor cell populations

K

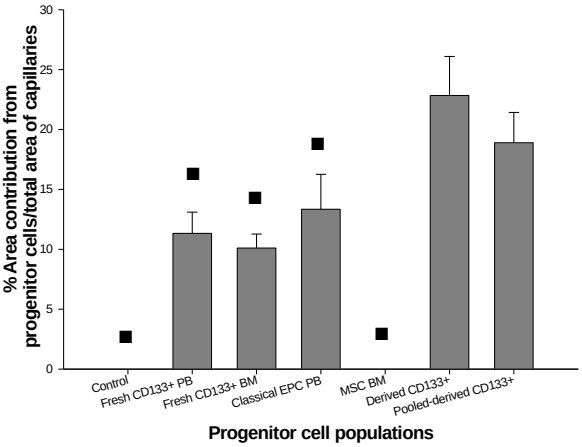
% Area contribution from progenitor cells/total area of capillaries
0
5
10
15
20
25
30
■
■
■
■
Control
Fresh CD133+ PB
Fresh CD133+ BM
Classical EPC PB
MSC BM
Derived CD133+
Pooled-derived CD133+
Progenitor cell populations

Figure 2-4: Cell vasulogenesis.

A-H, Representative images of the contribution of progenitor cells (red) to the formation of capillary structures with HUVECs: (A) HUVEC alone (control); (B) fresh $CD133^+$ PB cells; (C) fresh $CD133^+$ BM cells; (D) PB "classical" endothelial progenitor cells (EPCs); (E) BM MSCs; (F) BM MSCs with DAPI-stained HUVECs; (G) derived $CD133^+$ PB cells; and (H) pooled-derived $CD133^+$ PB cells. Scale bar = 150 μm. (I) Average complete area of tubule structure formation with different progenitor cell populations. Derived and pooled-derived $CD133^+$ PB cells had significantly greater capillary formation compared to fresh $CD133^+$ from PB ($^*P \leq .007$), MSC from BM ($^\wedge P < .001$) and control ($^{\#}P < .05$). (J) Derived and pooled-derived $CD133^+$ progenitors and fresh $CD133^+$ PB cells had significantly greater complete tube length formation compared to control. $^*P < .01$ versus control; $^\blacksquare P < .001$ versus all cell populations. (K) Derived $CD133^+$ progenitors had the greatest physical contribution compared to all groups except the pooled-derived $CD133^+$ cells. $^\blacksquare P < .001$ versus derived and pooled-derived $CD133^+$ PB cells.

Discussion

Preclinical and early clinical trials have suggested that transplantation of progenitor cells have the potential to improve the function of an ischemic and/or infarcted myocardial territory (Assmus et al. 2002; Stamm et al. 2003; Bartunek et al. 2005; Hofmann et al. 2005; Stamm et al. 2007; Suuronen et al. 2007; Zhang et al. 2008). However, it still remains unknown which cell source or cell type is optimal for vascular regeneration and myocardial functional restoration. It will be crucial to elucidate the basic biology and characterization of specific populations, and compare them with respect to their functional properties to optimize significant clinical benefits. In this regard, the current study demonstrated the successful expansion of human $CD133^+$ PB progenitors, which appear to be of superior vasculogenic potential for myocardial cell therapies based on *in vitro* comparison studies.

Previous studies showed that autologous $CD133^+$ cells enhanced myocardial perfusion and global function (Bartunek et al. 2005; Suuronen et al. 2006; Stamm et al. 2007). However, the frequency of $CD133^+$ progenitors in the blood and BM is low, and their mechanism and function in therapeutic vasculogenesis or cell therapy remain unclear. In this study, we examined $CD133^+$ cells to better characterize these progenitors and also expanded their number for increased relevance for cell-based therapy. A nearly 11-fold expansion of pooled-derived $CD133^+$ PB cells was achieved by serial removal of the non-adherent $CD133^+$ cells every 2 days over a period of 8 days, generated from culture of the $CD133^-$ fraction of PB-MNCs. These cells also expressed CD34 and VEGFR-2 (56.2 to 69.4%), suggesting that serial expansion generated progenitor cells similar to circulating $CD133^+CD34^+VEGFR\text{-}2^+$ EPCs (Peichev et al. 2000). To a lesser

extent (3-fold expansion), $CD133^+CD34^+VEGFR\text{-}2^+$ cells were also derived from the culture of $CD133^-$ cells after a 2-week period. Our data indicate that the reduced cell expansion observed with this protocol likely resulted from the inhibitory effects of other $CD133^+$ cells in the culture. Specifically, $CD133^+$ cell generation was significantly inhibited by the presence of whole PB-MNC supernatant or $CD133^+$ cells, suggesting that the removal of $CD133^+$ cells creates an environment conducive to $CD133^+$ cell generation. Conversely, direct contact with $CD133^+$ cells and/or the release of cytokines/soluble factors from these cells may inhibit $CD133^+$ generation by paracrine mechanisms.

Direct comparison of the derived $CD133^+$ cells with several commonly used progenitors showed that the "classical" EPC population had the greatest migratory potential response to VEGF. "Classical" EPCs consist of a heterogeneous mix of cells including those of monocytic, hematopoietic and endothelial lineage; and their greater migratory potential may be related to interactions between cell populations (Shantsila et al. 2007). Notably, it was observed that migration was enhanced for both fresh and derived $CD133^+$ PB progenitors when combined with $CD133^-$ cells or their supernatant. VEGFR-2 expression on these cells was also investigated to try to explain this improved migration because VEGF was the chemotactic agent used. For fresh $CD133^+$ cells, VEGFR-2 expression was increased significantly when incubated with $CD133^-$ cells. However, for derived $CD133^+$ cells, the expression of VEGFR-2 (already at approximately 96%) was not significantly changed after co-culture with $CD133^-$ cells. This can partly explain the greater improvement in migration for fresh $CD133^+$ PB cells compared to that of derived $CD133^+$ PB cells. Therefore, one important mechanism by

which interaction with $CD133^-$ cells may improve migration of the $CD133^+$ progenitor cells is increased VEGFR-2 expression.

Since $CD133^+$ cell migration was significantly increased by co-culture with the $CD133^-$ cell supernatant, it is likely that paracrine effects through the secretion of cytokines and chemokines are involved in regulating cell function. The $CD133^-$ supernatant expressed elevated levels of GRO, IL-1β, IL-6, IL-8, IL-10, MCP-1, MIP-1β, RANTES, and NAP-2 compared to control media. Therefore, provision of cytokines and growth factors from other circulating cell populations may be involved in regulating the migratory capacity of $CD133^+$ progenitor cells. In addition, recent evidence suggests that neovascularization/vasculogenesis of the dysfunctional myocardium from paracrine and humoral factors, as well as secondary recruitment of host cells are the likely mechanisms leading to functional improvement in CAD patients (Ruel et al. 2002; Yoon et al. 2005).

This study also revealed that derived $CD133^+$ cells are functionally more potent than several other select progenitor cells with respect to their vasculogenic potential *in vitro*. Overall, the derived $CD133^+$ cells demonstrated significantly greater contribution to form capillary-like structures *in vitro* (incorporation, total capillary area, and length). The capacity of freshly isolated $CD133^+CD34^+VEGFR\text{-}2^+$ cells to yield endothelial cells has recently been questioned (Case et al. 2007). However, the greater direct incorporation of derived $CD133^+$ progenitor cells into capillary-like structures observed in this study suggests that these cells may have improved endothelial differentiation. It is possible that intercellular interaction between different cell types is required for optimal function of the $CD133^+CD34^+VEGFR\text{-}2^+$ population, a consideration not explored in the previous study. Alternatively, greater paracrine effects of derived $CD133^+$ cells on the HUVECs is

suggested by the greater total capillary area and length seen with the addition of derived $CD133^+$ cells compared with the other progenitor populations.

Interestingly, the 2 cell populations from the BM differed in their *in vitro* vasculogenic potential: the fresh $CD133^+$ fraction contributed to capillary-like formation, whereas the cultured MSCs did not. Although these are *in vitro* results, this is consistent with recent evidence demonstrating that different cell populations from the BM differ in their vasculogenic potential (Copland et al. 2008). Also, it has been demonstrated that without prior environmental conditioning or differentiation into endothelial cells, the ability of MSCs to contribute to capillary-like structures in Matrigel is compromised (Annabi et al. 2003). It was shown that the ability of the BM population to contribute in vasculogenesis was associated with the positive expression of endothelial cell surface markers CD34, VEGFR-2 and/or CD31 (Annabi et al. 2003).

However, the limitations of this study need to be acknowledged. First, all functional evaluations and comparisons were performed in *in vitro* assays. Nevertheless, previous studies have reported that similar results were obtained in *in vitro* migration and vasculogenesis assays versus *in vivo* studies (Heeschen et al. 2004; Matsuura et al. 2009).

Second, in this study, only VEGF-induced migration capability was assessed. Several chemokines and growth factors have been shown to be responsible for stem cell homing and migration to the myocardium, such as VEGF, stromal cell-derived factor 1, MCP-3, hepatocyte growth factor, fibroblast growth factor 2, and insulin-like growth factor 1. These different factors recruit and regulate different stem cell populations. VEGF is a potent and highly specific mitogen for EPCs, and previous data indicates that

VEGF overexpression improves EPC migratory, adhesive, and proliferative capabilities both *in vitro* and *in vivo* (Iwaguro et al. 2002).

To our knowledge, this is the first study to directly compare the functional properties of five commonly used progenitor cell populations in simple *in vitro* experiments, in an effort to elucidate the vasculogenic potential of these cells. Derived $CD133^+$ cells appear to be a superior source of vasculogenic cells for transplantation based on this study. Also, interactions (cytokine/paracrine mechanism) between cell populations *in vitro* were observed to improve the migratory function of $CD133^+$ progenitor cells, which may have implications for clinical applications as well. Therefore, derived $CD133^+$ PB cells merit further investigation as potentially more effective and potent endothelial progenitors for cardiac cell-based therapy. Interactions between cell populations also require further attention in order to improve current cell-based vasculogenic therapies. An optimal cell population for cell-based vasculogenic treatment may exist: (1) that is likely a combination of different subtypes that can augment/participate in vasculogenesis; and/or (2) that requires interaction with the host cells for maximal therapeutic effect.

In conclusion, despite heightened expectations, the benefits of cell-based cardiac therapy have not yet been established in patients. The field must remain willing to return to the laboratory in order to improve our mechanistic understanding and refine our therapeutic approaches. The present study, albeit *in vitro*, attempted to perform this by comparing different cell populations for the first time, by investigating cell-cell and cell-soluble factor interactions, and by testing a method to expand a rare progenitor identified as being more vasculogenically potent than other commonly used cell populations.

Supplemental Materials and Methods

Isolation of $CD133^+$ Cells From PB

Total PB-MNCs were freshly isolated from the blood of human donors by using Histopaque1077 (Sigma) densitygradient centrifugation of buffy coats. On the initial day of PB-MNC isolation, $CD133^+$ cells were separated from PB-MNCs by using CD133-microbeads and a magnetically activated cell sorter (autoMACS; Miltenyi Biotech, Bergisch–Gladbach, Germany), thereby providing day 0 (fresh) $CD133^+$ cells and $CD133^-$ PB cells.

Expansion of $CD133^+$ Cells From $CD133^-$ PB Fractions

$CD133^-$ fractions were plated on fibronectin-coated, 12-well culture plates (Becton Dickinson, Mississauga, Canada) at a density of 1×10^6 cells/cm2 in EBM-2 supplemented with EGM-2-MV-SingleQuots (Clonetics) containing 5% fetal bovine serum, 50 ng/mL human VEGF, 50 ng/mL human insulin-like growth factor 1, and 50 ng/mL human epidermal growth factor. Two different protocols were used to obtain derived $CD133^+$ PB cells. Cells in protocol 1 had fresh media added to the wells every 3 days without aspiration of the old media. After 14 days, both adherent and nonadherent cells were collected and separated by means of autoMACS to obtain derived $CD133^+$ PB cells. In protocol 2 the nonadherent population was removed every 2 days over a period of 8 days and separated with the autoMACS machine to collect $CD133^+$ cells. The generated $CD133^+$ cells were cryopreserved in 1-mL aliquots with 10% dimethyl sulfoxide in complete media. After 8 days, cryopreserved cells from days 0, 2, 4, 6 and 8 were thawed and combined to constitute the pooled–derived $CD133^+$ population (hereafter referred to as pooled–derived $CD133^+$ PB cells).

Isolation of EPCs

Briefly, total human PB-MNCs were cultured in supplemented EBM-2 media on fibronectin-coated tissue-culture plates (1×10^6 MNCs/cm^2) for 4 days. The adherent cells, hereafter referred to as ‘‘classical’’ EPCs, were then collected.

Isolation of $CD133^+$ Cells and MSCs From BM

Donor marrow was aspirated from the sternum with a standard marrow aspiration needle and washed in Hanks balanced salt solution (Gibco Invitrogen, Burlington, Canada) to obtain BM cells. Bone marrow was digested completely with collagenase type I (250 U/mL, Gibco Invitrogen), and the cell suspension was filtered with a 70-mm nylon cell strainer (Becton Dickinson). Isolated BM-MNCs were separated from the $CD133^-$ fraction by means of autoMACS to obtain day 0 (fresh) $CD133^+$ BM cells. The filtered cell suspension was washed and plated at 1.3×10^6 cells/cm^2 in Dulbecco’s modified Eagle’s medium supplemented with 10% fetal bovine serum (Gibco Invitrogen), 2 mmol/L L-glutamine (Sigma), and 100 U/mL penicillin/streptomycin (Gibco Invitrogen) to obtain *ex vivo* expanded MSCs. After 4 days, the nonadherent cells were removed. The media was replaced every 3 days for 2 weeks or until the adherent MSC population was 80% to 90% confluent. The phenotype of the MSC population was characteristically $CD29^+CD44^+CD45^-$ (data not shown).

CHAPTER 3: MANUSCRIPT #2

Introduction to Manuscript #2

In addition to insufficient numbers of therapeutic cells, stem cell therapy is also hindered by a low rate of cell engraftment and persistence in the target tissue. With the advances in biotechnology, tissue engineered biomaterials provide the possibility to improve transplanted cell retention, survival, and function. Previous work indicated that a collagen-based matrix can support multiple tissues and cell types, thus might constitute suitable delivery vehicles for cell transplantation (Li et al. 2003; Suuronen et al. 2006). My group and others have reported that collagen-based delivery matrices improve the functional results of cell therapy (Kutschka et al. 2006; Suuronen et al. 2006). However, further understanding their mechanisms and local effects is limited to the histological examination. In this study, to investigate the effects of a collagen-based delivery matrix on transplanted human CPCs, PET imaging with ^{18}F-FDG cell labeling was used for assessing the ability of a collagen-matrix to improve the early retention of transplanted CPCs in a rat ischemic hindlimb model.

Circulation Cardiovascular Imaging 2008; 1: 197-204

Collagen-based Matrices Improve the Delivery of Transplanted Circulating Progenitor Cells: Development and Demonstration by *ex vivo* Radionuclide Cell Labeling and *in vivo* Tracking with Positron Emission Tomography

Yan Zhang, MD, MSc; Stephanie Thorn, MSc; Jean N. DaSilva, PhD; Marc Lamoureux, BSc; Robert A. deKemp, PhD; Robert S. Beanlands, MD; Marc Ruel, MD, MPH; and Erik J. Suuronen, PhD

From the Division of Cardiac Surgery (Y.Z., M.R., E.J.S.); Cardiac PET Centre, Division of Cardiology (Y.Z., S.T., J.N.D., M.L., R.A.D., R.S.B.); the Department of Cellular and Molecular Medicine (Y.Z., S.T., J.N.D., R.S.B., M.R., E.J.S.); and the Molecular Function and Imaging Program (all authors), University of Ottawa, Ottawa, Canada

Correspondence to Erik J. Suuronen or Marc Ruel, Division of Cardiac Surgery, University of Ottawa Heart Institute.

© 2008 American Heart Association, Inc.

DOI: 10.1161/CIRCIMAGING.108.781120

Contributions of Authors

Experiments described in this manuscript were designed and executed by myself, with practical help from Ph.D. candidate Stephanie Thorn. Radiochemist Dr. Jean DaSilva provided the radioisotope for cell labeling. Physicists Dr. Robert deKemp and M.Sc. candidate Marc Lamoureux provided input on the experiments needed for estimating in vivo parameters for use in PET imaging. Dr. Rob Beanlands provided a clinical perspective on the data. Work performed was supervised by Drs. Marc Ruel and Erik Suuronen.

Abstract

Background: Collagen delivery matrices have been reported to improve the results of cell therapy, but knowledge of their mechanisms of action is limited. To evaluate whether a collagen delivery matrix improves engraftment posttransplantation, 2-[^{18}F]fluoro-2-deoxy-D-glucose (^{18}F-FDG) was used to label transplanted circulating progenitor cells (CPCs) and track them *in vivo* with positron-emission tomography.

Methods and Results: Efficiency of ^{18}F-FDG cell labeling was CPC-concentration dependent (r=0.61, P<0.001) but not ^{18}F-FDG-dose dependent. Labeled human CPCs (2×10^6) were injected with or without a collagen-based matrix in the ischemic hindlimb of rats (n=12 per group) 2 weeks after femoral artery ligation. Imaging of labeled cells, acquired by small animal positron-emission tomography at 150 minutes postinjection, revealed greater CPC retention in the ischemic hindlimb and less nonspecific leakage to other tissues (retention ratio, 0.44±0.08) when CPCs were delivered within the collagen matrix, compared with cells injected alone (0.22±0.13, P=0.040) and with ^{18}F-FDG injected with or without the matrix (0.10±0.05 and 0.11±0.05, respectively; p<0.005). Tissue radionuclide biodistribution was performed after completion of positron-emission tomography imaging. When ^{18}F-FDG-labeled cells were injected with the collagen matrix, accumulation was significantly increased (by 69.6%; P=0.021) in the target ischemic hindlimb muscle, and significantly reduced (by 14.8 to 31.4%; P<0.05) in non-specific tissues, compared with cells injected alone. Histology confirmed the increased retention in target tissue associated with the matrix.

Conclusions: Early posttransplantation, a collagen matrix enhances progenitor cell retention and limits distribution to non-specific tissues, as measured by the use of ^{18}F-

FDG labeled cells and positron-emission tomography imaging and confirmed by biodistribution and histology.

Key Words: stem cells; tissue engineering; transplantation; ischemia; imaging

Introduction

Growing evidence from experimental studies (Kocher et al. 2001; Orlic et al. 2001) and clinical trials (Wollert et al. 2004; Assmus et al. 2006; Abdel-Latif et al. 2007; Patel et al. 2007) suggest that cell therapy can restore perfusion and improve function in ischemic and/or infarcted myocardium. Circulating progenitor cells (CPCs) have been shown to contribute to neovascularization in ischemic tissues, where they may differentiate into endothelial cells *in situ* and result in "vasculogenesis" (Kawamoto et al. 2003; Ruel et al. 2004; Numaguchi et al. 2006). CPCs can be obtained by non-invasive means, thus providing the potential for autologous clinical use.

However, stem/progenitor cell therapy is hindered by a low rate of engraftment and low persistence of cells in the target tissue. Depending on the method of delivery and the cell fraction used, transplanted cells can quickly fade from the target tissue in a matter of hours to a few days (Cho et al. 2007; Doyle et al. 2007). Therefore, insufficient cell numbers and inadequate cellular interactions may not allow for an optimal therapeutic effect. Furthermore, delivery of cells to other non-specific body sites constitutes an unwanted potential side effect. Considering the rapid loss of the delivered cells and the modest benefits of cardiac cell therapy using bone-marrow derived cells observed in clinical studies (Abdel-Latif et al. 2007; Patel et al. 2007), it is likely that improvements in stem/progenitor cell delivery, engraftment and survival will be needed for more effective restoration of myocardial function.

Previous work, including our own, has shown that tissue engineered collagen-based matrices can support multiple tissues and cell types (Suuronen et al. 2004; Suuronen et al. 2006), and constitute suitable cell delivery vehicles (Kofidis et al. 2005;

Suuronen et al. 2006; Suuronen et al. 2006). It has been hypothesized that the collagen, which mimics the extracellular matrix, may provide local physical retention and a good platform for cell seeding during direct cell transplantation (Suuronen et al. 2006). However, the evaluation of the ability of matrices to improve cell viability and engraftment has so far been limited primarily to histological assessment of tissue at a single time point. This study was therefore designed to use *in vivo* imaging to examine one mechanism by which a collagen matrix may enhance the short-term effects of CPC transplantation through improved early retention of transplanted cells.

To this end, we employed small animal positron emission tomography (PET), which is an advanced nuclear imaging technology with high sensitivity and high spatial resolution. PET not only provides the potential for determining the nature of transplanted cells and of their progeny *in vivo*, but also offers serial monitoring capabilities that add to the clinical relevance of this modality. PET imaging with 2-[^{18}F]fluoro-2-deoxy-D-glucose (^{18}F-FDG) cell labeling has been used to track a few types of cells, such as monocytes, bone marrow-derived cells, hematopoietic stem cells, in animal (Qian et al. 2007) and human studies (Hofmann et al. 2005; Kang et al. 2006). However, use of ^{18}F-FDG to label CPCs for the assessment of delivery matrix effects on transplanted cells has not been reported.

In the present study, we evaluated the feasibility of using ^{18}F-FDG to label CPCs for tracking by small animal PET, and examined the effect of collagen-based matrices on the early retention of transplanted CPCs and their distribution to non-specific tissues in a rat model of hindlimb ischemia.

Methods

Cell Isolation and Culture

Human CPC procurement procedures were approved by the Human Research Ethics Board of the University of Ottawa Heart Institute. Total peripheral blood mononuclear cells were freshly isolated (with informed consent) from the blood of volunteer, healthy human donors by Histopaque 1077 (Sigma-Aldrich, Oakville, Canada) density-gradient centrifugation of buffy coats, as described previously (Ruel et al. 2005). Briefly, cells were cultured on fibronectin-coated plates in endothelial basal medium (EBM-2; Clonetics, Guelph, Canada) supplemented with EGM-2-MV-SingleQuots (Clonetics) (Ruel et al. 2005). After 4 days, the adherent population (CPCs) was collected.

Collagen Matrix Preparation

Similar to methods described previously (Suuronen et al. 2006), collagen-based matrices (pH 7.5) were prepared on ice. Briefly, matrices consisted of a mixture of blended neutralized type I rat tail tendon collagen (0.4%, wt/vol; Becton Dickinson, Mississauga, Canada) and chondroitin 6-sulfate (1:6, wt/wt; Sigma), cross-linked with 0.02% (vol/vol) glutaraldehyde and followed by glycine termination of unreacted aldehyde groups. This formulation allowed the matrix to thermogel at 37°C, following injection into animal tissue.

^{18}F-FDG Cell Labeling

CPCs were incubated with ^{18}F-FDG at 37°C for 30 minutes in a 15-mL centrifuge tube (Fisher Scientific, Ottawa, Canada), under sterile conditions. Various dose ranges of ^{18}F-FDG (0.5 to 4.0 mCi [18.5 to 148 MBq], 4.1 to 6.0 mCi [151.7 to 222 MBq] and 6.1 to

8.0 mCi [225.7-296 MBq]) and different concentrations of CPCs (2×10^6 cells, in 1, 3 or 5mL of media) were tested, in order to optimize the efficiency of the labeling procedure. In select experiments, insulin (0.1 U/mL) and heparin (10 U/mL) were added to the incubation in an attempt to improve labeling efficiency. At the end of incubation, cells were washed in PBS to remove unbound radioactivity. The radioactivity was measured both in cells and in the supernatant, by using a dose-calibrator (Capintec, Ramsey, NJ). With correction for radiolabel decay, cell-labeling efficiency was calculated as the activity in cells over the total activity used in the incubation.

Stability and Viability of Labeled Cells

To assess the stability of the labeling procedure, labeled cells were rinsed and centrifuged, and the cell pellet was resuspended in 2 mL PBS and incubated at 37°C for 2 hours. The retention of ^{18}F-FDG within CPCs was calculated as above. To determine the effects of labeling on cell viability, labeled or non-labeled cells (1×10^6) suspended in 1.0 mL EBM were plated and incubated for an additional 0.5 hours, 24 hours or 5 days. Cell viability was assessed using the Vi-CELL analyzer (Beckman Coulter, Mississauga, Canada) with a Trypan Blue Dye Exclusion Method.

Retention of ^{18}F-FDG in Matrices

^{18}F-FDG-labeled CPCs (1×10^6) in 50 μL of PBS or ^{18}F-FDG alone (using the same radioactivity and volume as the labeled CPCs) were added to the matrix solution (450 μL) on ice. Gels were plated at 500 μL per well in 24-well flat-bottom plates (VWR, Mississauga, Canada) and incubated at 37°C for 60 minutes to allow complete gelation of the matrix. Matrix gels were transferred into 2 mL PBS and incubated at 37°C for 2

hours. After incubation, the radioactivity in matrices was counted to determine the retention of ^{18}F-FDG in matrices. Controls consisted of 1×10^6 ^{18}F-FDG-labeled cells in 500μL PBS.

Hind limb Ischemia Animal Model

Procedures were performed with the approval of the University of Ottawa Animal Care Committee, in accordance with the National Institutes of Health's Guide for the Care and Use of Laboratory Animals. The left proximal femoral artery of anaesthetized (2% isoflurane) 8- to 9-week-old Sprague Dawley rats (Charles River, Wilmington, Mass) was ligated to induce ischemia, as previously described (Takeshita et al. 1998). Survival for all treatment groups was 100%. Two weeks after ligation, anaesthetized rats randomly received one of the following treatments, administered by intramuscular injection into the ischemic thigh muscle, using a 28-gauge needle: (1) 2×10^6 ^{18}F-FDG-labeled CPCs (34.7 to 56.9 μCi) in 400 μL of matrix (n=15); (2) 2×10^6 ^{18}F-FDG-labeled CPCs (32.0 to 61.0 μCi) in 400μL PBS (n=15); (3) ^{18}F-FDG (54.9 to 130.2 μCi) in 400 μL of matrix (n=12); or (4) ^{18}F-FDG (51.9 to 148.4 μCi) in 400 μL PBS (n=12).

Small Animal PET Imaging for Localization of ^{18}F-FDG-Labeled CPCs

For some animals (n=3 to 4 per treatment group), whole body ^{18}F-FDG images (150 minutes post-injection) were acquired for 15 minutes using the Inveon small animal PET scanner (Siemens, Knoxville, Tenn). Images were reconstructed using OSEM2D, resulting in a reconstructed image resolution of ≈1.3 mm. To determine relative retention in the injected hind limb, Inveon Research Workplace (Siemens, Knoxville, Tenn) was used to draw one cuboid volume that completely encompassed the hind limb, and a

second cuboid volume that contained the whole body. After correcting for injected activity, total counts in both volumes were expressed as a retention ratio of hind limb/whole-body counts.

Biodistribution of ^{18}F-FDG Labeled CPCs

Although under anesthetic, rats were euthanized by cervical dislocation (at 180 minutes post-injection) and their tissues were dissected. Biodistribution of the specific radioactivity accumulation in different tissues was determined by a γ counter (PerkinElmer Life and Analytical Sciences, Waltham, Mass), and the tissues were weighed. Data are expressed as percentage of the injected dose per gram of wet tissue for all tissues other than the ischemic hind limb, and as percentage of the injected dose per organ for the ischemic hind limb, in order to account for differences in harvested and injected hind limb tissue locations (Thackeray et al. 2007).

Immunofluorescence Assessment

Hind limb muscles were dissected from 0.5 cm above to 0.5 cm below the marked injection site, fixed with 4% paraformaldehyde, and sectioned at 2.5 mm thickness to ensure equivalent sampling. Tissue samples were stored in 10% neutral buffered formalin, paraffin embedded, and slides were prepared using 5-μm serial sections. According to the manufacturer's protocol, transplanted human EPCs were localized by immunofluorescence staining using anti-human mitochondria antibodies (1:40; Chemicon, Temecula, Calif). The sections were mounted with mounting medium containing 4′,6-diamidino-2′-phenylindole (DAPI, Vector Laboratories, Burlingame,

Calif) to labeled cell nuclei. The percentage of transplanted cells per field of view was calculated from 4 random sections at different levels as:

$$\frac{\text{number of human mitochondria}^{+}\text{DAPI}^{+}\text{ cells}}{\text{number of DAPI}^{+}\text{ cells}} \times 100\%$$

Statistical Analysis

Data are expressed as mean ± SD. Statistical analyses between groups were performed with a one-way analysis of variance. For multiple comparison of ^{18}F-FDG PET imaging, a Bonferroni correction was applied to each test. Correlation analyses were performed by linear regression. Differences with $P<0.05$ were considered statistically significant.

Statement of Responsibility

The authors had full access to and take full responsibility for the integrity of the data. All authors have read and agree to the manuscript as written.

Results

^{18}F-FDG Cell Labeling Efficiency Depends Primarily on the Concentration of CPCs

Using 1×10^6 CPCs, there was no correlation between the retention and the amount of ^{18}F-FDG in the incubation (Table 3-1). Therefore, within the ^{18}F-FDG dose range used, CPC labeling efficiency was not ^{18}F-FDG-dose dependent ($P=0.18$, n=5/group).

A total of 2×10^6 CPCs and 2 mCi ^{18}F-FDG were incubated in three different volumes (Figure 3-1A). The highest ^{18}F-FDG retention in CPCs (7.6±4.4%, n=12) was

obtained in the most concentrated group (ie, 1 mL total incubation volume). ^{18}F-FDG accumulation decreased as incubation volumes were increased, indicating that the labeling efficiency of ^{18}F-FDG was dependent on the concentration of CPCs (r=0.61, P<0.001, n=9), with an overall labeling efficiency range of 1.5 to 12% (Figure 3-1B). Additional experiments revealed that insulin and heparin did not increase the retention of ^{18}F-FDG in CPCs (data not shown).

Table 3-1 Retention of ^{18}F-FDG in CPCs

Dose (mCi)	CPC ($\times 10^6$)	FDG accumulation in cells (%)
0.5-4.0	1.0	1.5±0.6
4.1-6.0	1.0	1.6±0.5
6.1-8.0	1.0	1.4±0.5

n=5 per group

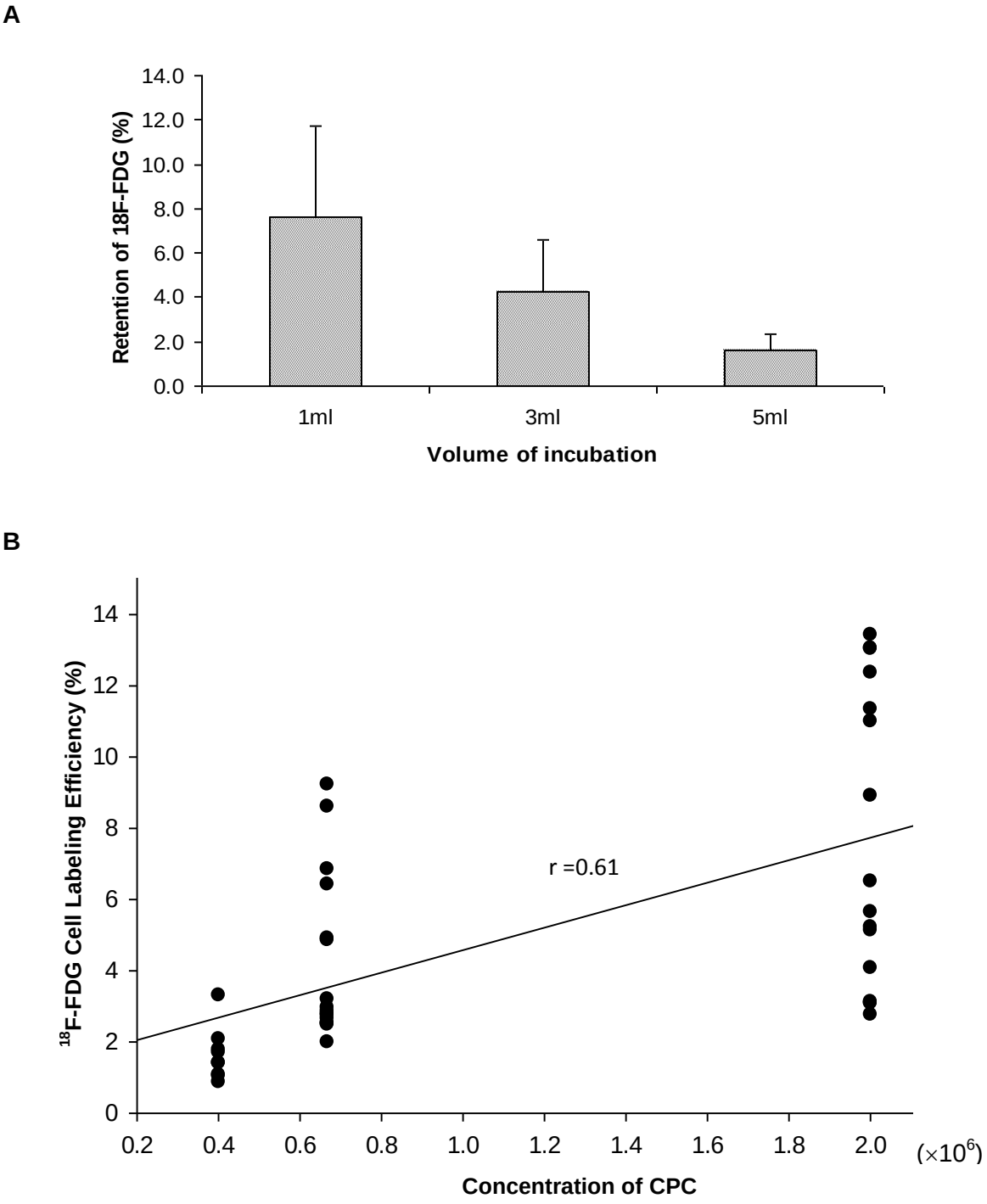

Figure 3-1: The effect of CPC concentration on cell labeling efficiency.

A, The maximum labeling efficiency (7.6±4.4%) was obtained in the group with 2×10^6 CPCs in 1mL total incubation volume (n=12 per group). B, The labeling efficiency was proportional to CPC concentration (r=0.61, P<0.001, n=9 per group).

Labeled CPCs Exhibit Good Short-term Stability and Viability

The retention of ^{18}F-FDG in CPCs was 42.1±3.1% (n=6) after a 2-hour incubation, indicating that labeled cells showed efflux of radioactivity into media.

To investigate the effect of ^{18}F-FDG labeling on cells, labeled cell viability was measured at 0.5 hour, 24 hours or 5 days after labeling. As shown in Figure 3-2, radiolabeling had no effect on CPC viability (P=0.21) up to 24 hours postlabeling. However, there was a slight reduction in viability (-15.9±6.6%) after 5 days (P<0.05).

^{18}F-FDG Radioactivity Postlabeling Indicates Persistence in Cells Rather Than Non-specific Retention in the Matrix

To evaluate whether matrices retain ^{18}F-FDG and may interfere with PET imaging of labeled CPCs, the retention of ^{18}F-FDG in matrices was measured *in vitro* under non-flow conditions. After 2-hour incubation, the retained ^{18}F-FDG radioactivity of labeled cells within the matrix was 32.3±6.9%, whereas the ^{18}F-FDG radioactivity of labeled cells alone was 26.8±3.0% (Figure 3-3), with no significant difference between the 2 groups (P= 0.11). Retained ^{18}F-FDG radioactivity in the collagen matrix alone (without cells) was only 4.1±1.0%, and significantly less than the other 2 groups (P<0.005).

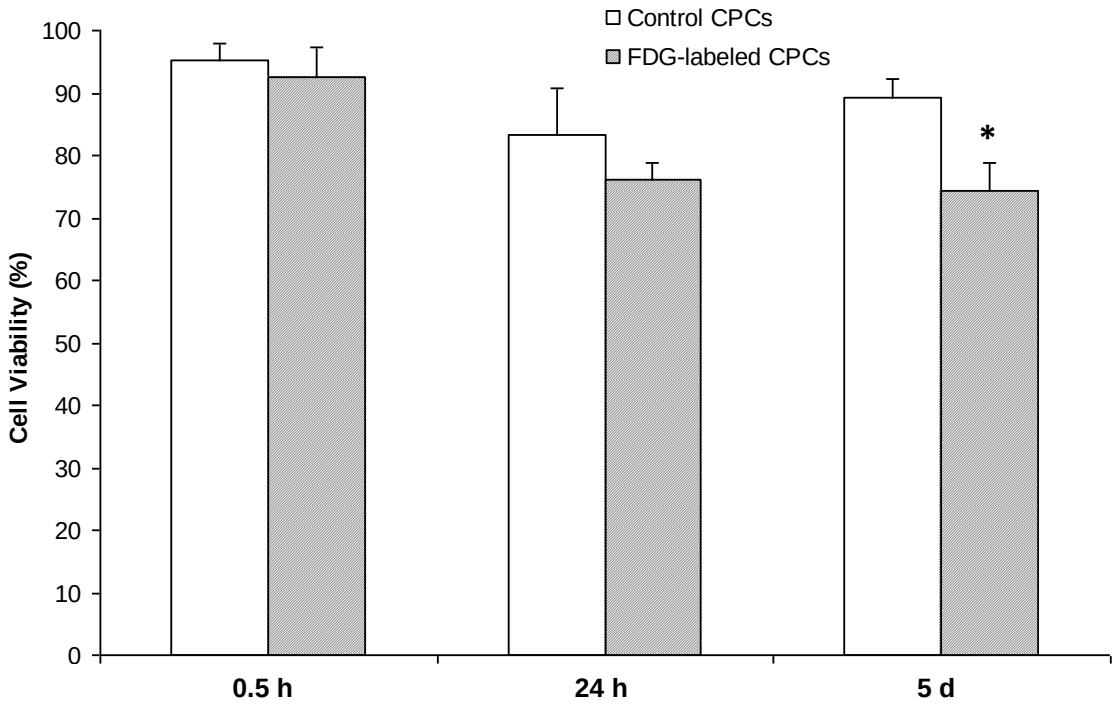

Figure 3-2: The effect of ^{18}F-FDG labeling on cell viability.

No difference was observed in the short-term (0.5 and 24 hours) viability between radiolabeled cells and unlabeled controls; however, lower cell viability was observed in labeled CPCs after 5 days post-labeling (n=6 per group). ***P*<0.05.

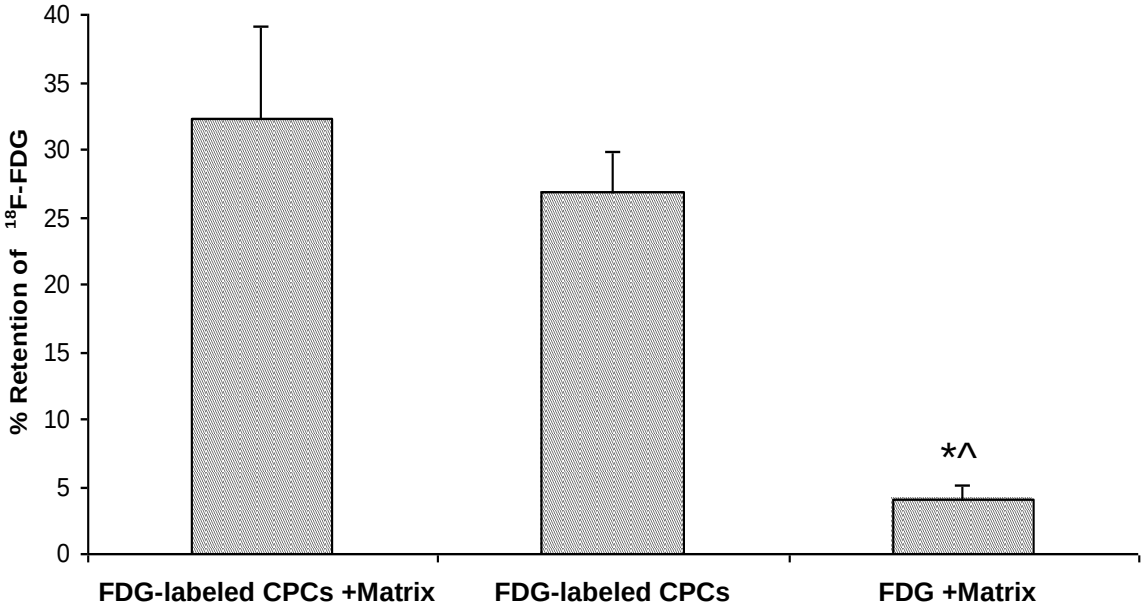

Figure 3-3: The effect of matrices on the retention of ^{18}F-FDG radioactivity.

There was no significant difference (P=0.11, n=5 per group) between the retention of ^{18}F-FDG-labeled cells in the matrix (32.3 ± 6.9%) and the retention of ^{18}F-FDG in labeled cells (26.8 ± 3.0%). However, the collagen matrix retained significantly less ^{18}F-FDG (4.1±1.0%) than the other 2 groups (n=5 per group) *****P< 0.005 versus FDG-labeled CPCs with matrices; ^P< 0.005 versus FDG-labeled CPCs.

Collagen Matrices Maintain Labeled Cells Within the Target Tissue and Minimize Delivery to Nonspecific Tissues and Organs

Determination by PET Imaging of ^{18}F-FDG Labeled Cells

Small animal PET whole-body imaging was performed in rats after treatment with ^{18}F-FDG-labeled cells with or without the matrix, in order to assess the ability of matrices to improve retention of the transplanted CPCs in the hind limb. At 150-minute postinjection (Figure 3-4), greater signal intensities in the ischemic hind limb relative to the whole body were observed when CPCs were delivered with the matrix. The retention ratio of ^{18}F-FDG radioactivity in the ischemic hind limb to whole-body ^{18}F-FDG radioactivity for hind limbs receiving CPCs in the matrix (0.44±0.08) was significantly greater than that observed for labeled CPCs in PBS (0.22±0.13; P=0.040), and to ^{18}F-FDG injected in the matrix and in PBS (0.10±0.05 and 0.11±0.05, respectively; P<0.005). PET imaging results also indicate that the accumulation of ^{18}F-FDG in heart, bladder and other nonspecific organs was lower when CPCs were delivered with matrix versus the other treatment groups (Figure 3-4).

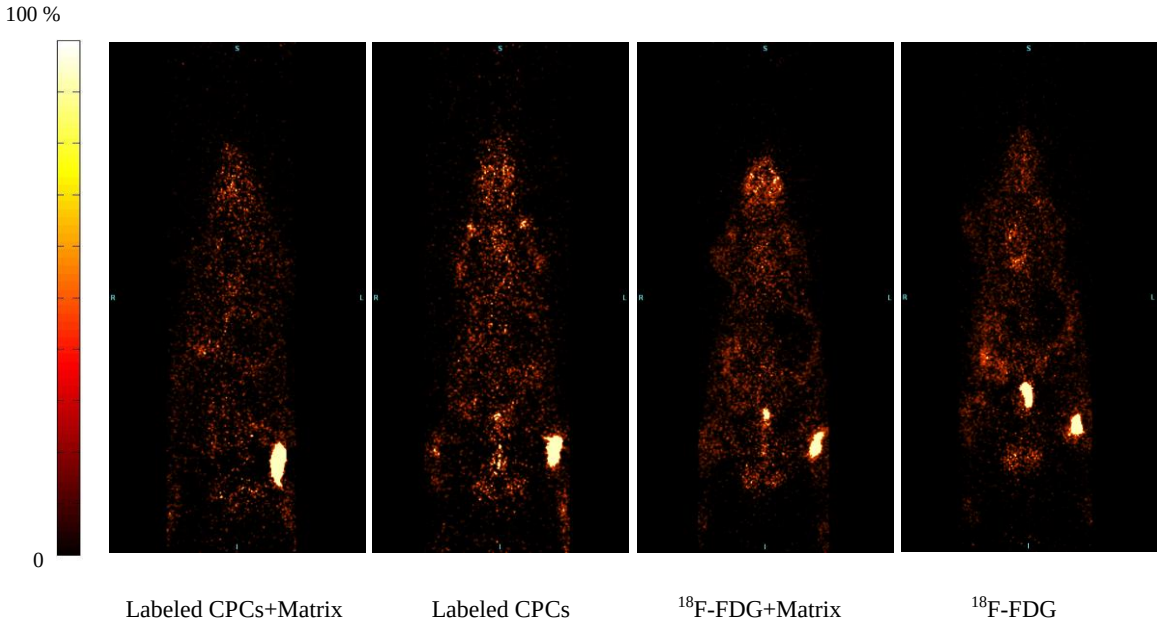

Figure 3-4: Small animal PET whole-body images at 150 minutes postinjection.

Images of transplanted ^{18}F-FDG-labeled CPCs delivered with the matrix showed significantly higher hind limb/whole-body retention ratios indicating minimized signals in the non-specific organs, and less clearance through the bladder compared to the other groups. Images are normalized based on the injected activity of ^{18}F-FDG to be visualized on a common scale.

Determination by Biodistribution of ^{18}F-FDG-Labeled Cells

For confirmation, biodistribution of the specific radioactivity accumulation in different organs was determined after completion of PET scans. As shown in Figure 3-5, with use of the matrix there was a significant increase in retention (69.6%; P=0.021) of ^{18}F-FDG-labeled CPCs within the ischemic hind limb muscle, and an overall reduction (by 14.8 to 31.4%; P<0.05) of labeled cell distribution to nontarget tissues, including the heart, lung, kidney, spleen, liver and brain.

Determination by Immunofluorescence Analysis of Transplanted Cells

The retention of transplanted human CPCs in the ischemic hind limb was also confirmed by immunofluorescence analysis, using anti-human mitochondria antibody and DAPI (Figure 3-6). The percentage of cells per field of view that were transplanted cells was greater in the ischemic hind limb of rats injected with cells + matrix (3.0±2.1%) compared with injection of cells alone (1.9±0.8%, P=0.048). The retention ratio calculated from PET images correlated with the number of transplanted cells in the hind limb as determined by immunofluorescence (r=0.845, P=0.017).

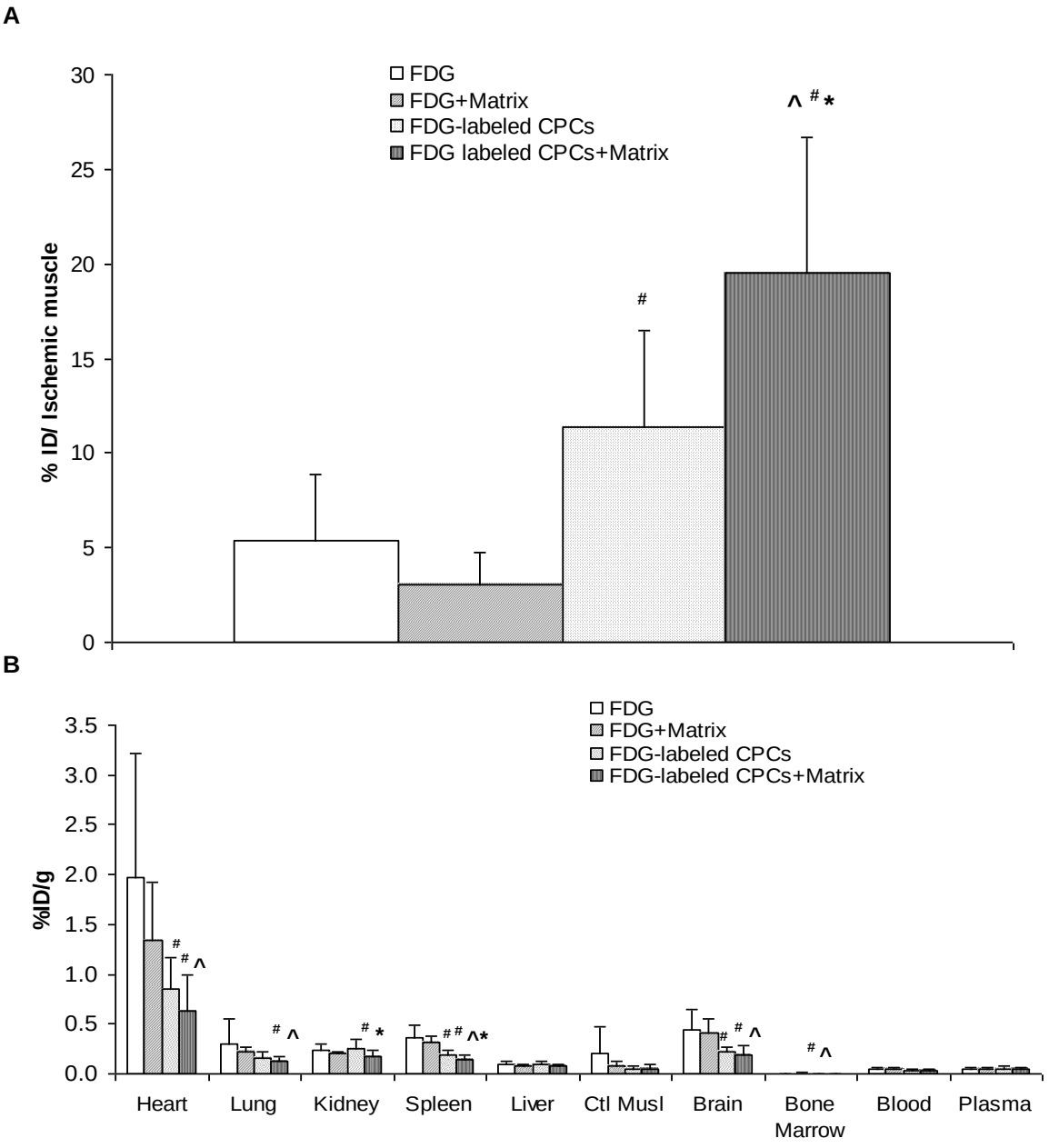

Figure 3-5: Biodistribution of ^{18}F-FDG accumulation in different organs 180 minutes after injection.

A, Radioactivity in the ischemic hind limb muscle. Distribution of ^{18}F-FDG-labeled CPCs in the group delivered in matrix was significantly greater in the target tissue (ischemic hind limb). B, Radioactivity in the nonspecific tissues. There was an overall reduction of labeled-cell distribution in kidney, spleen, and other nonspecific tissues. $^{\#}P<0.05$, versus FDG (n=12); $\wedge P<0.05$, versus FDG with the matrix (n=12); $\mathbf{*}P<0.05$, versus FDG-labeled CPCs (n=15).

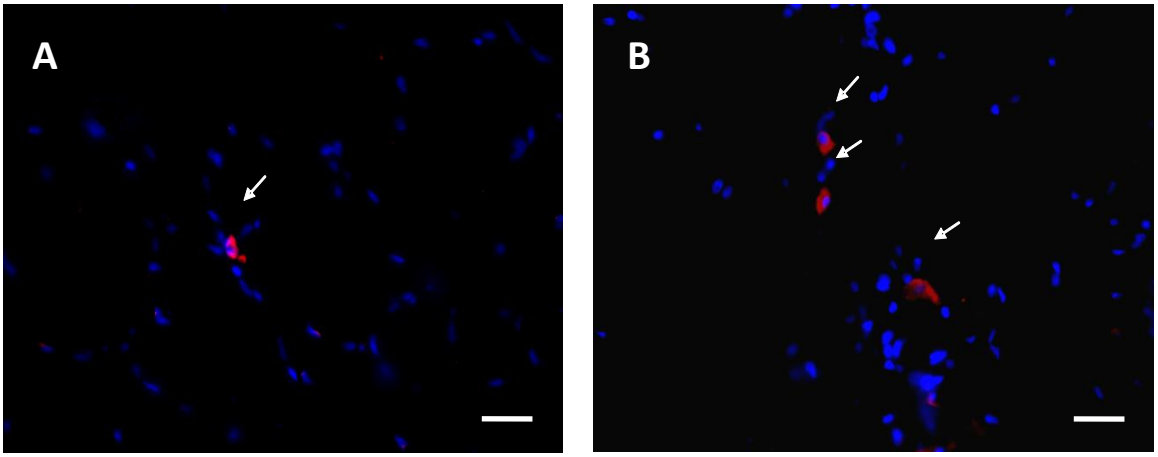

Figure 3-6: Identification of the transplanted cells.

Identification of the transplanted cells (arrows) in the ischemic hindlimb of rats by human-specific anti-mitochondrial antibody (red fluorescence, cytoplasm). The slices are also stained by 4′,6-diamidino-2′-phenylindole (blue fluorescence, nucleus). A, The hindlimb muscle injected with ^{18}F-FDG-labeled human CPCs; B, The hindlimb muscle injected with ^{18}F-FDG-labeled human CPCs delivered in the matrix. There were more transplanted CPCs in the hindlimb with injection of cells delivered in the matrix (P<0.05). Scale bar = 50 μm.

Discussion

The main findings of this study are: (1) that use of a collagen-based matrix increased the early retention of CPCs delivered *in vivo* (observed only 2 to 3 hours post-transplantation); (2) that a collagen-based matrix minimized the distribution of CPCs to nonspecific tissues; (3) that ^{18}F-FDG is a usable tracer for monitoring transplanted CPCs, and provides a promising platform for the development of non-invasive PET imaging approaches for trafficking of CPC delivery within matrices in real time; and (4) that the success of the PET imaging methods in evaluating the effect of the matrix on CPC transplantation was validated by 2 conventional methodologies (biodistribution and immunofluorescence). Our study therefore introduces a novel concept that in addition to improving the long-term engraftment of transplanted cells, a collagen delivery matrix may also enhance the short-term effects of cell therapy since differences in cell retention were observed at an early stage posttransplantation.

Stem cells and/or progenitor cells are being widely investigated as a potential therapy for ischemic heart disease. Satisfactory cell deposition and engraftment in the target area are considered likely therapeutic prerequisites. The use of CPCs for cardiac angiogenic activity has previously resulted in some benefits, but the retention and survival of implanted cells in the myocardium is only between 1 and 10% (Aicher et al. 2003). The development of tissue engineered matrices for the delivery and support of transplanted cells has recently attracted interest in the cardiac field. Collagen-based biomaterials have been developed to support cell growth and for the restoration of myocardial infarction (Ozawa et al. 2002; Kofidis et al. 2003; Boccafoschi et al. 2005; Kutschka et al. 2006). The advantages of collagen matrices are their large surface area for

cell seeding, porosity for capillary in-growth, stability for mechanical support, biodegradability, and minimal immunogenicity (Kofidis et al. 2003; Boccafoschi et al. 2005). Previous work from our group indicated that *in vitro* adhesion of the CPC derived $CD133^+$ cells was greatest on a collagen type I substrate; and use of a collagen-based matrix for the delivery of CPCs into ischemic hind limbs of rats improved the retention of the transplanted cells and increased tissue vascularization, as determined by immunohistochemical analysis performed 2 weeks after transplantation (Suuronen et al. 2006).

In this study, noninvasive *in vivo* PET imaging and subsequent biodistribution and immunofluorescence analysis demonstrated related observations at earlier time points after transplantation than previously investigated. CPC retention in the ischemic hind limb muscle was ≈11% of injected dose at 180 minutes after injection without the matrix. With use of the matrix, retention was enhanced by ≈70% in the target tissue.

To date, cardiac cell therapy has resulted only in modest clinical benefits (Abdel-Latif et al. 2007; Patel et al. 2007), perhaps limited by the low retention and survival of implanted cells. It has been demonstrated that the loss of injected cells from the target tissue occurs at an early stage post-transplantation (Aicher et al. 2003; Cho et al. 2007; Doyle et al. 2007), but their effects can be sustained by host tissues that are induced by the transplanted cells to express humoral factors involved in angiogenesis, antiapoptosis, and chemoattraction of bone marrow cells (Cho et al. 2007). Therefore, the observation that our collagen matrix improved the very early retention of cells within the target tissue suggests that its use may confer enhanced short-term therapeutic cell effects in addition to its benefits to long-term cell engraftment. It is conceivable that by minimizing the

rapid loss of transplanted cells, the collagen matrix may augment and/or prolong the cell transplant-mediated host humoral response.

The ability to assess the engraftment and survival of transplanted cells is also of importance for the study of cell-based therapeutic strategies. Traditionally, the fate of transplanted cells is assessed by postmortem histological examination at a single time point in animal studies. For visualization, *ex vivo* cell labeling methods are used prior to transplantation using a vital dye (eg, 4',6-diamidino-2'-phenylindole), a thymidine analog (eg, 5-bromodeoxyuridine) or a conventional reporter gene (eg, green fluorescent protein). Alternatively, established radioisotope methods used in clinical nuclear medicine offer an attractive option for cell imaging, with the advantage of non-invasive cell tracking at several time points. The present study demonstrated that PET imaging with ^{18}F-FDG cell labeling was feasible for the assessment of CPC retention and distribution in the early stages of transplantation with and without a matrix. To our knowledge, this is the first study using PET imaging to investigate and demonstrate the effect of collagen matrices on cell transplantation *in vivo*.

^{18}F-FDG is an attractive radiotracer for labeling stem cells since it enables PET imaging of cell tracking *in vivo*, and exploits normal metabolic activity of target cells, thereby reducing any risk of functional alteration. In this study, we successfully labeled human CPCs with ^{18}F-FDG with minimal alteration of viability. The viability of labeled cells was preserved up to 24 hours, with a slight subsequent reduction observed at 5 days. Our results also demonstrated that cell labeling efficiency of ^{18}F-FDG was CPC-concentration dependent but not FDG-dose dependent. Similar observations have been reported in studies using ^{111}In or ^{99m}Tc (Rao et al. 1982; Ecclestone et al. 1990).

Because only viable cells will retain ^{18}F-FDG in the cytoplasm, an added benefit to its use is that retention of ^{18}F-FDG might reflect the viability state of the cells (Kang et al. 2006). However, a possible limitation of labeling cells with ^{18}F-FDG is that significant leakage of the radiotracer after initial cellular accumulation may occur. Several studies using ^{18}F-FDG have reported a labeling efficiency of less than 10% for some types of stem cells due to a high efflux rate in the first hour post-labeling. Ma et al (Ma et al. 2005) showed that rat mesenchymal stem cells can be labeled with ^{18}F-FDG but 98% release of the radiotracer occurs in the washing process. Our results also showed a significant rate of radiolabel release from CPCs during the washing process. Stability studies on labeled cells showed a ≈ 50% label loss after 2-hour incubation. Although insulin has been shown to improve ^{18}F-FDG retention in cells, it was not effective in improving the labeling efficiency in CPCs (Kang et al. 2006). It is possible that CPCs may have an insufficient level of G-6-phosphatase activity, or perhaps insulin does not have an inhibitory effect on G-6-phosphatase activity in CPCs (Paik et al. 2002). Importantly, despite the dosage loss, the radioactivity could still be monitored by PET *in vivo*.

Another limitation of ^{18}F-FDG cell labeling is the rather short half-life of ^{18}F (110 minutes) that only permits the monitoring of cell fate for several hours. Advances in nanotechnology are enabling the development of new PET agents with improved sensitivity for the tracking of cells using longer-lived radionuclides. For example, ^{64}Cu-labeled nanoparticles have been used to image the macrophages in inflammatory atherosclerosis (Nahrendorf et al. 2008), and although not yet widely available, agents such as these may provide an appealing alternative for long-term or repeated imaging.

In summary, ^{18}F-FDG is a usable tracer for monitoring transplanted CPCs, and provides a promising platform for the development of non-invasive PET imaging approaches for trafficking of CPC delivery within matrices in real-time. This study used PET imaging and traditional confirmatory techniques to demonstrate that collagen-based matrices significantly improved the very early retention of transplanted CPCs in the ischemic tissue, and limited their non-specific distribution. This mechanism conferred by the matrix may have implications on the effects of cell therapy at the early stages after transplantation in addition to the long-term benefits of improved cell engraftment.

Sources of Funding

This work was supported by the Heart and Stroke Foundation of Ontario (Program Grant, PRG 6242; grant NA5905 to Drs. Ruel and Beanlands; and grant NA6121 to Dr. Suuronen), the Canadian Institutes of Health Research (grant MOP-77536 to Drs. Ruel and Suuronen) and by the Canadian Foundation for Innovation (award 7346 to Dr. Ruel). Dr. Beanlands is a Career Investigator of the Heart and Stroke Foundation of Ontario and Dr. Zhang is the recipient of an Ontario Graduate Scholarship in Science and Technology.

Disclosures

None

Clinical Perspective

Regenerative medicine for the treatment of cardiac disease is rapidly developing. However, our understanding of the efficacy of cell therapies and of the adjuvant role of tissue engineered materials, such as collagen matrices, is largely limited to postmortem histological assessment, which is unsuitable for clinical use. As a noninvasive molecular imaging modality, PET imaging can be applied longitudinally and has the capability to assess biological processes at the molecular and cellular levels. The current study used 18F-FDG cell labeling and PET imaging to monitor the distribution of transplanted endothelial progenitor cells in real time and to better understand the role of delivery matrices in cell therapy. By using this imaging technique, we found that a collagen-based matrix can improve the early retention of transplanted cell in the target tissue. We believe with further refinement, molecular imaging techniques of transplanted cells will contribute to the elucidation of the optimal stem cell type(s) and dose, the evaluation of adequate administration methods, the assessment of delivery of the cells and biopolymers, and the development of novel tissue engineering strategies. Therefore, tissue engineering and PET imaging could help expand the clinical applications of cell therapies in years to come.

CHAPTER 4: MANUSCRIPT #3

Introduction to Manuscript #3

In the previous manuscript, I reported a significant leakage of ^{18}F-FDG from labeled cells. Although ^{18}F-FDG-CPCs could be detected by PET, a more stable labeling approach would still be desirable. I next proposed to evaluate ^{18}F-HFB as a new radioligand, which might be a superior cell tracker for PET. To evaluate the feasibility of ^{18}F-HFB to label human CPCs for cell tracking, PET imaging was performed to monitor cell homing and retention of intramyocardially injected CPCs in a rat myocardial infarction model. The use of ^{18}F-HFB was compared with the properties of ^{18}F-FDG labeling for PET imaging of transplanted CPCs.

Manuscript Submitted to Cell Transplantation 2011; CT-0438 (under revision)

^{18}F-FDG Cell Labeling may Underestimate Transplanted Cell Homing: More Accurate, Efficient and Stable Cell Labeling with Hexadecyl-4-[^{18}F]fluorobenzoate for In Vivo Tracking of Transplanted Human Progenitor Cells by Positron Emission Tomography

Yan Zhang, MD, MSc; Jean N. DaSilva, PhD; Tayebeh Hadizad, PhD; Stephanie Thorn, MSc; Drew Kuraitis, BSc; Jennifer M. Renaud, MSc; Ali Ahmadi, MD, MSc; Myra Kordos; Robert A. deKemp, PhD; Rob S. Beanlands, MD; Erik J. Suuronen, PhD; and Marc Ruel, MD, MPH

From the Division of Cardiac Surgery (Y.Z., D.K., A.A., E.J.S., M.R.); Cardiac PET Centre, Division of Cardiology (J.N.D., T.H., S.T., J.M.R., M.K., R.A.D., R.S.B.); and the Molecular Function and Imaging Program (all authors), University of Ottawa Heart Institute; the Department of Cellular and Molecular Medicine (Y.Z., J.N.D., S.T., D.K., A.A., R.S.B., E.J.S., M.R.), University of Ottawa

Correspondence to Marc Ruel or Erik J. Suuronen, Division of Cardiac Surgery, University of Ottawa Heart Institute.

Running title: *In Vivo* CPC Tracking with ^{18}F-HFB Labeling

Word count: Total 6,518 Abstract 291

Contributions of Authors

Experiments described in this manuscript were designed and executed by myself, with practical help from Ph.D. candidates Stephanie Thorn (implementation of animal model) and Drew Kuraitis (analysis of histological examination). Radiochemists Drs. Jean DaSilva and Tayabeh Hadizad provided the knowledge and synthesis of radioisotopes for cell labeling. Myra Kordos operated the PET scanner to acquire PET images. Physicists Dr. Robert deKemp and Jennifer Renaud provided input on the relevance of obtained data for the interpretation of PET data. Dr. Rob Beanlands provided a clinical perspective on the data. I worked on manuscript preparation and submission under the guidance and supervision of Drs. Marc Ruel and Erik Suuronen.

Abstract

Cell therapy is expected to restore perfusion and improve function in the ischemic/infarcted myocardium; however, the biological mechanisms and local effects of transplanted cells remain unclear. To assess cell fate *in vivo*, hexadecyl-4-[^{18}F]fluorobenzoate (^{18}F-HFB) cell labeling was evaluated for tracking human circulating progenitor cells (CPCs) with positron emission tomography (PET), and was compared to the commonly used 2-[^{18}F] fluoro-2-deoxy-D-glucose (^{18}F-FDG) labeling method in a rat myocardial infarction model. CPCs were labeled with ^{18}F-HFB or ^{18}F-FDG *ex vivo* under the same conditions. ^{18}F-HFB cell labeling efficiency (23.4±7.5%) and stability (4h, 88.4±6.0%) were superior to ^{18}F-FDG (7.6±4.1% and 26.6±6.1%, respectively; $p<0.05$). Neither labeling approach significantly altered cell viability, phenotype or migration potential up to 24h post-labeling. Two weeks after left anterior descending coronary artery ligation, rats received echo-guided intramyocardial injection in the infarct border zone with: ^{18}F-HFB-CPCs; ^{18}F-FDG-CPCs; ^{18}F-HFB; or ^{18}F-FDG. Dynamic PET imaging of both ^{18}F-HFB-CPCs and ^{18}F-FDG-CPCs demonstrated that only 16-37% of the initial injection dose (ID) was retained in the injection site at 10min post-delivery, and remaining activity fell significantly over the first 4h post-transplantation. The ^{18}F-HFB-CPC signal in the target area at 2h (23.7±14.7%ID/g) and 4h (17.6±13.3%ID/g) post-injection was greater than that of ^{18}F-FDG-CPCs (5.4±2.3%ID/g and 2.6±0.7%ID/g, respectively; $p<0.05$). Tissue biodistribution confirmed the higher radioactivity in the border zone of ^{18}F-HFB-CPC rats. Immunostaining of heart tissue sections revealed no significant difference in cell retention between two labeled-cell transplantation groups. Good correlation with biodistribution results was observed in the ^{18}F-HFB-CPC rats

(r=0.81, p<0.05). Compared to ^{18}F-FDG, labeling human CPCs with ^{18}F-HFB provides a more efficient, stable, and accurate way to quantify the distribution of transplanted cells. ^{18}F-HFB cell labeling with PET imaging offers a better modality to enhance our understanding of early retention, homing, and engraftment with cardiac cell therapy.

Key Words: stem cells; myocardial infarction; transplantation; cell tracking; positron emission tomography

Introduction

Despite considerable advances in cardiovascular therapeutics over the past few decades, our ability to effectively treat myocardial infarction and subsequent congestive heart failure remains limited by the fact that necrotic or scarred myocardium cannot be restored. Cell–based regenerative therapy is a promising strategy for myocardial repair. Initial animal studies and clinical trials have demonstrated that intramyocardial injection of circulating progenitor cells (CPCs) can restore regional perfusion and improve function in the ischemic/infarcted myocardium (Kawamoto et al. 2003; Hendrikx et al. 2006). However, further understanding the biological mechanisms and local effects of transplanted cells remains mostly restricted to post-mortem histological assessment (Yukawa et al. 2009), which is a single time point analysis and unpractical with human subjects. Little quantitative data on the biodistribution and *in vivo* kinetics of transplanted stem/progenitor cells in the myocardium and the whole body have been reported. Therefore, the development of non-invasive imaging approaches for monitoring the fate and tissue distribution of transplanted cells would provide useful insights.

Positron emission tomography (PET) is a well-developed tool for studying myocardial blood flow, metabolism and cardiac function, and is proving to be useful for evaluating cell therapeutic responses. As an advanced nuclear imaging technology, PET combines high sensitivity, good spatial resolution, and whole body imaging to track transplanted stem cells (Zhang et al. 2008). Therefore, PET can be used as a non-invasive imaging technique to assess cell fate longitudinally. Moreover, PET provides the potential for quantification of cell numbers in specific tissues of interest. PET imaging techniques have been proposed and evaluated in several cell delivery models (Adonai et

al. 2002; Aicher et al. 2003; Hofmann et al. 2005). To implement PET cell imaging, it is important to develop a stable radiolabeling method without altering cell viability or function. One common approach to assess the distribution pattern of transplanted cells with PET is 2-[^{18}F] fluoro-2-deoxy-D-glucose (^{18}F-FDG) cell labeling (Hofmann et al. 2005). Our group has used this technique to evaluate the ability of tissue-engineered matrices to improve the early retention of transplanted human CPCs in an ischemic hindlimb model (Zhang et al. 2008). Although ^{18}F-FDG labeled cells could be detected by PET, we and others have also observed significant leakage of ^{18}F-FDG from labeled cells (Adonai et al. 2002; Zhang et al. 2008).

Hexadecyl-4-[^{18}F]fluorobenzoate (^{18}F-HFB), a lipophilic long-chain ester derivative, is a novel radioligand that is absorbed into the cell membrane, and thus might be a superior cell tracker for PET imaging. Recently, it has been used to image rat mesenchymal stem cells (MSCs) by micro-PET after intravenous injection to healthy animals (Ma et al. 2005). However, use of ^{18}F-HFB to label human cells for the assessment of cardiac cell therapy has not been reported. In addition, it has not been compared to other commonly used cell tracking methods, such as ^{18}F-FDG, nor has its cytotoxic effect on labeled cells been evaluated.

In this study, we evaluated ^{18}F-HFB labeling properties for monitoring intramyocardially injected CPCs with PET imaging in a rat myocardial infarction (MI) model. Also, we assessed ^{18}F-HFB cytotoxicity, and the possibility of ^{18}F-HFB labeling for the evaluation of human CPCs delivered in a collagen matrix. All *in vitro* and *in vivo* studies of ^{18}F-HFB labeling were compared to an ^{18}F-FDG labeling approach.

Materials and Methods

Radiotracer Synthesis

^{18}F-HFB was synthesized by a 3-step procedure according to previously described methods (Ma et al. 2005). Briefly, the triflate precursor was synthesized after esterification of 4-(*N*,*N*-dimethylamino)benzoyl chloride (Sigma-Aldrich, Oakville, Canada) with 1-hexadecanol (Sigma-Aldrich). ^{18}F-HFB was produced by ^{18}F-substitution and purified by high-performance liquid chromatography with 20-40% yield (decay corrected) and high radiochemical purity (>99%). Pure ^{18}F-HFB was dissolved in 10% DMSO/saline.

Cell Isolation and Culture

Human CPC procurement was approved by the Human Research Ethics Board of the University of Ottawa Heart Institute. After acquiring informed consent from healthy human donors, total peripheral blood mononuclear cells (PBMNCs) were freshly isolated from human peripheral blood by Histopaque 1077 (Sigma-Aldrich) density-gradient centrifugation. Subsequently, PBMNCs were cultured on fibronectin-coated plates in endothelial basal medium (EBM-2; Clonetics, Guelph, Canada) supplemented with EGM-2-MV-SingleQuots (5% fetal bovine serum, vascular endothelial growth factor (VEGF), insulin-like growth factor-1, and human epidermal growth factor). After 4 days, the adherent population (CPCs) was collected as described previously (Ruel et al. 2005).

Cell Radiolabeling

Harvested CPCs were incubated with ^{18}F-HFB for 30 minutes in a sterile centrifuge tube under various conditions, including different dose ranges of ^{18}F-HFB (0.4-0.6 mCi, 1.5-

2.5 mCi or 5.0-7.0mCi), different concentrations of CPCs (2.0×10^6 cells in 1, 3, or 5 mL PBS) and different temperatures (4, 22, or 37°C). In parallel experiments, CPCs were labeled with ^{18}F-FDG under these same conditions. At the end of incubation, cells were washed to remove unbound radioactivity. The radioactivity was measured both in cells and in the supernatant, by using a dose-calibrator (Capintec, Ramsey, NJ). With correction for radiolabel decay, cell-labeling efficiency was calculated as the activity in cells over the total activity used in the incubation.

Cell Labeling Stability

Radiolabeled cells were resuspended in 2 mL PBS and incubated at 37°C for 2 hours and 4 hours. The retention of ^{18}F-HFB or ^{18}F-FDG within CPCs was calculated.

Viability of Labeled CPCs

The relative survival of labeled cells was evaluated by using the Vi-CELL analyzer (Beckman Coulter, Mississauga, Canada) with a Trypan Blue Dye Exclusion Method. Radiolabeled or unlabeled CPCs (1×10^6) suspended in 1.0 mL EBM were plated, and viability was assessed after an incubation of 2, 4, 24 hours or 5 days. Cell viability was also measured with CPCs incubated with non-radioactive HFB.

Phenotype of Labeled CPCs

The phenotype of ^{18}F-HFB-CPCs and ^{18}F-FDG-CPCs was assessed by flow cytometry analysis (FACSAria cell sorting system; BD Biosciences, San Jose, CA) using CD144, vascular endothelial growth factor receptor-2 (VEGFR-2), L-selectin (CD62L), and CD34 antibodies (Becton Dickinson, Mississauga, Canada) at 24 hours post-labeling.

Migratory Potential of Labeled CPCs

In vitro cell migration assays were performed as described previously (Zhang et al. 2010). Briefly, ^{18}F-HFB-CPCs, ^{18}F-FDG-CPCs, or unlabeled controls were incubated with 4'6-diamidino-2'-phenylindole (DAPI, Molecular Probes, Eugene, OR), and then 2×10^4 cells were placed separately in the upper chamber of a modified Boyden chamber with VEGF-free media. The lower chamber contained serum-free media with 50ng/mL VEGF (Sigma-Aldrich). After 24 hours of incubation, cells that migrated into the lower chamber were counted in 6 random high powered fields.

Retention of ^{18}F-HFB in Matrices

Collagen-based matrices (pH ~7.5) consisted of a mixture of blended neutralized type I rat tail tendon collagen (0.4%, wt/vol; Becton Dickinson, Mississauga, Canada) and chondroitin 6-sulfate (1:6, wt/wt; Sigma), cross-linked with 0.02% (vol/vol) glutaraldehyde (Zhang et al. 2008). ^{18}F-HFB-CPCs (1×10^6, in 50 μL PBS) or ^{18}F-HFB alone was added to the matrix solution (450 μL) on ice. Matrix mixture was plated and incubated at 37°C for 60 minutes to allow complete gelation. Matrix gels were then transferred into 2 mL PBS and incubated at 37°C for 2 hours. Before and after incubation, the radioactivity in matrices was measured.

Myocardial Infarction Animal Model

Procedures were performed with the approval of the University of Ottawa Animal Care Committee, in accordance with the Canadian Council on Animal Care's Guide to the Care and Use of Experimental Animals. Sprague Dawley rats (8-9 weeks old, Charles River, Wilmington, MA) were anesthetized (2% isoflurane, inhaled), intubated and ventilated,

and then the heart was exposed via a sternotomy. Subsequently, a 7-0 suture was placed in the anterior myocardium at one thirdof the length of the heart, towards the apex, so that the left coronary anterior descending artery was completely ligated to induce MI (Suuronen et al. 2007). After two weeks, the survival for all animals was 77.3%.

Echo-guided Cell Delivery

Two weeks after ligation, MI rats were anesthetized and anchored in a supine position. Echocardiography was performed with a Vevo770 system (VisualSonics, Toronto, Canada) in B mode with the use of a 716 series real-time microvisualization (RMV) scanhead probe. Rats randomly received one of the following treatments in 50 µL PBS (n=8/group), administered by echo-guided intramyocardial injection into the infarct border zone with a 27-gauge needle: (1) 2×10^6 ^{18}F-HFB-CPCs; (2) 2×10^6 ^{18}F-FDG-CPCs; (3) ^{18}F-HFB; or (4) ^{18}F-FDG. To this end, the syringe was secured in a micromanipulator (VisualSonics), and both the needle and RMV scanhead probe were aligned before the injection procedure (Rodriguez-Porcel et al. 2005; Yeghiazarians et al. 2009). The needle was retracted from the ultrasound field of view with the use of the micromanipulator until the needle tip was in the desired location within the heart, which was proximal to the infarct area (defined by poor wall motion). The cell mixture was then injected into the border zone of the anterior wall.

PET Imaging for Localization of Labeled CPCs In Vivo

For some animals (n=5/group), ^{18}F-PET images were acquired using the Inveon small animal PET scanner (Siemens, Knoxville, TN) for cell localization at 10 minutes, 2 hours, and 4 hours post-injection. ^{13}N-NH_3 PET imaging was also performed for

anatomic delineation of the heart and liver. Image reconstruction resulted in an image resolution of approximately 1.3 mm. ^{18}F-microPET image data were analyzed in three cardiac axes (axial, coronal and sagittal) with the Inveon Research Workplace, and fused with ^{13}N-NH_3 images. Regions of interest (ROIs) were manually drawn around the injection site, normal myocardium, lung, and liver by visual inspection. The same ROIs were used at the three scan time points. The radioactivity of each ROI was expressed as percentage of the injected dose per gram (%ID/g) for all tissues, and the percentage of the injected dose (%ID) was also calculated in the MI border zone as %ID/g × ROI volume (cm^3, assuming a tissue density of 1g/cm^3) to determine the relative retention of injected cells in the target site.

Biodistribution of Labeled CPCs

After PET scan completion (at 5 hours post-injection), rats were sacrificed and tissues were harvested. Biodistribution of the radioactivity accumulation in different tissues was determined by a gamma counter (PerkinElmer Life and Analytical Sciences, Waltham, MA), and the tissues were weighed. Data were expressed as %ID/g.

Immunofluorescence Assessment of Transplanted Human CPCs

Hearts were sliced into 3 sections: the infarct centre, the border zone, and the normal myocardium. Tissue samples were fixed with 4% paraformaldehyde and embedded in paraffin, and slides were prepared in 5 μm serial sections. Transplanted human CPCs were localized by immunofluorescence staining with anti-human mitochondria antibodies (1:40; Chemicon, Temecula, CA). The sections were mounted with mounting medium containing DAPI (Vector Laboratories, Burlingame, CA). The percentage of transplanted

human cells ((number of human mitochondria^{+}DAPI^{+} cells ÷ number of DAPI^{+} cells) ×100) per field of view (/FOV) was calculated from 4 random slides of each section as described previously (Zhang et al. 2008).

Statistical Analysis

Data are expressed as mean ± standard deviation (SD). Statistical analyses between groups were performed with a one-way analysis of variance, with Bonferroni corrections as appropriate. Correlation analyses were performed by linear regression. Differences with $p<0.05$ were considered statistically significant.

Results

Ex Vivo CPC Labeling Efficiency

The factors influencing cell labeling efficiency were studied to determine the optimal labeling conditions for *in vivo* tracking studies. There was no correlation between the cell uptake and the amount of radiotracer in the incubation for both ^{18}F-HFB (p=0.78, n≥5/dose range) and ^{18}F-FDG (p=0.46, n≥4/dose range) groups (Figure 4-1A).

CPCs (2×10^6) were incubated with ^{18}F-HFB or ^{18}F-FDG in 3 different volumes (1, 3, and 5mL) resulting in different cell concentrations (2×10^6, 0.7×10^6 and 0.4×10^6 CPCs/mL). Labeling efficiency in 5 mL was 8.3±3.4% (^{18}F-HFB) and 1.6±0.7% (^{18}F-FDG), and in 3mL was 11.4±3.9% (^{18}F-HFB) and 4.2±2.3% (^{18}F-FDG). As shown in Figure 4-1B, labeling efficiency was significantly increased for both ^{18}F-HFB and ^{18}F-FDG labeling when incubation was performed in 1mL (23.4±7.5% and 7.6±4.1%,

respectively; $p<0.05$). A cell concentration–dependent incorporation of ^{18}F-HFB labeling ($r=0.81$, $p<0.05$) was observed with an overall labeling efficiency of 4.2-48.4%.

Three different temperatures (4°C, 22°C, and 37°C) were also tested. The highest retention of ^{18}F-HFB (31.6±3.2%) and ^{18}F-FDG (5.6±1.4%) in CPCs was obtained when labeling occurred at 37°C (Figure 4-1C).

On the basis of these results, in subsequent *in vitro* and *in vivo* experiments, 2×10^6 CPCs were incubated with 2 mCi of radiotracer (^{18}F-HFB or ^{18}F-FDG) in 1mL at 37°C. Overall, with any given condition, ^{18}F-HFB labeling efficiency was better than that of ^{18}F-FDG (all $p<0.05$).

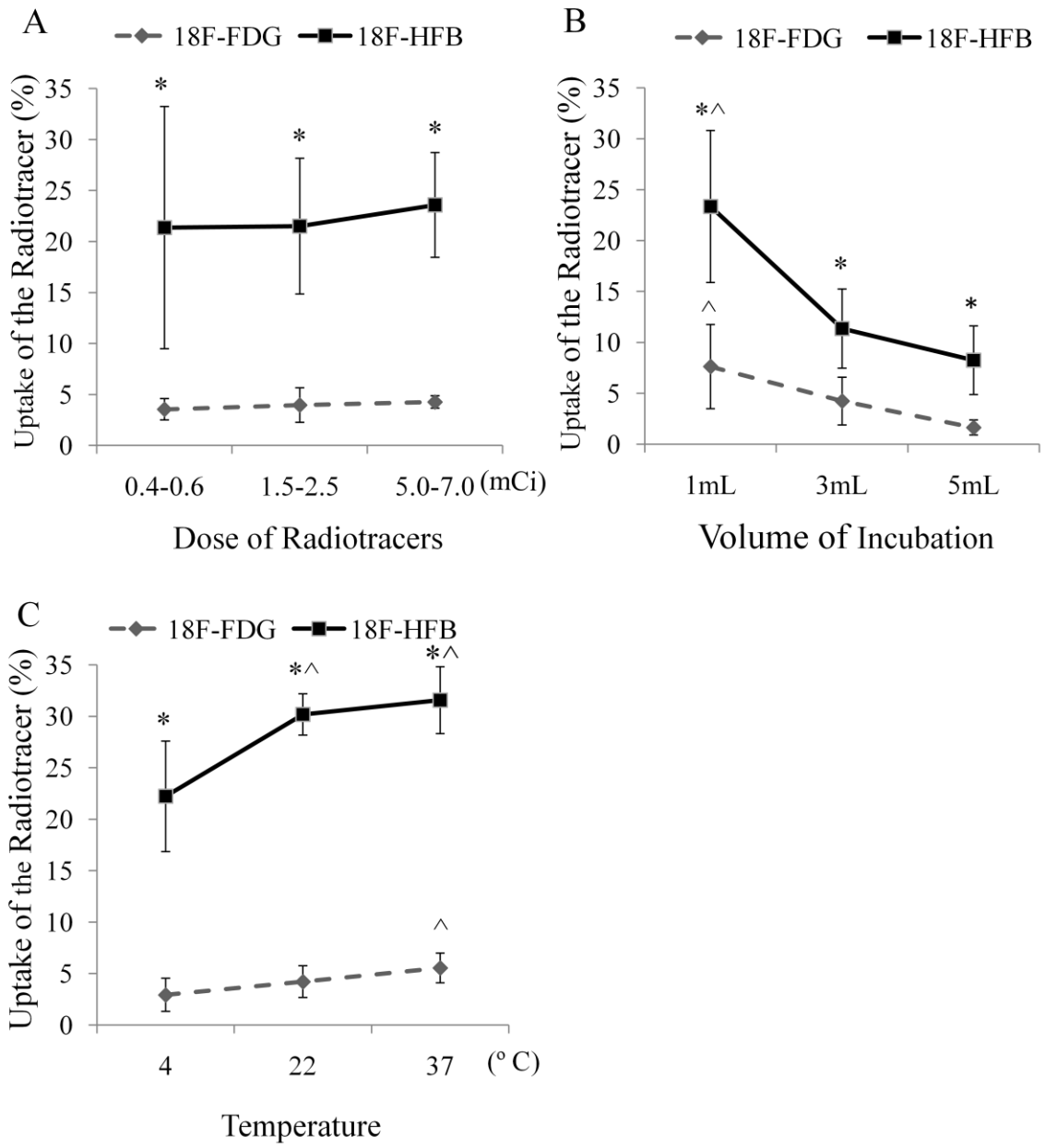

Figure 4-1: Cell labeling efficiency of ^{18}F-HFB and ^{18}F-FDG.

A) The effect of radiotracer dose on labeling efficiency; B) the effect of cell concentration on labeling efficiency; and C) the effect of temperature on labeling efficiency (*****p<0.05 versus ^{18}F-FDG labeling; ^p<0.05 versus other conditions within group; n≥4/group).

Labeling Stability

To evaluate the efflux rate of ^{18}F-HFB and ^{18}F-FDG from the cells, the retention of radioactivity in labeled CPCs was measured. After a 2h- or 4h- incubation, the retention of ^{18}F-HFB in labeled CPCs (91.6±5.1% and 88.4±6.0%, respectively) was significantly higher compared to ^{18}F-FDG-CPCs (42.5±4.3% and 26.6±6.1%; $p<0.05$), demonstrating greater labeling stability of ^{18}F-HFB -CPCs (Figure 4-2).

Cytotoxicity of Labeling in CPCs

To investigate the effect of radiolabeling on cells, CPC viability at 0, 2, 4, 24 hours, and 5 days post-labeling was measured (Figure 4-3A). There were no significant differences among ^{18}F-HFB-CPCs, ^{18}F-FDG-CPCs and the unlabeled controls in the first 4 hours. At 24 hours post-labeling, however, a reduction in ^{18}F-HFB-CPC viability (65.8±13.3%) was observed compared to the controls (81.8±6.9%, $p<0.05$). After 5 days, there was a loss in viability for both ^{18}F-HFB-CPCs (62.5±10.4%) and ^{18}F-FDG-CPCs (72.1±14.7%) compared to the unlabeled cells (84.0±13.3%, $p<0.05$). To further investigate whether the increased radioactivity in ^{18}F-HFB-CPCs or the HFB compound itself cause cell death, we also incubated CPCs with non-radioactive HFB. There was no significant difference between HFB-CPCs (68.7±7.0%) and ^{18}F-HFB-CPCs in 24h cell viability. However, viability of HFB-CPCs (69.7±14.7%) at 5 days was better than ^{18}F-HFB-CPCs, but less than the controls, suggesting that both increased radioactivity and HFB itself contributed to the death of ^{18}F-HFB-CPCs.

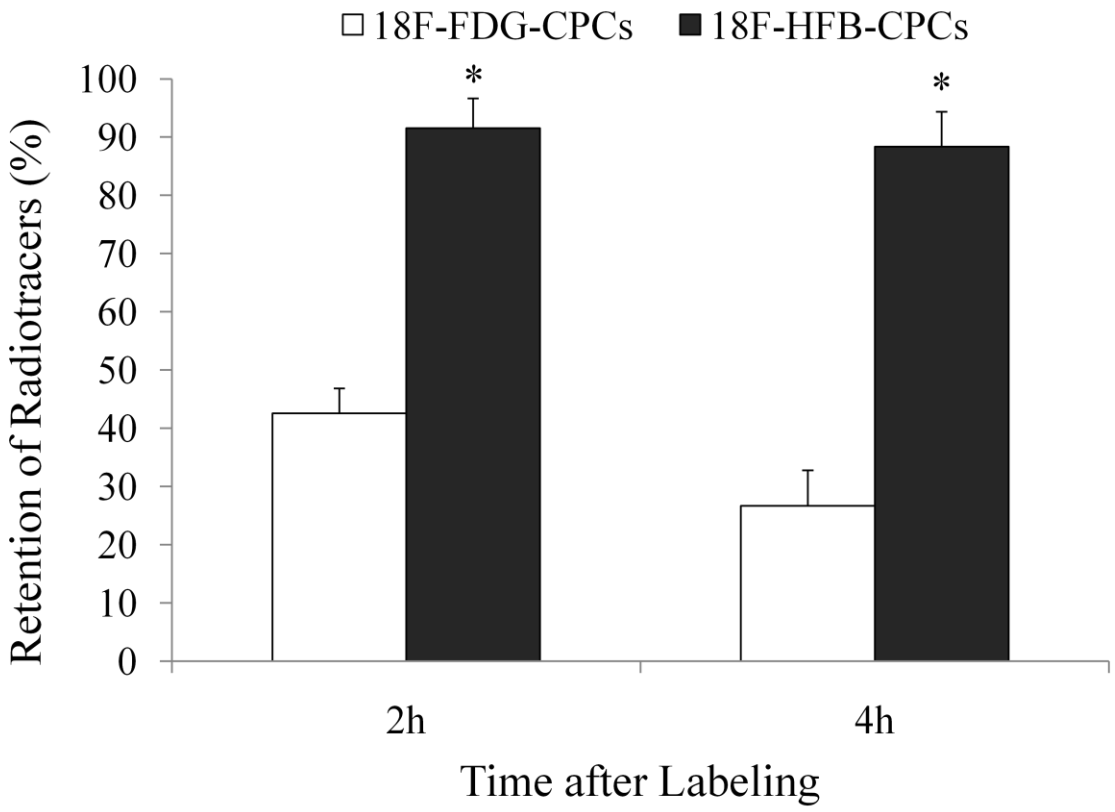

Figure 4-2: Stability of radiolabeling in ^{18}F-HFB-CPCs and ^{18}F-FDG-CPCs.

After a 2h- or 4h- incubation, the retention of ^{18}F-HFB in labeled CPCs was significantly higher than ^{18}F-FDG-CPCs (*p<0.05 versus ^{18}F-FDG-CPCs; n=5/group).

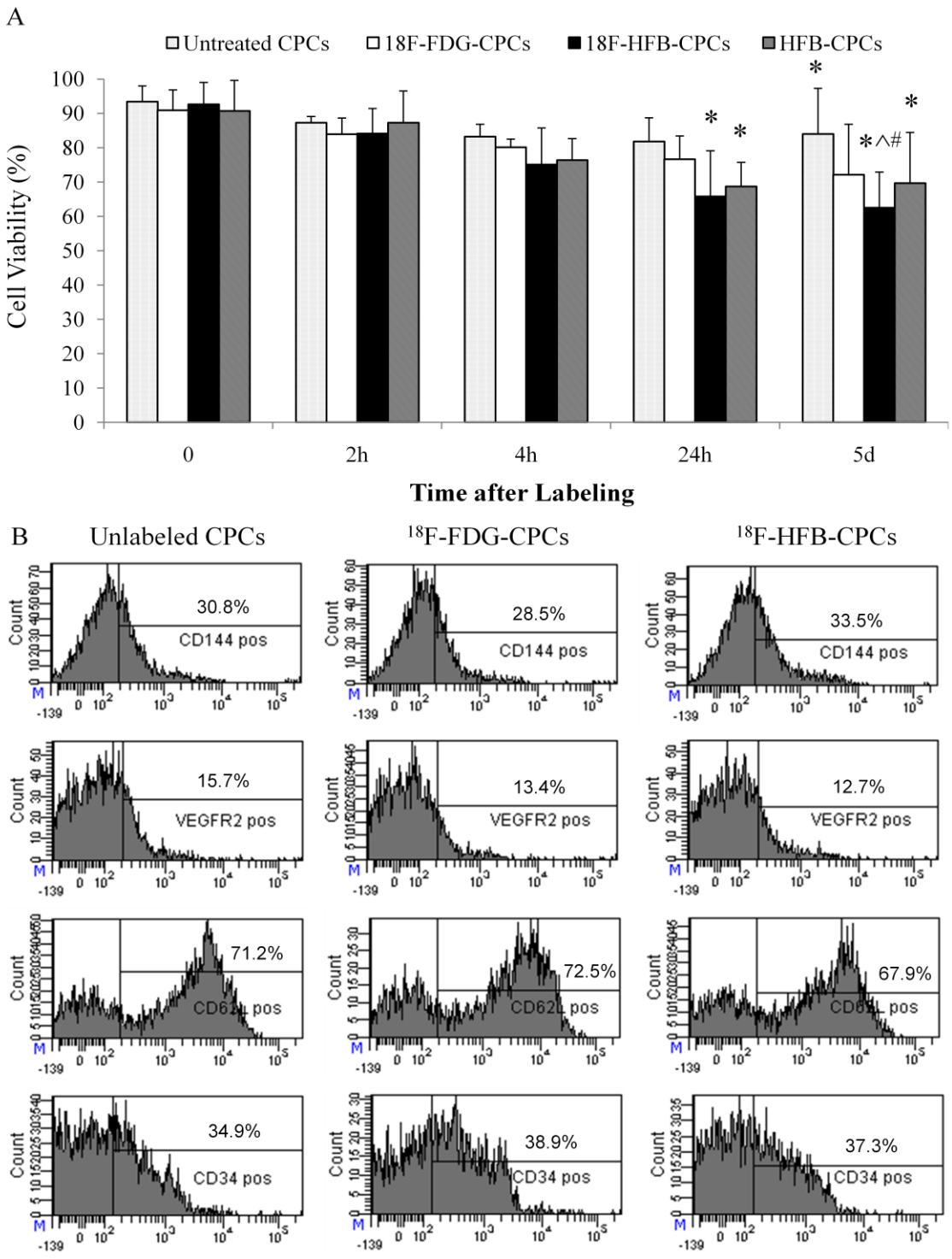

Figure 4-3: The effect of radiolabeling on cell phenotype and function.

A) Labeled cell viability. (*p<0.05 versus untreated CPCs; ^p<0.05 versus ^{18}F-FDG-CPCs; $^{\#}p$<0.05 versus HFB-CPCs; n=6 per group) B) Representative flow cytometric analysis of cell phenotype at 24 hours post-labeling. The expression of CD144, VEGFR-2, CD62L and CD34 on the unlabeled CPCs, ^{18}F-FDG-CPCs, and ^{18}F-HFB-CPCs.

Table 4-1 Cell phenotypes and function at 24 hours post-labeling

Cell Types	Expression of Cell Markers (%)				Cell Migration (cell number /field of view)
	CD144	VEGF-R2	L-selectin	CD34	
Unlabeled CPCs	20.5±14.1	12.7±4.1	72.9±2.5	34.9±8.3	58.5±26.4
^{18}F-FDG-CPCs	22.1±10.8	15.8±7.8	67.1±8.6	37.4±12.0	60.0±27.3
^{18}F-HFB-CPCs	22.2±12.0	10.9±2.6	68.9±5.6	38.0±12.2	56.5±19.6

n=6 per group

The phenotype of labeled CPCs was confirmed at 24 hours post-labeling by cell surface marker expression analysis of $CD144^+$, $VEGF\text{-}R2^+$, $L\text{-}selectin^+$, and $CD34^+$ (Figure 4-3B and Table 4-1). There was no significant difference among these three groups for any of the markers (all $p \geq 0.30$), suggesting that neither radiolabeling method affected the phenotype of CPCs.

To define whether radiolabeling induces the cytotoxicity in cell function, *in vitro* migration potential of labeled cells was tested (Table 4-1). The number of migrating cells /FOV was not significantly different between ^{18}F-HFB-CPCs, ^{18}F-FDG-CPCs, and unlabeled controls (p=0.90), indicating the functional activity of human CPCs to migrate in response to VEGF in an *in vitro* assay was not affected by ^{18}F-HFB or ^{18}F-FDG radiolabeling.

In Vitro Retention of ^{18}F-HFB or ^{18}F-HFB-CPCs in the Collagen Matrix

To identify whether collagen matrices retain ^{18}F-HFB, the retention of ^{18}F-HFB in matrices was measured *in vitro*. When ^{18}F-HFB was added directly to the matrix, 65.9±5.4% ^{18}F-HFB was retained in the matrices after its gelling. After a 2h- incubation, 93.4±1.4% of this retained activity was still in the matrix, while the radioactivity of ^{18}F-HFB-CPCs within the matrix was 90.5±6.0%, and the radioactivity of ^{18}F-HFB-CPCs alone was 86.6±3.5%, with no significant difference among these three groups (p= 0.14, Figure 4-4). The retained radioactivity of ^{18}F-HFB alone without cells in the collagen matrix was significantly higher than that of ^{18}F-FDG alone in the matrix (4.1±1.0%, p<0.005).

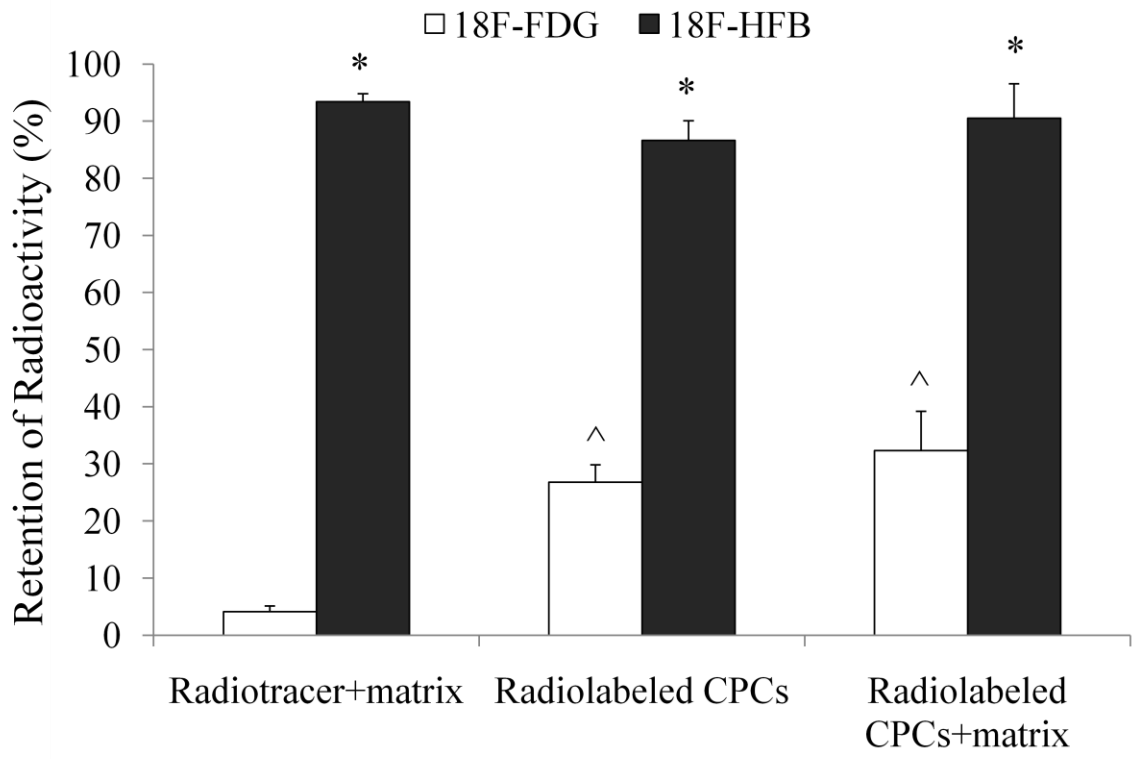

Figure 4-4: ^{18}F-HFB retention in matrices.

There was no difference between ^{18}F-HFB+matrix, ^{18}F-HFB-CPCs and ^{18}F-HFB-CPCs+matrix. However, retention of ^{18}F-HFB in the matrix was significantly higher than that of ^{18}F-FDG (*p<0.05 versus all ^{18}F-FDG groups; ^p<0.05 versus ^{18}F-FDG +matrix; n≥4/group).

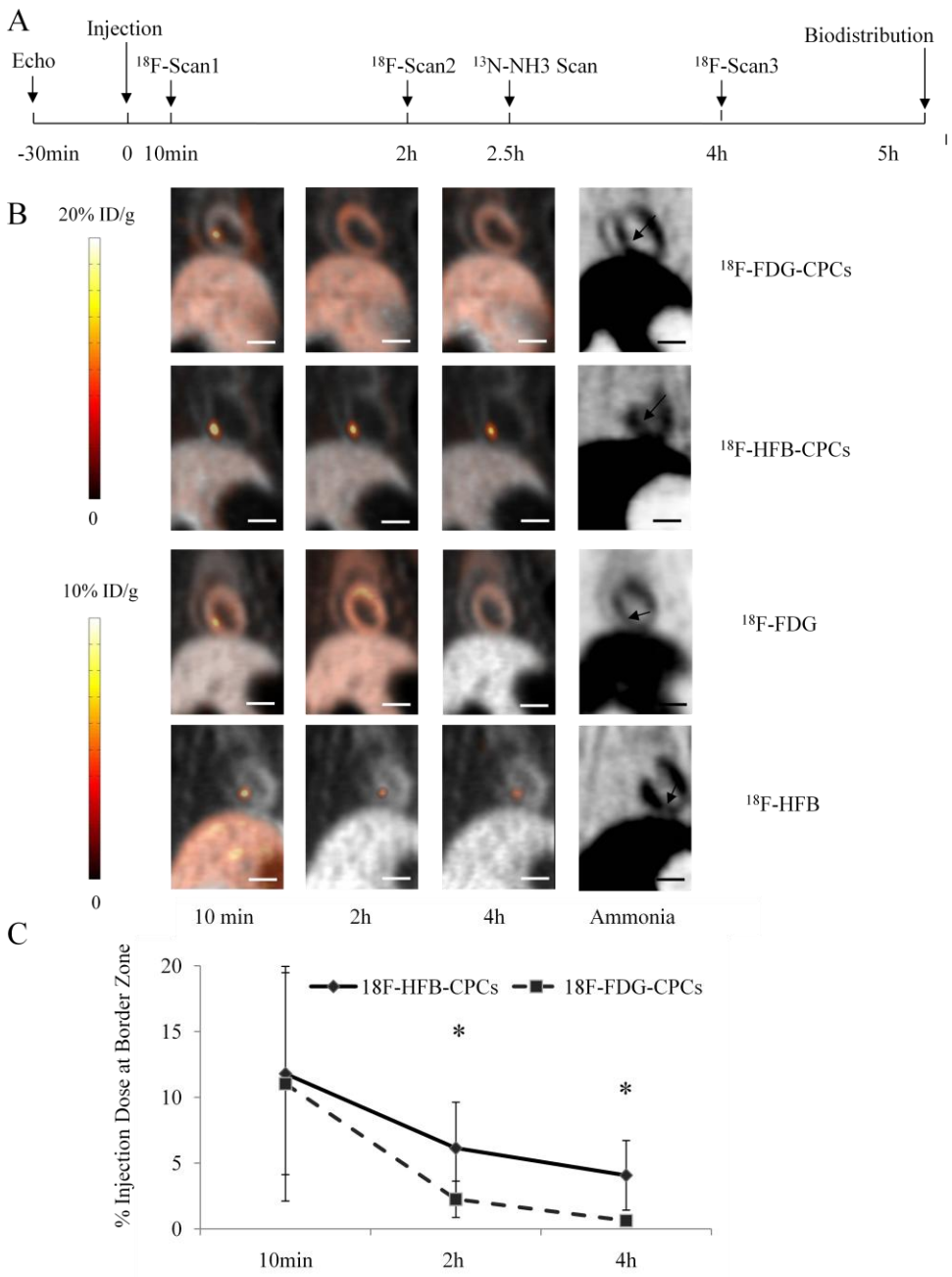

Figure 4-5: Dynamic PET imaging of labeled-CPCs after intramyocardial injection.

A) Flow diagram of *in vivo* study; B) PET fusion image (coronal view) of ^{13}N-NH$_3$ (gray) and ^{18}F (color) indicated the distribution of transplanted cells or radiotracers in the MI rat at 10 minutes, 2 hours and 4 hours post-injection; ^{13}N-NH$_3$ image showing reduced myocardial perfusion in the infarct area, (arrows). Scale bar = 10 mm; C) Kinetics of transplanted CPCs at the border zone of infarcted myocardium (*****p<0.05 versus ^{18}F-FDG-CPCs, n=5/group).

Dynamic PET Imaging and Cell Kinetics of Transplanted CPCs in Myocardium

The range of radioactivity of injected ^{18}F-HFB-CPCs was 0.6-10.9MBq (0.02-0.29mCi), and cell viability was 86.6-94.3%; while the range of activity of ^{18}F-FDG-CPCs was 0.5-3.5MBq (0.01-0.10 mCi), and cell viability was 88.1-93.5%.

After cell delivery, PET images of rats were acquired (Figure 4.5A). Dynamic PET imaging (Figure 4-5B) delineated the myocardial infarct area (ammonia images) and demonstrated the kinetics of transplanted CPCs (fusion images) in the myocardium and other organs (such as liver and lungs). Only a small portion of transplanted cells was retained in the injection site of both ^{18}F-HFB-CPC (11.8±7.7%ID) and ^{18}F-FDG-CPC (11.0±8.9%ID) rats at 10 minutes post-transplantation. In images of the ^{18}F-HFB-CPC rats, radioactivity in the infarct border zone progressively declined to 6.9±3.5%ID after 2 hours and 4.7±2.7%ID after 4 hours. However, this was greater than that observed for ^{18}F-FDG-CPCs (2.5±1.2%ID and 1.4±0.5%ID at 2 and 4 hours, respectively; $p<0.05$; Figure 4-5C).

Outside the injection site, some activity was present in the normal myocardium, lungs, liver, and other tissues (Figure 4-6). At 10 minutes post-injection (Figure 4.6A), a transient high lung uptake was observed in ^{18}F-HFB-CPC (2.3±0.9%ID/g) and ^{18}F-FDG-CPC (2.3±1.9%ID/g) rats. In animals treated with ^{18}F-HFB alone, a different tracer distribution was observed, with an obvious high liver activity (5.1±2.4%ID/g); whereas high uptake was visible in the normal myocardium of ^{18}F-FDG rats (1.3±0.3%ID/g). At 2 hours post-injection (Figure 4-6B), the most notable change was the relocation of activity from the injection site to the normal myocardium of ^{18}F-FDG-CPC rats. At 4 hours post-injection (Figure 4-6C), retention of ^{18}F-HFB-CPCs in the border zone (17.6±13.3%ID/g)

was still observed. In contrast, there was no significant difference between the activity of injection site and normal myocardium of ^{18}F-FDG-CPC rats (2.6±0.7%ID/g versus 2.4±0.4%ID/g). In both ^{18}F-HFB-CPC and ^{18}F-FDG-CPC groups (1.6±0.6%ID/g and 1.9±1.1%ID/g, respectively), a slightly higher uptake was detected in the liver compared to ^{18}F-HFB and ^{18}F-FDG rats.

Radionuclide Biodistribution of CPCs in Rats

Consistent with the *in vivo* ^{18}F-HFB-CPC images, the majority of the radioactivity was detected in the border zone at 5 hours after intramyocardial injection of CPCs. Tissue radionuclide biodistribution (Figure 4-7) indicated that 17.2±8.9%ID/g was detected in the border zone of ^{18}F-HFB-CPC rats, compared to only 3.1±1.5 %ID/g in ^{18}F-FDG-CPC rats (p<0.05). No significant radioactivity was detectable in the normal myocardium of ^{18}F-HFB-CPC (0.7±0.6%ID/g) and ^{18}F-HFB (0.5±0.4%ID/g) rats, whereas ^{18}F-FDG-CPC (3.0±1.6 %ID/g) and ^{18}F-FDG (3.7±1.7%ID/g) rats showed relative high uptake in this region. Outside the border zone, liver, spleen, lung and bone marrow showed cell accumulation in cell transplantation rats.

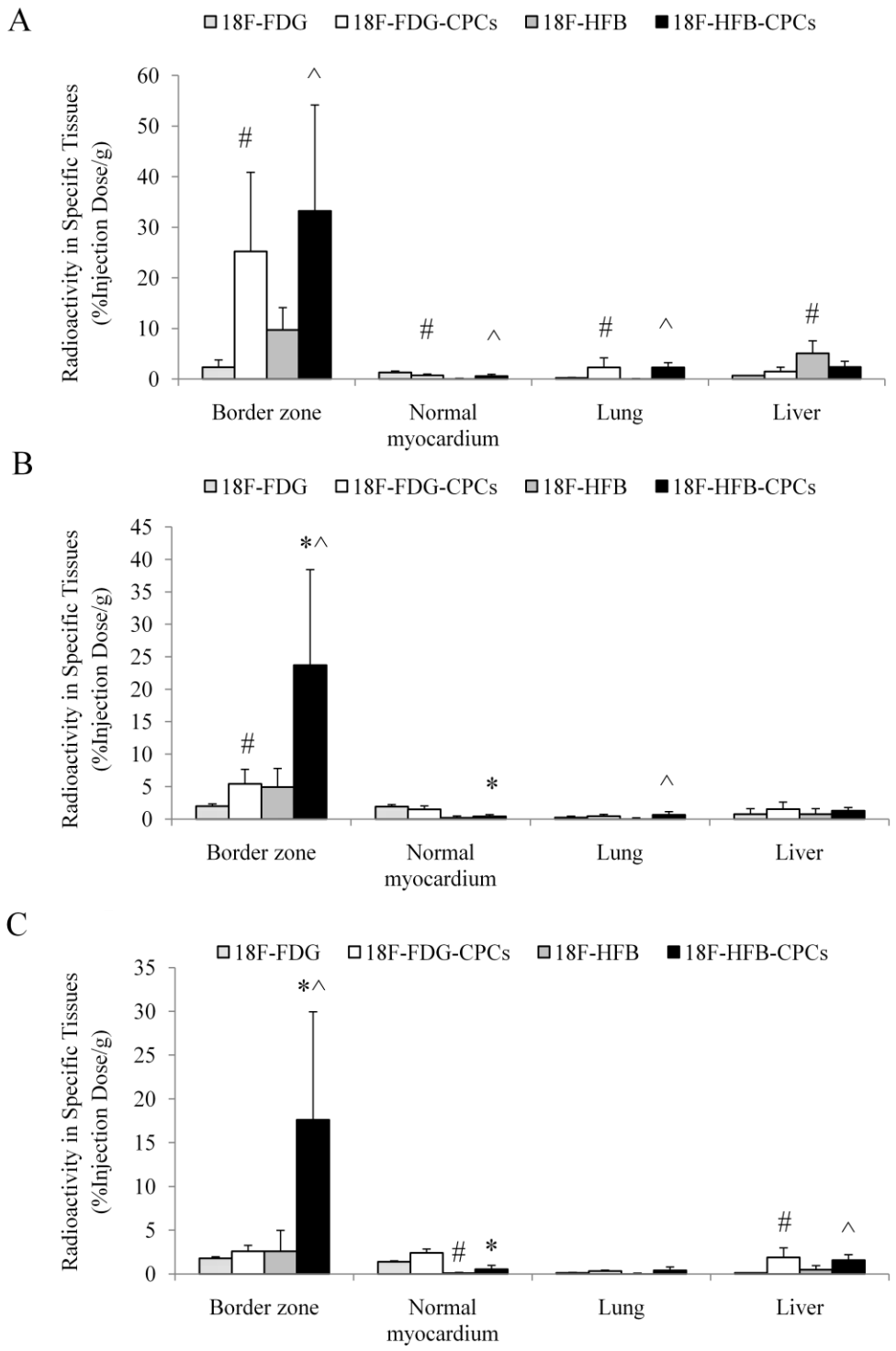

Figure 4-6: The dynamic distribution of transplanted CPCs.

PET images indicated radioactivity measured at the border zone, normal myocardium, lung and liver at: A) 10 minutes post-injection; B) 2 hours post-injection; C) 4 hours post-injection (*****p<0.05 versus ^{18}F-FDG-CPCs; ^p<0.05 versus ^{18}F-HFB; $^{\#}p$<0.05 versus ^{18}F-FDG; n=5/group).

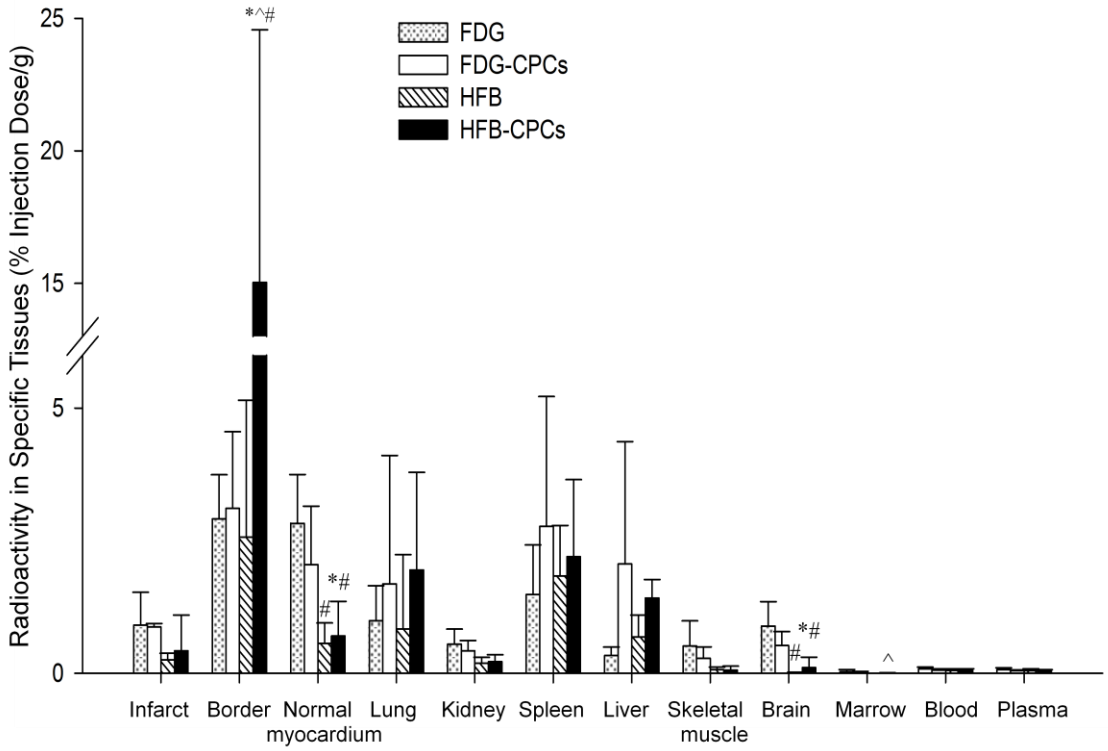

Figure 4-7: Biodistribution of radioactivity in different organs at 5 hours post-injection.

The activity of ^{18}F-HFB-CPCs in the border zone of infarcted myocardium was greater than that of ^{18}F-FDG-CPCs (*p<0.05 versus ^{18}F-FDG-CPCs; ^p<0.05 versus ^{18}F-HFB; $^{\#}p$<0.05 versus ^{18}F-FDG).

Detection of Transplanted CPCs by Immunofluorescence

To confirm the results obtained by PET imaging and radiotracer biodistribution, and to gain further insight into transplanted CPC incorporation in the myocardium, immunofluorescence was performed on heart tissue sections. In the heart of cell-transplanted rats, injected CPCs (human mitochondria^{+} cells) were found predominantly in the border zone (Figure 4-8A-B). In contrast, transplanted cells were rarely detectable in the infarct scar and normal myocardium. There was no significant difference in the percentage of transplanted cells /FOV at the border zone between ^{18}F-HFB-CPC rats (3.0±0.7%) and ^{18}F-FDG-CPC rats (2.6 ±0.6%, p=0.21). To further evaluate the accuracy of ^{18}F-HFB and ^{18}F-FDG labeling, a correlation between immunostaining and biodistribution results was analyzed. Better correlation was observed for the ^{18}F-HFB-CPC group (r=0.81, p<0.05; Figure 4-8C), compared to that of ^{18}F-FDG-CPCs (r=0.51, p<0.05; Figure 4-8D).

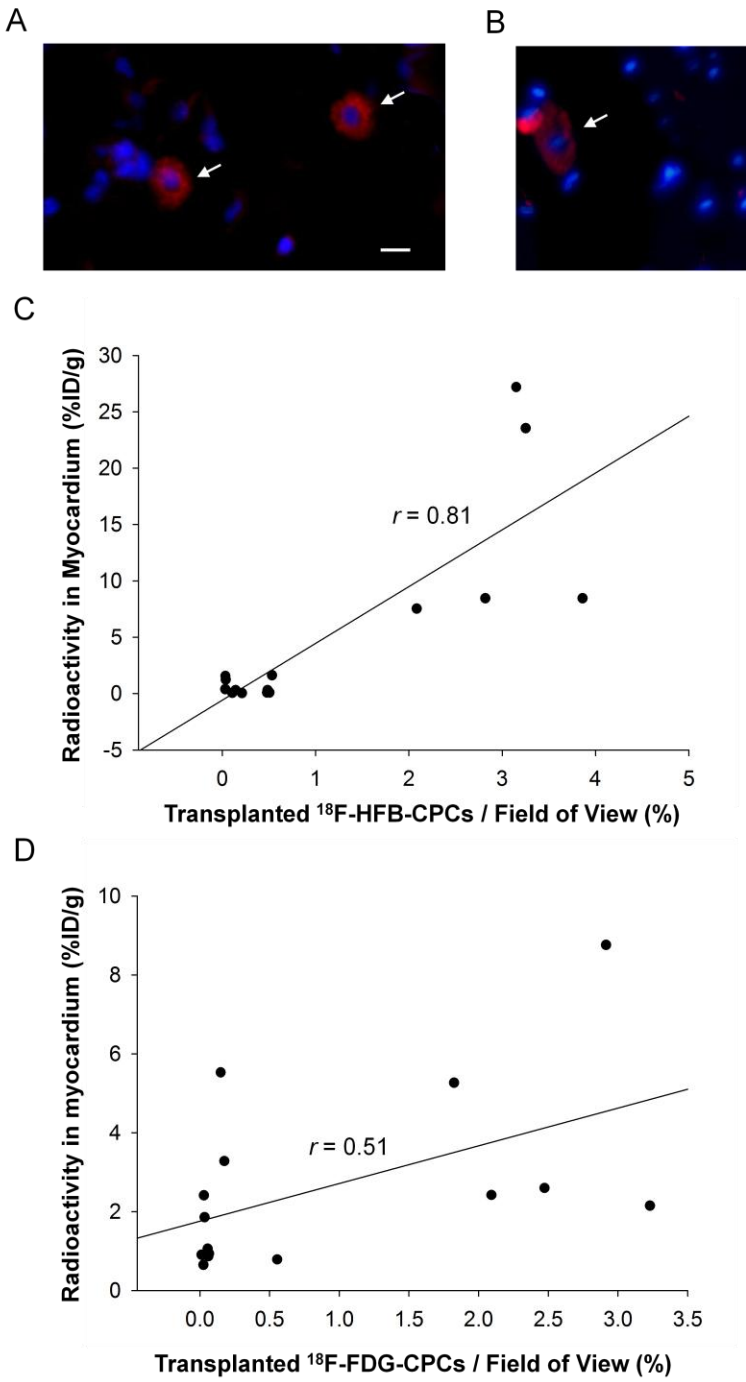

Figure 4-8: Immunofluorescence identification of transplanted cells in the border zone of infarcted myocardium.

A-B) Transplanted CPCs (arrows) in the border zone of A) ^{18}F-HFB-CPC and B) ^{18}F-FDG-CPC rats identified by specific anti-human mitochondria (red, cytoplasm) and DAPI (blue, nucleus). Scale bar = 12.5 µm; C-D) Correlation between immunofluorescence and radionuclide biodistribution of C) ^{18}F-HFB-CPCs and D) ^{18}F-FDG-CPCs in rat hearts. A better correlation was observed for the ^{18}F-HFB-CPC group.

Discussion

The results of our study demonstrate that labeling with ^{18}F-HFB is a feasible method to assess the homing and tissue distribution of transplanted human CPCs *in vivo* with PET. Labeling CPCs with ^{18}F-HFB provided a more efficient, stable, and accurate way to quantify cell distribution compared to the more commonly used ^{18}F-FDG labeling method. PET imaging of ^{18}F-HFB-CPCs revealed a significant cell washout from the myocardium immediately after intramyocardial injection, with only a small proportion (2-7%) of transplanted CPCs remaining in the border zone of infarcted myocardium 4 hours after delivery.

Consistent with previous use in rat MSCs (Ma et al. 2005), ^{18}F-HFB uptake into human CPCs was modest (12-48%), and ^{18}F-HFB is efficiently retained in CPCs over 4 hours (77-95%) *in vitro*. Optimal labeling efficiency was obtained at 37°C and high cell concentration conditions. In the comparison study, ^{18}F-FDG, the widely available radiotracer, showed a low labeling efficiency of less than 10%, with a high efflux (only 22-33% retained in CPCs) over the same time period. Overall, the labeling efficiency and stability for ^{18}F-HFB was significantly higher than ^{18}F-FDG. This may be due in part to the uptake and retention mechanism of ^{18}F-FDG, which depends on cell glucose transporters. ^{18}F-FDG remains trapped within the cells as the fructose-6 phosphate analogue (^{18}F-FDG-6P), except when it is dephosphorylated to ^{18}F-FDG by glucose-6-phosphatase (Plathow et al. 2008). Consequently, the ^{18}F-FDG labeling method is likely better suited for cells with low levels of glucose-6-phosphatase; and this may partly explain the difference in labeling efficiency of ^{18}F-FDG in various cell types (Hofmann et al. 2005; Rini et al. 2006). In contrast, ^{18}F-HFB, a lipophilic molecule, incorporates

within the cell membrane, and is independent of any receptor-mediated effect. The calculated logP value for ^{18}F-HFB is 10.189 (for ^{18}F-FDG, it is -2.0085); since a high logP value is indicative of hydrophobic molecules that cannot be dissolved directly in an aqueous buffer, it is easily understandable that ^{18}F-HFB sticks and is retained in the lipophilic cell membrane.

PET imaging demonstrated a greater signal of ^{18}F-HFB-CPCs in the injection site compared with ^{18}F-FDG-CPCs a few hours after cell transplantation. There was no significant difference in the distribution of ^{18}F-HFB-CPCs and ^{18}F-FDG-CPCs at 10 minutes post-injection. However, after 2 and 4 hours, the signal intensity of ^{18}F-HFB-CPCs was much greater than that of ^{18}F-FDG-CPCs. In contrast, the radioactivity was high in the normal myocardium of ^{18}F-FDG-CPC rats at this time period. However, immunofluorescence examination revealed that transplanted human CPCs were rare in the normal myocardium. We consider the well-known efflux of ^{18}F-FDG from labeled cells as the main reason for the high uptake in this area. Consistent with the PET images of free ^{18}F-FDG, the normal myocardium exhibited a high portion of activity that was unbound ^{18}F-FDG, and not transplanted ^{18}F-FDG-CPCs. We also found that ^{18}F-HFB radioactivity was rarely taken up by infarcted and normal myocardium. Therefore, ^{18}F-HFB cell labeling may be more reliable method for assessing the distribution of transplanted human CPCs, especially in the myocardium.

PET imaging indicated an ^{18}F-HFB-CPC-associated distribution of radioactivity, which is markedly different from the distribution of the free ^{18}F-HFB after intramyocardial injection. Up to 4 hours after injection, radioactivity was predominantly located in the border zone (injection site) of ^{18}F-HFB-CPC rats. Immnunostaining

revealed many intact CPCs in this region and good correlation between the histological examination and tissue radionuclide biodistribution results. Although few transplanted cells were found in the infarct scar area, cytokines and growth factors might recruit transplanted cells to the injured territory (Takahashi et al. 1999; Shintani et al. 2001). It is known that acute ischemia enhances the expression of chemoattractants and cytokines mediating homing of CPCs. However, the infarct centre may lack living cells and, thus may not furnish the necessary instructive signals and/or blood flow for the delivery of oxygen and nutrients needed for transplanted cell survival and differentiation (Dimmeler et al. 2005). Therefore, the border zone might be the better region for stem cell delivery, homing and engraftment.

Our findings also demonstrated a negative effect of ^{18}F-HFB on cell viability after 24 hours, although no significant alteration was observed in cell phenotype and migration ability at this time point. At 5 days post-labeling, both ^{18}F-HFB and ^{18}F-FDG reduced cell viability. Further investigation indicated free HFB is partly responsible for the observed cell death. We also found that labeling with ^{18}F-HFB using the same concentration of CPCs (2×10^6 cell/mL) but a higher radioactivity (259-296MBq) resulted in significant cell death (data not shown). Although the mean labeling efficiency was not changed, the radioactivity in single cells increased. In accordance with previous studies (Botti et al. 1997; Brenner et al. 2004), the increased radioactivity could be another cause of cell death. This is the first study investigating the cytotoxicity of ^{18}F-HFB labeled cells. Although cultivated CPCs showed a low sensitivity to irradiation-induced cell dysfunction, we would still recommend the use of a combination of radiolabeled cells with unlabeled cells in clinical trials (Hofmann et al. 2005). For future studies in cell

imaging with radiolabeling, it will be necessary to carefully check for radiation-induced impairment of cell viability and function. Another limitation of ^{18}F-HFB is the short half-life (110 minutes) of ^{18}F, so that cell homing, retention and survival can be assessed only in the first few hours. Other PET isotopes with longer half-lives may be worth pursuing. For example, ^{64}Cu-pyruvaldehyde-bis-(N^4-methylthiosemicarbazone) (half-life of 12.7 hours) has been used for tracking C_6 rat glioma cells up to 24-36 hours (Adonai et al. 2002). Another commonly used imaging technique considered for cell tracking is magnetic resonance imaging (MRI), in which cells are labeled with iron oxide (Nohroudi et al. 2010) or paramagnetic particles (Mai et al. 2009). However, MRI signals cannot reliably indicate whether cells are dead or alive. While short-term monitoring of cells does not give insight into the long-term engraftment and function of the therapeutic cells, without the initial homing event, the cells cannot exert either their paracrine or regenerating effects.

In this study, we used an echo-guided intramyocardial injection technique to deliver cells into the target site of rat myocardium in a closed-chest fashion with a high success rate. By using this novel approach, we can remove the animals with unsuccessful injections from the study at the time of the injection to assure uniformity of the study groups. Successful injection was corroborated by PET images. Although the fusion (injection sites) and ^{13}N-NH_3 (infarct areas) PET images are shown at different slices, the maximum distance between the injection site and infarct scar was less than 3mm, confirming cell delivery to the border zone.

The use of circulatory stem cells for therapy is an attractive approach considering the noninvasive nature of cell procurement (Zhang et al. 2010; Suuronen et al. 2006).

Experimentally, the administration of CPCs to ischemic or infarcted myocardium has resulted in increased blood vessel formation, decreased infarct size, and improved ventricular function (Kawamoto et al. 2003). Reports have also shown that CPCs can prevent cardiomyocyte apoptosis, reduce remodeling and improve cardiac function in areas of neovascularized ischemic myocardium (Kocher et al. 2001). Intramyocardial delivery of CPCs has recently been shown to enhance left ventricular ejection fraction recovery in patients after AMI (Losordo et al. 2007). Previous work using ^{111}In-oxine-labeled human PBMNCs has demonstrated that the intramyocardial injection technique displayed greater delivery efficiency compared with intracoronary and interstitial retrograde coronary venous delivery in an ischemic swine model (Hou et al. 2005). In our study, intramyocardial injection resulted in about 20% of transplanted CPC retention at 10 minutes post-injection; but subsequently, some injected cells moved to the pulmonary circulation, liver, spleen and bone marrow. Therefore, the absolute number of CPCs engrafted in the heart is still rather low, which is in accordance with previous studies (Hou et al. 2005). A low rate of cell persistence is a potential limitation for cell therapy. One may speculate that the use of tissue engineered scaffolds will enhance the local retention and therapeutic effects of cells in the injured myocardium (Suuronen et al. 2006; Suuronen et al. 2008). We have previously used ^{18}F-FDG labeling to successfully assess the ability of tissue-engineered matrices to improve the early retention of transplanted progenitor cells (Zhang et al. 2008). The current study suggests that ^{18}F-HFB may also be suitable for such an application. Unlike ^{18}F-FDG, for which only 10-20% was retained in the matrix, the collagen matrices can bind 60-75% of ^{18}F-HFB and about 90% of this activity will remain in the collagen matrix after a 2h- incubation. However,

the leakage of ^{18}F-HFB from labeled CPCs is minimal (only 8-15% after 4 hours). Although this small amount of activity may be trapped in the matrix, it will be insignificant compared to the activity retained by ^{18}F-HFB-CPCs in the matrix. Therefore, it is possible that ^{18}F-HFB may be usable as a tracer to assess the location and fate of injected biomatrices in future studies. Therefore, ^{18}F-HFB with PET imaging could be used to screen various bioengineering, pharmacological or genetic techniques that may enhance myocardial homing and therapeutic efficacy of transplanted stem cells (Ruel et al. 2008).

Conclusions

In summary, the results of this study demonstrate that ^{18}F-HFB is a usable tracer for *in vivo* monitoring of transplanted human CPCs in a rat model of myocardial infarction. ^{18}F-HFB labeling with PET imaging can help evaluate the efficacy of stem cell delivery and retention in the target tissue quantitatively. Compared to ^{18}F-FDG, the potential of ^{18}F-HFB labeling to detect differences in cell homing between the border zone and normal myocardium suggests that this method may provide a better modality to enhance our understanding of early retention, homing, and engraftment with cardiac cell therapy.

ACKNOWLEDGMENTS

This work was supported by the Heart & Stroke Foundation of Ontario (program Grant, PRG 6242; grant NA5905 to Drs. Ruel and Beanlands; grant T6793 to Dr. Suuronen), the Canadian Institutes of Health Research (grant MOP-77536 to Drs. Ruel and Suuronen) and the Canadian Foundation for Innovation (award 7346 to Dr. Ruel). Dr. Zhang and S. Thorn are recipients of Doctoral Research Awards from the Heart and Stroke Foundation of Canada. D. Kuraitis was supported by a Canadian Institutes of Health Research Canadian Graduate Scholarship.

DISCLOSURES

None

CHAPTER 5: MANUSCRIPT #4

Introduction to Manuscript #4

Direct cell radiolabeling methods with PET have been used to track transplanted stem cells noninvasively. However, this technique can only monitor the cells for several hours due to the short half-life of PET radioisotopes. For the long-term evaluation of transplanted cell fate and for further investigation of the role of delivery matrices in cell therapies, reporter gene-based cell labeling is being developed. To apply the reporter gene-based PET imaging, the first step is to deliver the PET reporter gene to the target cells. In this study, I transduced human CPCs with lentiviral vectors to express PET reporter gene: the herpes simplex virus thymidine kinase (HSV1-*tk*) or its mutant HSV-*sr39tk*.

Nuclear Medicine Biology (to be submitted)

Development of Reporter Gene PET Imaging Techniques for Long-term Assessment of Transplanted Human Circulating Progenitor Cells

Yan Zhang[a,b], Patrick G. Burgon[a,c], Drew Kuraitis[a,b], Suzanne Crowe[a], Branka Vulesevic[a,b], Joseph C. Wu[d], Jean N. DaSilva[a,b], Rob A. deKemp[a,b], Robert S. Beanlands[a], Erik J. Suuronen[a,b,*], Marc Ruel[a,b,*]

[a] University of Ottawa Heart Institute

[b] Department of Cellular and Molecular Medicine, University of Ottawa

[c] Department of Biochemistry, University of Ottawa

[d] Department of Medicine (Division of Cardiology), Department of Radiology, Stanford University School of Medicine

* Corresponding authors: Marc Ruel or Erik J. Suuronen, Division of Cardiac Surgery, University of Ottawa Heart Institute.

Running title: PET reporter gene delivery into human CPCs

Contributions of Authors

Experiments described in this manuscript were designed and executed by myself, with assistance from Dr. Patrick Burgon, and practical help from Ph.D. candidate Drew Kuraitis. Suzanne Crowe and Branka Vulesevic obtained data for the flow cytometry analysis. Drs. Jean DaSilva and Robert deKemp provided input on the radioprobe and PET imaging aspects of the data. Dr. Rob Beanlands provided a clinical perspective on the data. Work performed was supervised by Drs. Marc Ruel and Erik Suuronen.

Abstract

Introduction

To develop *in vivo* positron emission tomography (PET) imaging for the investigation of cell fate and function, PET reporter genes were delivered to human circulating progenitor cells (CPCs) for monitoring transplanted cell homing and engraftment over the long-term.

Methods

Human CPCs were transduced with one of two lentiviral particles: LV-GFP-iresTK or LV-*Fluc*-RFP-tTK. The transduction efficiency was determined by flow cytometry analysis. Expression of herpes simplex virus type I thymidine kinase (HSV1-*tk*) was assessed by Western blot. The transduced CPCs were isolated by fluorescence-activated cell sorting, and the stability of reporter expression was evaluated. The effect of transduction on CPC morphology, viability and function was also determined.

Results

The mean transduction efficiency was 15% (LV-GFP-iresTK, MOI of 10) and 13% (LV-*Fluc*-RFP-tTK, MOI of 50). Western blot analysis confirmed HSV1-*tk* protein expression in transduced CPCs. There was no significant difference in cell viability between the transduced CPCs and the untreated controls at a MOI of 50 or below. However, a reduction was observed in cell viability of CPCs transduced with LV-*Fluc*-RFP-tTK at an MOI of 100. Both transduced and control CPCs exhibited similar rounded or spindle shapes. Cell migration and angiogenesis potentials were not adversely affected by lentiviral transduction. After 4 weeks, 80.3±8.4% of the sorted cells continued to express the reporters.

Conclusion

Quiescent human CPCs transduced with lentiviral vectors show stable expression of reporter genes. The reporter gene approach may be developed for tracking transplanted CPCs noninvasively by PET, while preserving the cell's morphology, viability, migration and angiogenesis capabilities.

Key words: circulating progenitor cells; reporter gene; gene delivery; lentiviral transduction; positron emission tomography

Introduction

Many studies demonstrate that circulating progenitor cells (CPCs) have considerable potential for the treatment of tissue ischemia and myocardial infarction (Assmus et al. 2002). Because they can be isolated from the peripheral blood of adult patients, CPCs are the one of most accessible cell types for autologous cell therapy. To better define whether a CPC and its progeny can contribute to the repair of injured tissue, noninvasive approaches for long-term follow-up studies are needed.

One recent major advance in the field of clinical molecular imaging has come into play in the form of reporter gene techniques that enable the study of stem cell therapy over a long time period. Positron emission tomography (PET) imaging appears to be a choice to monitor the engrafted cells, due to its high sensitivity and suitable spatial resolution. By appropriate reporter gene transfer into CPCs, it may be possible to assess the fate of transplanted cells *in vivo* with PET imaging. Reporter gene-based PET imaging was initially described by Tjuvajev et al in 1995 (Tjuvajev et al. 1995). An approach was developed to visualize the expression of the viral enzyme, herpes simplex virus type I thymidine kinase (HSV1-*tk*). Since then, HSV1-*tk* has been the most commonly used reporter gene for PET applications. Recently, a "second generation" mutant HSV1-*tk* reporter gene, HSV1-*sr39tk* (a deletion in the first 135bp that contains the nuclear location signal) has been developed. It was reported that HSV1-*sr39tk* might provide a further increase in imaging sensitivity compared to HSV1-*tk* (Yaghoubi et al. 2006).

To implement reporter gene-based PET imaging of cells, the reporter must be introduced into the target cells. To this end, a variety of methods, including transfection

of plasmid DNA, transduction with viral vectors, or incorporation into the DNA of genetically engineered animals, has been developed (Sharma et al. 2002). As the most commonly used method for gene delivery, viral vectors can generally provide sufficient transfection efficiency for most types of cells (Kay et al. 2001). Different viruses, such as retroviruses, lentiviruses, adenoviruses, and adeno-associated viruses, have been used as transfer vectors. However, adenoviral vectors can not give the gene integration. For retroviral mediated gene delivery, the cells need to be dividing, so that their nuclear membranes are broken down, for the gene to enter and intergrate into the chromosomes of target cells. Currently, due to these limitations, the use of PET reporter genes is not well-documented in primary adult stem cells (such as human CPCs).

Compared to other vectors, lentiviruses offer unique versatility and robustness as vehicles for gene delivery (Tiscornia et al. 2006). The reporter gene delivered by lentiviruses can be stably integrated into the host cell genome, thus the reporter will not be lost or diluted upon cell division, resulting in long-term expression of transgene both *in vitro* and *in vivo* (Romano et al. 1999). Because their preintegration complex can get through the intact membrane of the cell nucleus, lentiviral vectors can transduce a wide range of cell types (dividing and non-dividing cells), thus might be a good candidate of gene delivery vectors for the study of human CPCs.

In this study, to enable future investigatation of cell fate and function by PET imaging, we delivered HSV1-*tk* and HSV1-*sr39tk* to human CPCs by using two lentiviral vectors: LV-GFP-iresTK expressing genes that encode the enhanced green fluorescence protein (GFP) and HSV1-*tk*, and LV-*Fluc*-RFP-tTK, which carries a triple-fusion reporter

(TFR) construct consisting of firefly luciferase (*Fluc*), monomeric red fluorescence protein (RFP), and HSV1-*sr39tk* (truncated HSV1-*tk*, tTK) genes.

Methods

Purification of Plasmids

The transfer vector plasmid, pCMV-GFP-iresTK (Addgene, Cambridge, MA) or pUb-*Fluc*-RFP-tTK (kindly provided by Dr. Joseph Wu at Stanford University) was purified by QIAGEN purification kit (QIAGEN, Mississauga, ON, Canada). The structure of pCMV-GFP-iresTK was confirmed by restriction enzyme analysis and polymerase chain reaction. The expression of HSV1-*sr39tk* and RFP in pUb-*Fluc*-RFP-tTK was confirmed by DNA sequencing using the following primers: 1) TK_1: CAC GGG ATG GGG AAA ACC; 2) TK_2: ATC GCC TTC ATG CTG TGC TAC; 3) TK_3: GTT CCA TGC ACG TCT TTA TCC TG; 4) RFP_1: CTC CGA GGA CGT CAT CAA GTT C; 5) RFP_2: CCC ACA ACG AGG ACT ACA CCA T.

Production of Lentiviral Particles

The self-inactivating bicistronic lentiviral vector LV-GFP-iresTK was produced by transient co-transfection into HEK-293T cells with pCMV-GFP-iresTK, psPAX2, and pMD2.G plasmids (Addgene) by using the calcium-phosphate precipitation method (Naldini et al. 1996). Sixteen hours after transfection, the medium (Dulbecco's modified Eagle's medium supplemented with 10% fetal bovine serum and 1% penicillin /streptomycin solution) was changed. Lentiviral supernatant was collected from the first (24 hours) and second (48 hours) harvests, and then filtered through a 0.45-μm filter. The vector particles were concentrated by ultracentrifugation at 19,500 rpm in a Beckman

SW32 Ti rotor for 2 hours. The supernatant was discarded and the pellet was resuspended in 300 µL PBS. The concentrated vector was used directly or aliquoted, and stored at -80 ^{o}C.

Another lentiviral vector, LV-*Fluc*-RFP-tTK was produced by a 293FT cell transient system (Invitrogen, Burlington, Canada) with pUb-*Fluc*-RFP-tTK, psPAX2, and pMD2.G plasmids (Sun et al. 2009). Collected supernatant was centrifuged (1500*g*, 15 minutes), and then the clear supernatant was mixed with 5×PEG-it Lentivirus Concnetration Solution (System Biosciences, Mountain View, CA) overnight. After centrifugation (1500*g*, 30 minutes), the pellet of viral particles was resuspended in 300 µL PBS.

Titer of the Generated Viral Particles

Concentrated virus was titered on 293T cells, as described previously (Tiscornia et al. 2006). Briefly, 293T cells (1.0×10^{4}) were plated in a well of a 24-well plate and cultured overnight. Cells were 60-70% confluent at the time of transduction. The number of cells /well was counted before the transduction. A 10-fold serial dilution (from undiluted to a dilution of 10^{-6}) of viral particles in medium was added to the cells. After a 24-hour incubation, the medium was changed. After another 48 hours, the cells were observed under a fluorescence microscope and then examined by flow cytometry analysis. The titer of vector particles was calculated using the following formula:

$$\text{Vector Titer (pfu/mL)} = \frac{\text{Number of GFP}^{+}\text{ (or RFP}^{+}\text{) cells}}{\text{Dilution factor} \times \text{Volume}}$$

Preparation of Human CPCs and Collagen-based Matrices

Human CPC procurement was approved by the Human Research Ethics Board of the University of Ottawa Heart Institute. After acquiring informed consent from healthy human donors, total peripheral blood mononuclear cells (PB-MNCs) were freshly isolated from human peripheral blood by Histopaque 1077 (Sigma-Aldrich, Oakville, Canada) density-gradient centrifugation. Subsequently, PB-MNCs were cultured on fibronectin-coated plates in endothelial basal medium (EBM-2; Clonetics, Guelph, Canada) supplemented with EGM-2-MV-SingleQuots. After 4 days, the adherent population (CPCs) was collected as described previously (Ruel et al. 2005).

The collagen-based matrices (pH 7.5) were prepared on ice. Briefly, matrices consisted of a mixture of 0.4% blended neutralized type I rat tail tendon collagen (Becton Dickinson, Mississauga, Canada) and chondroitin 6-sulfate, cross-linked with 0.02% glutaraldehyde, followed by glycine termination of unreacted aldehyde groups (Zhang et al. 2008).

Human CPC Transduction

Human CPCs were transduced with LV-GFP-iresTK at increasing multiplicities of infection (MOIs) in the presence of polybrene (8 μg/mL) (Liu et al. 2006). After 16 hours of incubation, the medium was changed and cells were further cultured for 3 days.

The produced viral particle LV-*Fluc*-RFP-tTK was also used to transduce CPCs in RetroNectin-coated plates. After 2 days, lentiviral transduction was repeated to increase transduction efficiency (Yoon et al. 2010). Briefly, floating cells were harvested, washed with PBS and then resuspended in fresh EBM medium. Fresh medium was also

added to the adherent cells and recombined with the floating cells and new viral supernatant for an additional 2 days.

Expression of Reporter Proteins in Transduced CPCs and Transduction Efficiency

The transduction efficiency was determined by flow cytometry analysis of GFP or RFP expression. The expression of GFP or RFP was also examined under fluorescence microscopy. The expression of HSV1-*tk* protein in the transduced CPCs was assessed by Western blot.

Viability and Morphology of Transduced CPCs

Cell viability was assessed using the Vi-CELL analyzer (Beckman Coulter, Mississauga, Canada) with a Trypan Blue Dye Exclusion Method. The morphology of transduced CPCs was examined under bright-field microscopy. Untreated CPCs served as controls.

Cell Function of Transduced CPCs

In vitro assays were performed to assess cell migration and angiogenesis capacities, as described previously (Zhang et al. 2010). For cell migration, briefly, the transduced CPCs or untreated controls were incubated with 4'6-diamidino-2'-phenylindole (DAPI, Molecular Probes, Eugene, OR), and then 2×10^4 cells were placed separately in the upper chamber of a modified Boyden chamber with VEGF-free media. The lower chamber contained serum-free media with 50ng/mL VEGF (Sigma-Aldrich). After 24 hours of incubation, cells that migrated into the lower chamber were counted in six random high powered fields (HPFs).

For cell angiogenesis, transduced cells or untreated cells (1×10^4) were seeded onto solidified ECMatrix (Chemicon, Temecula, CA) with 1×10^4 human umbilical vein

endothelial cells (HUVECs, supporting cells). After 24 hours of incubation, images of six random HPFs were taken and the total tube length of capillaries was measured.

Stability of Reporter Gene Expression in Transduced CPCs

The transduced CPCs were isolated by Fluorescence Activated Cell Sorting (FACS, Becton Dickinson), and the sorted GFP^+ cells were then cultured for 3 days, 1 week, 2 weeks, 3 weeks, or 4 weeks. The maintenance of GFP expression in transduced cells was assessed by flow cytometry analysis. Also, sorted GFP^+ cells (1×10^5) were mixed with the collagen-based matrix, plated in a 24-well plate, and incubated at 37ºC. The expression of GFP in CPCs was examined under fluorescence microscopy every week up to 4 weeks.

Statistical Analysis

Data are expressed as mean ± standard deviation. Statistical analyses between groups were performed with a one-way analysis of variance, with Bonferroni corrections as appropriate. Correlation analyses were performed by linear regression. Differences with $p<0.05$ were considered statistically significant.

Results

Expression of Reporter Proteins in Transduced CPCs and Transduction Efficiency

The expression of reporter proteins in CPCs is shown in Figure 5-1. Flow cytometry analysis of GFP indicated a transduction efficiency of LV-GFP-iresTK at the three different MOIs (0.1, 1, and 10), with the greatest efficiency (15.1±5.6%) obtained at a

MOI of 10 (Figure 5-1 A). Western blot analysis confirmed HSV1-*tk* protein expression in transduced CPCs (Figure 5-1 B).

The mean transduction efficiency of LV-*Fluc*-RFP-tTK in CPCs was 2.2%, 2.6%, 3.8%, 6.9%, 9.9%, 13.3% and 15.9% at MOIs of 0.1, 0.5, 2.5, 12.5, 25, 50 and 100, respectively (Figure 5-1 C). A dose-response effect was achieved by transducing cells at increasing MOIs. Western blot analysis of HSV1-*tk* protein showed results similar to RFP flow cytometry results (Figure 5-1 D). The expression of RFP in CPCs could be visualized under fluorescence microscopy when MOI was 25 or above (Figure 5-1 E).

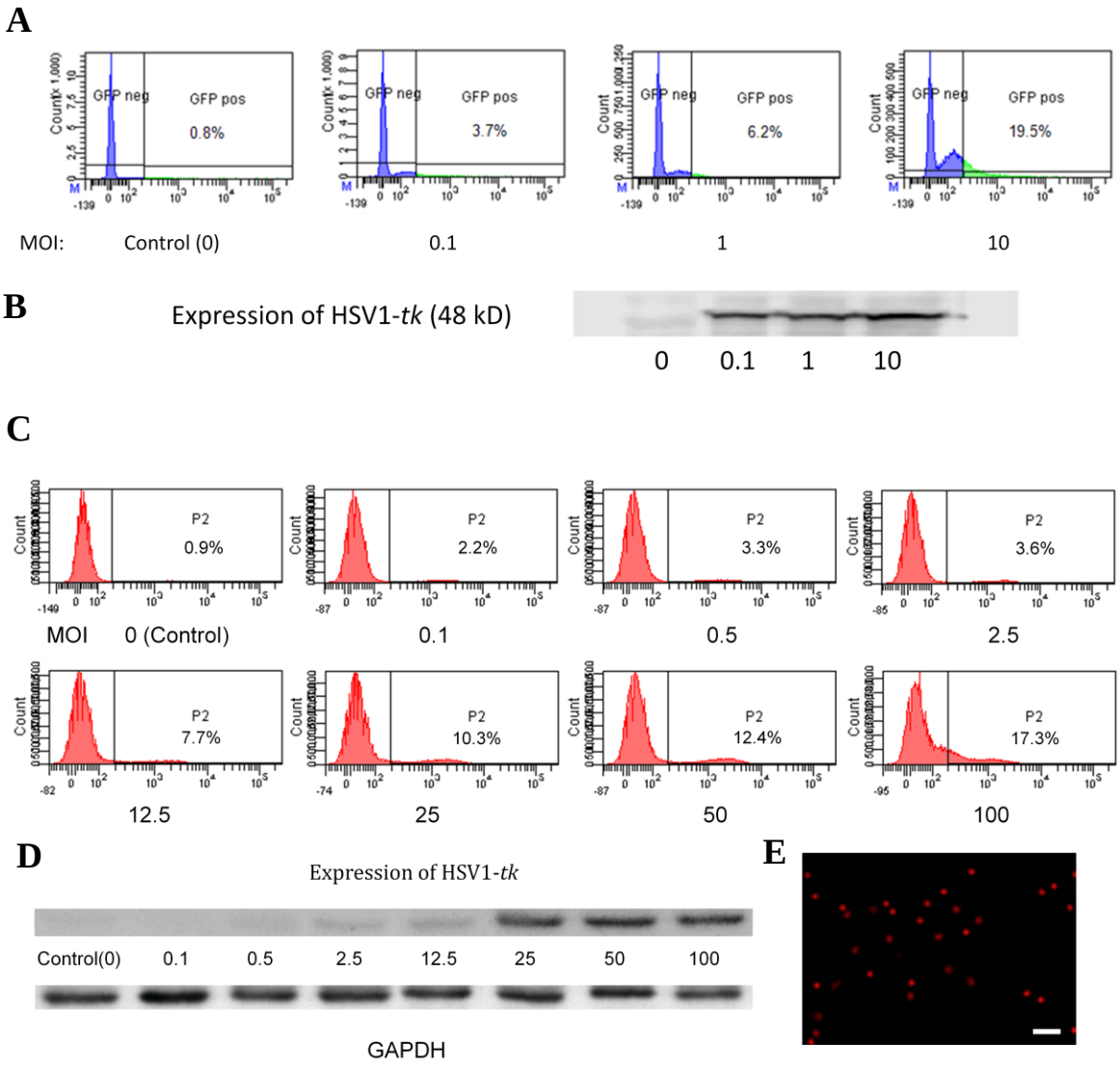

Figure 5-1: Expression of reporter proteins in transduced human circulating progenitor cells.

A-B) Cells transduced with LV-GFP-iresTK at different MOIs (0.1, 1 and 10): A) Flow cytometry analysis of GFP; B) Western blot of HSV1-*tk*. C-D) Cells transduced with LV-*Fluc*-RFP-tTK at increasing MOIs (0.1, 0.5, 2.5, 12.5, 25, 50, and 100): C) Flow cytometry analysis of GFP; D) Western blot of HSV1-*tk* and GAPDH; E) Visualization of RFP expression in transduced CPCs at a MOI of 50. Scale bar = 100µm.

Viability of Transduced CPCs

With LV-GFP-iresTK transduction (Figure 5-2 B), there was no significant difference in cell viability between the transduced CPCs (87.9±9.2%, at a MOI of 10) and the untreated controls (91.8±7.0%, p=0.62).

In the cell viability study of LV-*Fluc*-RFP-tTK transduction (Figure 5-2 C), no significant difference was observed at a MOI of 50 or below; however, there was a reduction in transduced CPC viability at a MOI of 100, compared to the untreated CPCs (66.2±9.5% versus 82.8±10.3%, p<0.05). Due to this reduction by LV-*Fluc*-RFP-tTK, LV-GFP-iresTK was used for the following studies.

Morphology of Transduced CPCs

Under the microscope, both transduced and control CPCs exhibited similar rounded or spindle shape morphology (Figure 5-2 A).

Function of Transduced CPCs

To further investigate possible cytotoxicity induced by lentiviral transduction, the migratory potential and angiogenic capacity of transduced cells were evaluated by using *in vitro* assays. The number of transduced CPCs that migrated (66.2±21.3 cells/field of view (FOV)) was not different from control cells (61.1±19.6 cells/FOV, p=0.7; Figure 5-3 A). In the angiogenesis assay, the total capillary tube length in cultures with transduced CPCs (5.6±0.6mm) was not different from cultures with control CPCs (5.7±0.5mm, p=0.8; Figure 5-3 B).

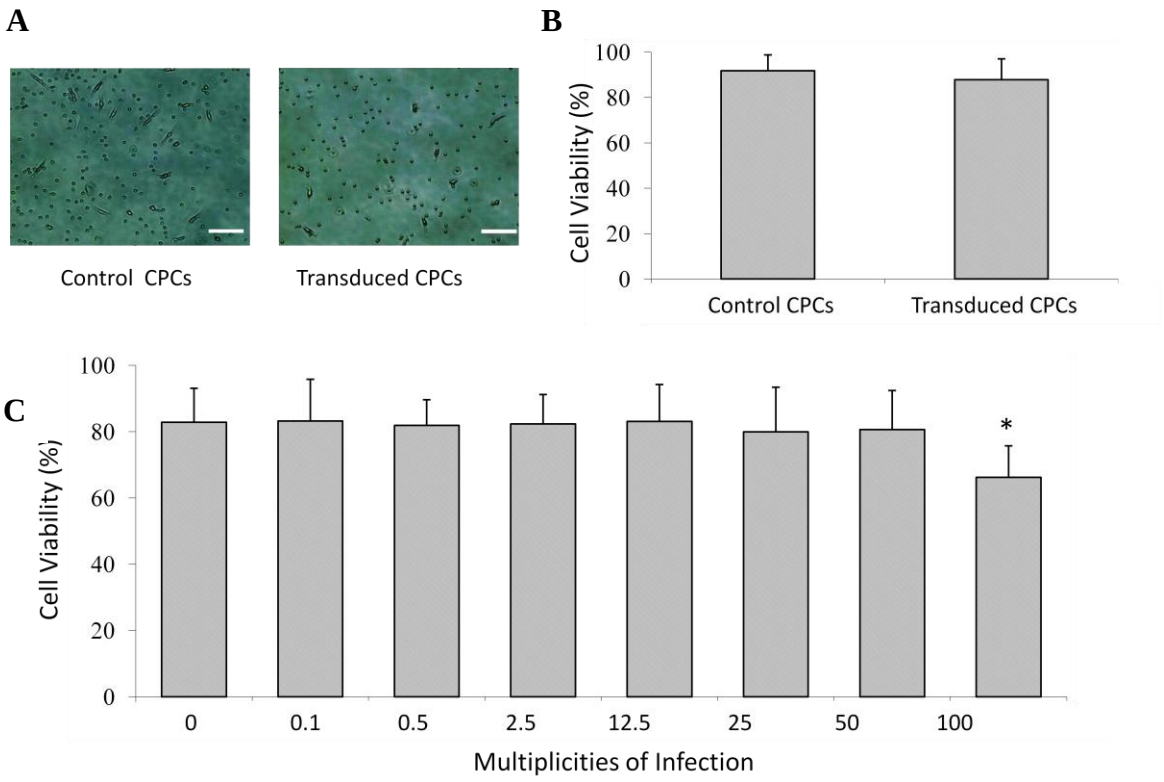

Figure 5-2: Morphology and viability of transduced circulating progenitor cells.

A) Transduced and control cells exhibited similar rounded or spindle shapes. Scale bar = 100µm. B) There was no significant in cell viability between the transduced CPCs with LV-GFP-iresTK at a MOI of 10 and the untreated controls (p=0.6). C) A reduction was observed in the cell viability of CPCs transduced with LV-*Fluc*-RFP-tTK at a MOI of 100 (*p<0.05, versus the control cells).

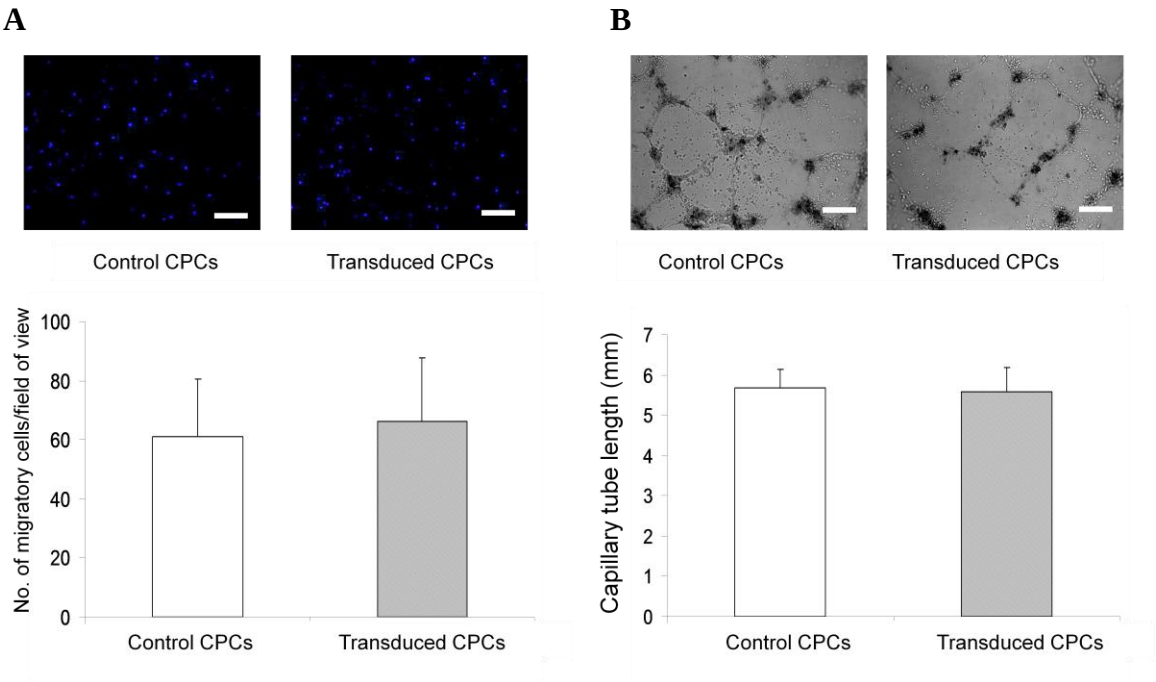

Figure 5-3: Cell function of transduced circulating progenitor cells.

A) Migration potential. B) Angiogenic capacity. Scale bar = 100μm. There was no significant difference in the number of migrating cells and the length of capillary tubes between transduced CPCs and the untreated controls (p=0.7 and p=0.8, respectively).

Stability of Reporter Gene Expression in Transduced CPCs

To test the stability of reporter gene expression in transduced cells, the maintenance of GFP expression in the sorted cells was examined by flow cytometry analysis at 3 days, 1 week, 2 weeks, 3 weeks, or 4 weeks after transduction. The result showed no significant difference up to 4 weeks after transduction (all $p>0.05$; Figure 5-4). After 4 weeks, 80.3±8.4 % of the transduced cells continued to express GFP, indicating stable transduction over this time period.

Potential of Tracking Transduced CPCs in Collagen Matrices

To evaluate the effect of matrices on transduced cells, transduced CPCs seeded in collagen matrices were examined by fluorescence microscopy every week for 4 weeks. As shown in Figure 5-5, the transduced cells could be visualized both within and without the matrix for up to 4 weeks.

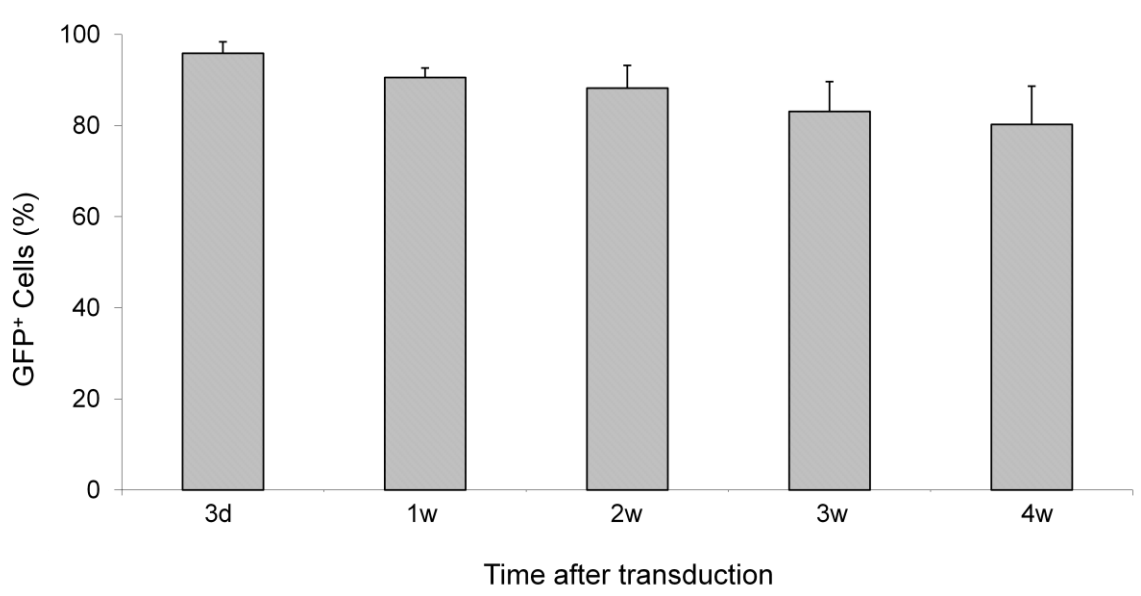

Figure 5-4: The maintenance of GFP expression in transduced circulating progenitor cells.

No significant difference was observed in the percentage of GFP^+ cells up to 4 weeks after transduction (all $p>0.05$).

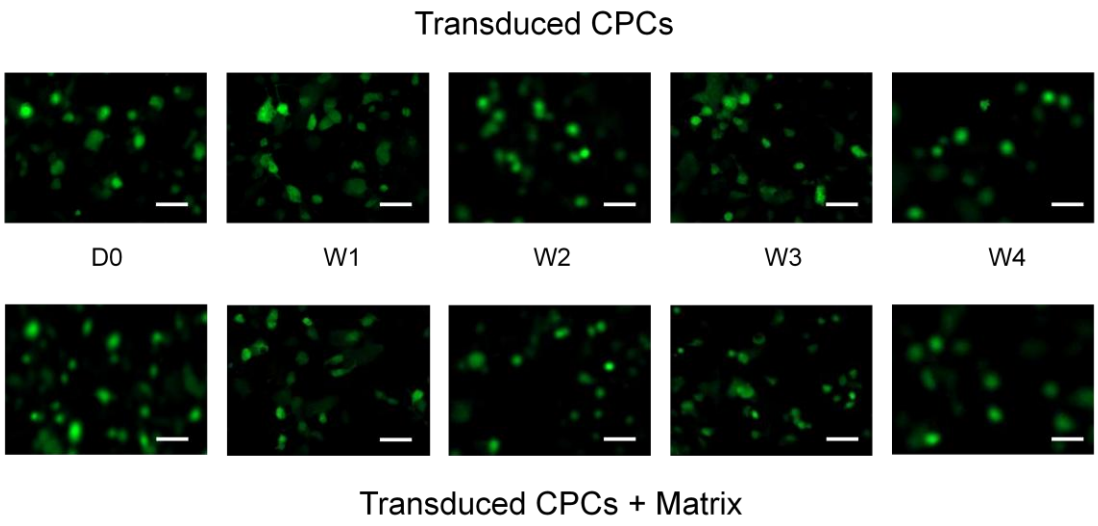

Figure 5-5: Representative images of GFP expression in the transduced CPCs.

The transduced cells could be visualized by fluorescence microscopy both within and without the collagen-based matrix at day 0, and at 1, 2, 3, and 4 weeks after transduction. Scale bar = 20 μm.

Discussion

Growing evidence from animal studies and clinical trials suggest that cell therapy can restore perfusion in ischemic tissues (Janssens et al. 2006) and bioengineered matrices can enhance functional results of cell therapy (Suuronen et al. 2006). *In vivo* cell tracking methods can help improve our understanding of the basic mechanisms of cell-based regenerative therapies and the effects of bioengineered matrices on transplanted cells. To this end, in this study, we successfully delivered two PET reporter genes (HSV1-*tk* and HSV1-*sr39tk*) by lentiviral transduction into human CPCs, Our results indicated that either LV-GFP-iresTK or LV-*Fluc*-RFP-tTK could be used to transduce human CPCs, without significantly altering cell morphology, viability, and function. The transduced CPCs showed stable expression of the introduced reporter genes for up to four weeks, thus providing the potential for noninvasive monitoring the transplanted cell fate during this time period.

Primary cells can be more difficult to transfect/transduce than similar immortalized cell lines (Hamm et al. 2002); therefore, obtaining efficient gene transfer in primary human CPCs could be challenging. In this study, we reported that the mean transduction efficiency of LV-GFP-iresTK in CPCs was about 15% at a MOI of 10, which is similar to a previous report that used Lenti-CMV-GFP to transduce HUVECs (Liu et al. 2006). Meanwhile, in LV-*Fluc*-RFP-tTK transduction, a dose-response effect was achieved by transducing cells with increasing MOIs; with a mean transduction efficiency of 13% and 16% at MOIs of 50 and 100, respectively. It has been previously demonstrated that LV-*Fluc*-RFP-tTK was capable of stably transducing human and mouse embryonic stem cells (Cao et al. 2006). In this study, to successfully transduce

human CPCs using the same vector, lentiviral transduction was repeated and a relatively high MOI was used.

PET reporter gene technology requires genetic modification, and it is unclear whether this may alter CPC viability and function. Because the HSV1-*tk* enzyme accumulates more in the cytoplasm rather than the nucleus, either LV-GFP-iresTK or LV-*Fluc*-RFP-tTK should induce less cellular toxicity (Ray et al. 2004). Our finding demonstrated no significant alteration in cell morphology, or migration and angiogenesis potential of transduced human CPCs with LV-GFP-iresTK. However, we reported a reduction in the viability of CPCs when transduced with the LV-*Fluc*-RFP-tTK at a high MOI of 100. In accordance with previous studies (McGinley et al. 2011), this observed cell death at the highest MOI may be, in part, due to a toxic effect of the transgene, or toxicity of the vector, which constitutes an area for future investigation. We suggest that the optimal MOI for different vectors and different cell types should be experimentally determined in the future studies. Although not evaluated in this study, genomic and proteomic studies from other groups have shown that reporter genes did not significantly affect differentiation or proliferation function of transducted cells (Wu et al. 2006; Wu et al. 2006).

The insertion of GFP or RFP reporter genes has gained popularity due to additional attractive features. It allows detection of the naturally fluorescent cytoplasmic protein by fluorescence microscopy or FACS in live cells. We used this technique to measure the transduction efficiency and purify the transduced CPCs. Specifically, successful transduction was verified by observing the GFP/RFP positive cells under a fluorescence microscope and the approximate transduction efficiency was calculated by

counting GFP/RFP positive and negative cells using flow cytometry. Generally, a transduction efficiency of 30-40% is sufficient for FACS, subsequent subculture and *in vivo* transplantation (Sun et al. 2009). However, our results indicated that slightly lower transduction efficiency (10-15%) was acceptable, but a higher number of starting cells for sorting is needed to be effective. Although transduced cells expressing the fluorescence gene are easily detectable or selected on a single cell level, concerns about immunogeneity and possible toxicity to living cells have been reported (Stripecke et al. 1999).

This study also evaluated the stability of lentiviral transduction in human CPCs and demonstrated that 80% of the successfully transduced CPCs continued to express the reporter protein after 4 weeks. During this time, CPCs may differentiate into endothelial cells or other mature cells. However, the reporter genes integrated stably into CPCs, and were not lost or diluted during cell division or differentiation that may have occurred *in vitro* culture or *in vivo* transplantation.

PET imaging may not only help provide novel insights into cell engraftment, proliferation, and survival, but may also serve to evaluate the effects that bioengineered materials have on transplanted cells. In this study, we investigated the effect of matrices on the expression of GFP in transduced CPCs. The results indicated that transduced CPCs in the matrices could be visualized up to 4 weeks, suggesting that the developed reporter gene techniques might provide the potential of tracking transduced CPCs delivered in a collagen-based matrix by using PET.

HSV1-*tk* and its mutant HSV1-*sr39tk* are the most commonly used reporter genes for PET applications, and several radiolabeled acyclo-guanosine and pyrimidine

nucleoside analogues have been investigated as reporter probes for imaging of HSV1-*tk* or HSV1-*sr39tk* (de Vries et al. 2002). Of the PET reporter probes evaluated, radioactivated (^{124}I- or ^{18}F-) 2' fluoro-β-D-arabinofuranosyluracil (FIAU) and 9-(4-[^{18}F]fluoro-3-hydroxymethylbutyl) guanine (^{18}F-FHBG) are the most extensively studied (Tjuvajev et al. 2002) and have already been studied in humans (Jacobs et al. 2001; Yaghoubi et al. 2001). *In vitro* and *in vivo* studies have indicated that HSV1-*sr39tk* is better able to utilize acycloguanosine substrates (such as FHBG) (Yaghoubi et al. 2006); while ^{18}F-FHBG is more sensitive for HSV1-*sr39tk*, and FIAU is more sensitive for HSV1-*tk* (Min et al. 2003; Buursma et al. 2006). Compared to the complicated procedures of FIAU synthesis, ^{18}F-FHBG can be synthesized within a reasonable time (95-100 min), at a high specific activity (>320mCi/μmol), and with high radiochemical purity (99%) (Alauddin et al. 1998). Therefore, HSV1-*sr39tk* and ^{18}F-FHBG have become a more popular PET reporter system in recent years. Use of a fluorescent protein (GFP or RFP) as the second reporter gene can help measure gene expression, select transgenic cells, study fusion genes or proteins, and investigate cell distribution by histological examination. GFP is the most popular reporter gene, and cell sorting for GFP is available in most institutions. Therefore, in this study, we evaluated two lentiviruses, LV-GFP-iresTK and LV-*Fluc*-RFP-tTK, to meet the needs of different sites.

The advantage of reporter gene PET imaging over radiotracer direct labeling PET imaging is that constitutive expression of the reporter protein allows for longitudinal tracking of cell survival and localization without the constraint of label decay. It is important to note that, because active transcription of the reporter gene is a prerequisite for synthesis of the reporter protein, only cells that are alive yield positive imaging

signals which indicate the cell survival. Furthermore, because the reporter gene integrates into the host cell's chromosome after stable transduction, the reporter gene is passed on from the mother cell to daughter cell. Genetic inheritance of the reporter gene thus permits monitoring of donor cell proliferation. In addition, HSV1-*tk* expression can also be used as a reporter for markers of gene therapy or cell-gene therapy. Using this reporter technique, therapeutic genes and gene-engineered cells will be quantifiable noninvasively within the host. Because the radiolabeled probe is administered before each imaging session, the lifetime does not become problematic for long-term studies. However, the attempt to use lentiviral-mediated reporter gene techniques in clinical trials has raised concerns about their safety including the risk of genetic recombination, and the generation of replication-competent virus in humans (Leyva et al. 2011). More recently, further modifications in the packaging and genetic components of viral genes have been reported in order to develop safer lentiviral vector systems (Levine et al. 2006).

Given the projected rapid growth of cellular therapy and bioengineering technology, it is expected that reporter gene imaging will play an increasingly important role in evaluating such therapies (Sheikh et al. 2006). Compared with other molecular imaging modalities, PET imaging with reporter gene-based cell labeling may provide more specific information on the number of surviving cells. Although the clinical potential of molecular imaging has yet to be realized, several new PET reporter gene systems are under development in an attempt to advance clinical applications. Recently, it was reported that human mitochondrial thymidine kinase type 2 (hTK2) reporter gene alone or fused with GFP, was used for preclinical evaluation in a mouse model (Ponomarev et al. 2007). Another study used the estrogen receptor ligand binding domain

(ER-LBD) as a reporter gene to monitor a transduced ES cell line in mice (Takamatsu et al. 2005; Furukawa et al. 2006). However, further work remains to be done in the development of safe, practical, highly sensitive, and specific quantitative PET imaging of reporter gene systems for meaningful clinical applicability.

Conclusion

In summary, quiescent human CPCs transduced with lentiviral vectors show stable expression of reporter genes. The reporter gene approach can be developed for tracking transplanted CPCs, while preserving the cells' morphology, viability, migration and angiogenesis capabilities. This technique may be used for the development of reporter gene PET imaging, to monitor the fate of transplanted cells noninvasively, longitudinally, and quantitatively, and thereby help elucidate the mechanisms and effectiveness of cell-based therapies and evaluate the long-term effect of bioengineered materials on delivered cells.

CHAPTER 6: GENERAL DISCUSSION

The main objective of cardiac cell therapy is to repair and/or replace parts of the damaged heart (Lovell et al. 2010). Adult stem cell transplantation appears to be a realistic and promising therapy for cardiac regeneration in ischemic or infarcted myocardium. However, recent results from many clinical trials have demonstrated only minimal favorable effects in patients (Welt et al. 2006). Therefore, to improve the applicability of cell therapy clinically, it is important to understand the behavior of transplanted cells, in order to overcome the hurdles of cardiac cell therapy. To this end, the present research addresses four significant needs in cardiac cell therapies: 1) increasing the number of available autologous adult stem cells; 2) investigating the optimal cell types for cardiac regeneration; 3) increasing the homing and engraftment of transplanted cells at sites of interest; 4) developing cell labeling methods to monitor transplanted cells *in vivo* in different target subjects and at different stages of cell delivery.

6.1 Successful Expansion and Characterization of Human $CD133^+$ cells

Currently, autologous stem or progenitor cells have been regarded as a leading candidate cell source for regenerative medicine. Since the identification of the CD133 antigen as a suitable stem cell marker, the possible use of $CD133^+$ cells in therapeutic applications opened a new promising field in the treatment of CAD. Early clinical studies demonstrated that transplanted bone marrow-derived $CD133^+$ cells improved cardiac function in MI patients probably as a result of neovascularization (Stamm et al. 2003; Stamm et al. 2007). General isolation protocols may be impractical from a clinical perspective due to the low frequency of $CD133^+$ cells from available sources for transplantation. Currently, $CD133^+$ cells for clinical use are isolated from bone marrow or peripheral blood of patients after the introduction of granulocyte colony-stimulating

factor (G-CSF). Although G-CSF treatment can effectively mobilize HSCs and EPCs to obtain increased cell numbers, many studies indicate that the response to SDF-1 and *in vivo* migratory capacity of G-CSF-mobilized cells was significantly reduced (Honold et al. 2006). It was also reported that G-CSF administration depressed the angiogenic potential of cells, and the benefit observed following implantation of cells mobilized by G-CSF might come only from a paracrine effect (Tura et al. 2010). This may partly explain why the therapeutic efficacy of $CD133^+$ cells (G-CSF-mobilized) in patients was much less than in animals (where fresh non-G-CSF-mobilized cells are generally used). These results beckon for more efficient methods of $CD133^+$ cell isolation and expansion. Therefore, the first specific aim focused on developing techniques that may help increase the cell number of human $CD133^+$ PB cells.

As reported in manuscript #1, a novel source of expandable $CD133^+$ cells can be generated from the $CD133^-$ fraction of human peripheral blood. Based on our *in vitro* comparison studies of cell function, the derived $CD133^+$ progenitors appear to have similar cell migration potential to the fresh $CD133^+$ cells, and a superior vasculogenesis capacity compared to fresh $CD133^+$ cells and other progenitors.

In this chapter, greater migration potential of the heterogeneous CPC population was described, and cytokine mechanisms appear to be involved. This suggests that cell interactions may be important in regulating functional characteristics of therapeutic cells, and that co-administration of different cell types may be superior to transplantation of a single cell population. Some studies demonstrated that combined transplantation of two cell populations or cells with growth factors results in the better function improvement, reduction of scar size and myocardial apoptosis in chronic ischemia (Bonaros et al. 2006;

Hahn et al. 2008). The unselected cell population or mixed population (such as CPCs) also shows the cell interaction, thus might be another optional cell type for cardiac therapy and worth further investigation.

6.2 Homing and Engraftment of CPCs within or without Collagen Matrices

Due to their ease of acquisition and their demonstrated therapeutic potential, CPCs have been regarded as a favorable cell type for therapy. But, before CPCs become more applied clinically, it is important to further understand the *in vivo* local effects and behavior of CPCs and their derivatives. To date, however, most of current *in vivo* studies about cell therapy are elucidated through post-mortem histological examination, which is a single time point analysis and does not allow for longitudinal observation, and which is impractical with human subjects. Recent advances in the field of molecular imaging have made it possible to noninvasively track transplanted cells over time. Most modalities require efficient cell labeling, and include direct cell labeling, or reporter gene approaches. Chapters 3, 4 & 5 focused on the utilization of PET imaging for *in vivo* assessment of cardiac cell therapy.

Another challenge in cardiac cell therapy is that transplanted cells have little success in homing and engrafting to areas of injury. With the advance of tissue engineering technology, delivery biomaterials are evolving to address this issue (Suuronen et al. 2006). Two common biomaterial approaches used to repair the injured heart are injectable hydrogels and surgically implanted tissue engineered grafts. The injectable collagen-based material used in this study is thermo-sensitive, and formed a gel at body temperature. Highly porous collagen lattice sponges can support the growth of

many types of tissues, and thus provide the potential for reducing physical infarct expansion, improving cell retention and survival, and inducing neovessel formation in the damaged myocardium (Glowacki et al. 2008). However, the biological mechanisms and local effects of collagen matrices after implantation remain to be fully elucidated. In chapter 3, we reported that PET imaging with ^{18}F-FDG direct cell labeling is a suitable tool to track transplanted human CPCs, and evaluate the effect of their delivery within collagen I-based matrices.

The distribution of human CPCs delivered with collagen matrices was assessed by whole body PET imaging in a rat ischemic hindlimb model. Only 11% of the locally transplanted CPCs were retained in the target site after intramuscular injection without the matrix. With use of the matrix, retention was enhanced by 70% in the ischemic tissue. This mechanism conferred by the matrix may have implications on the effects of cell therapy at the early stages after transplantation. Based on these results, PET imaging with ^{18}F-FDG cell labeling is a promising approach to monitor cell fate *in vivo* and better understand the role of delivery matrices in cell regenerative therapies.

The results indicated that ^{18}F-FDG is a sensitive and quantifiable marker of transplanted CPCs. However, we also reported a significant leakage (58%) of ^{18}F-FDG from labeled cells. Since the myocardium shows a high uptake of ^{18}F-FDG, a concern emerged that ^{18}F-FDG leakage might affect the positive identification of labeled CPCs in the heart. Therefore, we developed a more stable stem cell labeling method. In chapter 4, we evaluated the feasibility of ^{18}F-HFB to label human CPCs for cell tracking in a rat MI model and compared the properties of ^{18}F-HFB and ^{18}F-FDG labeling *in vitro* and *in vivo*. ^{18}F-HFB is efficiently retained in CPCs over 4 hours (77-95%). Consistent with the better

labeling efficiency and stability *in vitro*, PET imaging demonstrated a greater signal of ^{18}F-HFB-CPCs in the injection site compared with ^{18}F-FDG-CPCs a few hours after cell transplantation. A high portion of radioactivity was observed in the normal myocardium of ^{18}F-FDG-CPC rats was ^{18}F-FDG leaked from CPCs, rather than the CPCs themselves. The correlation between the PET image and histological examination indicated that ^{18}F-HFB cell labeling may be a more reliable method for assessing the distribution of transplanted human CPCs, especially in the myocardium. Although effects on cell viability and function studies were examined, there are still outstanding questions regarding long term radiation effects on the labeled cells.

Although such direct cell labeling allows high sensitivity PET imaging, its use is limited to tracking cells in the first hours to days after delivery, due to the short half-life of the radioisotopes. Therefore, longer-term studies will require other labeling approaches that are not affected by decay, and which are not diluted in cells undergoing division. Recently, the use of superparamagnetic iron oxide (SPIO) labeling with MRI imaging became one of the commonly approaches for long-term cell tracking. However, SPIO agents can be engulfed by macrophages after transplanted cell death (which may continue to produce signal even after cell death), and hence cannot be used to accurately monitor long-term cell survival and behavior (Bulte et al. 2004).

Unlike direct cell labeling, reporter genes are inherited genetically and can be used to monitor the survival and function of transplanted cells and their progeny for lifetime (Sun et al. 2009). The advantage of reporter gene PET imaging over radiotracer labeled PET imaging is that constitutive expression of the reporter protein allows for longitudinal tracking of cell survival and localization without the constraint of label

decay. To implement reporter-gene based cell labeling, it is first important to deliver the reporter gene of interest into the target cells. Because the use of PET reporter genes is not well-documented in primary human adult stem cells, proper *in vitro* experiments are needed prior to *in vivo* studies, to determine both efficiency and functionality of the inserted gene.

Although less time consuming, non-viral gene transfer methods and other viral gene delivery systems are inefficient at transfecting primary cells, such as the adult stem and progenitor cells typically used in cell therapy testing (Hamm et al. 2002). Lentiviral vectors, based on the disabled HIV genome, are attractive for the transduction of non-dividing or infrequently dividing cells, such as adult HSCs or CPCs (Naldini et al. 1996). In chapter 5, two lentiviral vectors, LV-GFP-iresTK and LV-*Fluc*-RFP-tTk, were used for delivery of the PET reporter gene to human CPCs. Although the efficiency of lentiviral transduction was limited to 15%, this approach still provides the potential to monitor the transplanted cells *in vivo* due to the sensitivity of PET, and the stability of reporter expression. Flow cytometry analysis indicated that 80% of CPCs still expressed the reporters after 4 weeks. In addition, the reporter technique used did not adversely affect cell migration and angiogenesis capabilities, important functions for angiogenic/cardiac cell therapy. Therefore, this technique should prove useful for the long-term assessment and optimization (e.g. cell type, biomaterial, and timing) of experimental cell therapies.

Despite the advantages discussed for reporter gene imaging, it does suffer from several drawbacks. First, the derivation of cells with stable reporter gene expression typically requires a lengthy incubation period (around 1 week), whereas preparation for

radionuclide direct cell labeling can be completed within 1 hour. Furthermore, the introduction of reporter genes has been documented to possess the potential to alter cellular genome and phenotype (Grabski et al.).

We hope reporter gene-based labeling may be used in conjunction with radiotracer direct cell labeling to answer a wide range of biological questions. The choice of whether to use physical cell labeling or reporter gene modalities for *in vivo* imaging of transplanted cells depends on the subject of investigation, the timeline of study, and the availability of equipment at a given institution (Sun et al. 2009).

6.3 Clinical Perspective and Future Directions

Cell therapy is rapidly advancing as a potential treatment for clinical use, in the midst of some concern within the scientific community that this may be occurring too quickly and too uncritically (Smith et al. 2008). It is important to realize that the field of cell therapy is at an early stage. Although some clinical trials are underway, a number of fundamental questions need to be addressed and resolved experimentally in the near future.

First, for clinical use, human cells and often autologous cells will still be the main applied cell source. Age and disease might affect the number and function of stem or progenitor cells (Dimmeler et al. 2008). For example, some studies have shown that CHF attenuated the cell number and increased the senescence of CPCs (Hill et al. 2003; Maltais et al. 2011). However, in Manuscript #1, we did not observe a significant functional impairment in the progenitors obtained from the 2 patients with heart failure (NYHA Class II), compared to the other donors (10 patients) although the number of samples were small. Therefore, we conclude that further preclinical studies on the

function of cells from patients are necessary. Some pretreatments or preconditions might be applied to improve the functional activity of patients' cells (Sasaki et al. 2006).

Second, homing and engraftment not only are regulated by multiple biological signaling cascades, but also may be critically affected by the delivery vehicles and the disease of patients (Chavakis et al. 2010). It might well be that different cell types and cell delivery methods are used for specific disease states depending on different cardiac pathologies. For example, the treatment that promotes cell survival or angiogenesis might be a good stage for AMI; while contractile cells or cells that can differentiate into contractile cells might be the best choice in CHF situation (Segers et al. 2008). Achieving the longer-term goal of true cardiac regeneration will probably require more than simply injecting the right type of cells in the right place at the right time. The development of tissue engineering for the delivery and support of transplanted cells has recently attracted interest in the cardiac field. The collagen-based injectable matrices used in this study might facilitate targeted, less invasive tissue restoration after myocardial injury including increased cell transplant survival, increased blood flow and improved cardiac function. Progress has also been made in improving cell homing and engraftment, using approaches including heat shock treatment (Zhang et al. 2001), overexpression of antiapoptotic proteins (Zhang et al. 2001; Mangi et al. 2003), or the addition of bioactive moieties to matrices (Suuronen et al. 2009), but there is still room for improvement.

There is clearly a long and arduous path ahead that is not helped by the lack of tools that we have for answering these questions in cell therapy. PET imaging with cell labeling developed in this thesis can help evaluate different treatment protocols of cardiac regeneration. Future research needs to focus on improving sensitivity while minimizing

radioactivity exclusion. With the increasing popularity and availability of PET instrumentation in medical practice, commercial radiopharmacy production and distribution are expected to be enhanced for both basic research and clinical studies. In addition, the use of PET imaging does not always need to be mutually exclusive. Multimodality imaging approaches (such as PET/CT or PET/MRI) may minimize the potential drawbacks inherent within a single modality, by using a tailored combination of two or more techniques to achieve the best approach for a given experiment.

6.4 Conclusions

In summary, cell number, fate and biodistribution are a key challenge in cell therapy applications. The ability to expand and track transplanted cells is necessary for clear understanding of cell therapy. Significant findings from this thesis and previous work (Suuronen et al. 2006; Suuronen et al. 2006) demonstrated that autologous adult stem cell can be expanded *ex vivo* and the derived $CD133^{+}$ might be a superior cell source for vascular regeneration. Furthermore, the ability to quantify cells using PET imaging with cell labeling techniques (Manuscript #2, 3 & 4) makes this approach ideal for *in vivo* tracking of transplanted human CPCs. In addition, successful cell delivery (retention and engraftment) for treatment of heart disease, as well as other disease states, is required in this field. Another finding from this thesis (Manuscript #2) demonstrated the capability of bioengineered matrices to enhance cell retention in the early stage of cell delivery. These findings open up additional questions as to where the cells reside and what mechanisms are involved thereafter. As our research continueds, by utilizing reporter gene technique (Manuscript #4), long-term studies of transplanted cells with PET imaging will become available in the near future at our institution. The ability to monitor the location, viability,

differentiation and proliferation of transplanted cell populations by PET imaging should similarly aid in the application of cell therapy protocols (Herschman 2004). The advent of PET imaging has brought about fundamental paradigm shifts in our approach to basic research and clinical use (Wang et al. 2009). In the laboratory setting, PET imaging provides innovative tools allowing dissection of the cellular and molecular features of various biologic processes in a living organism. In clinical practice, PET imaging holds the promise of becoming a key for disease diagnosis, disease characterization, and assessment of therapeutic response in cardiovascular medicine. It can be anticipated that cell preparation and delivery vehicles will undergo considerable development once the clinical benefit of cardiac cell therapy is clearly established.

REFERENCES

Abdel-Latif, A., R. Bolli, I. M. Tleyjeh, V. M. Montori, E. C. Perin, C. A. Hornung, E. K. Zuba-Surma, M. Al-Mallah and B. Dawn (2007). "Adult bone marrow-derived cells for cardiac repair: a systematic review and meta-analysis." Arch Intern Med **167**(10): 989-97.

Acton, P. D. and R. Zhou (2005). "Imaging reporter genes for cell tracking with PET and SPECT." Q J Nucl Med Mol Imaging **49**(4): 349-60.

Adonai, N., K. N. Nguyen, J. Walsh, M. Iyer, T. Toyokuni, M. E. Phelps, T. McCarthy, D. W. McCarthy and S. S. Gambhir (2002). "Ex vivo cell labeling with 64Cu-pyruvaldehyde-bis(N4-methylthiosemicarbazone) for imaging cell trafficking in mice with positron-emission tomography." Proc Natl Acad Sci U S A **99**(5): 3030-5.

Agbulut, O., S. Vandervelde, N. Al Attar, J. Larghero, S. Ghostine, B. Leobon, E. Robidel, P. Borsani, M. Le Lorc'h, A. Bissery, et al. (2004). "Comparison of human skeletal myoblasts and bone marrow-derived CD133+ progenitors for the repair of infarcted myocardium." J Am Coll Cardiol **44**(2): 458-63.

Aicher, A., W. Brenner, M. Zuhayra, C. Badorff, S. Massoudi, B. Assmus, T. Eckey, E. Henze, A. M. Zeiher and S. Dimmeler (2003). "Assessment of the tissue distribution of transplanted human endothelial progenitor cells by radioactive labeling." Circulation **107**(16): 2134-9.

Alauddin, M. M. and P. S. Conti (1998). "Synthesis and preliminary evaluation of 9-(4-[18F]-fluoro-3-hydroxymethylbutyl)guanine ([18F]FHBG): a new potential

imaging agent for viral infection and gene therapy using PET." Nucl Med Biol **25**(3): 175-80.

Alvarez-Dolado, M., R. Pardal, J. M. Garcia-Verdugo, J. R. Fike, H. O. Lee, K. Pfeffer, C. Lois, S. J. Morrison and A. Alvarez-Buylla (2003). "Fusion of bone-marrow-derived cells with Purkinje neurons, cardiomyocytes and hepatocytes." Nature **425**(6961): 968-73.

Anderson, D. J., F. H. Gage and I. L. Weissman (2001). "Can stem cells cross lineage boundaries?" Nat Med **7**(4): 393-5.

Annabi, B., Y. T. Lee, S. Turcotte, E. Naud, R. R. Desrosiers, M. Champagne, N. Eliopoulos, J. Galipeau and R. Beliveau (2003). "Hypoxia promotes murine bone-marrow-derived stromal cell migration and tube formation." Stem Cells **21**(3): 337-47.

Asahara, T., T. Murohara, A. Sullivan, M. Silver, R. van der Zee, T. Li, B. Witzenbichler, G. Schatteman and J. M. Isner (1997). "Isolation of putative progenitor endothelial cells for angiogenesis." Science **275**(5302): 964-7.

Assmus, B., J. Honold, V. Schachinger, M. B. Britten, U. Fischer-Rasokat, R. Lehmann, C. Teupe, K. Pistorius, H. Martin, N. D. Abolmaali, et al. (2006). "Transcoronary transplantation of progenitor cells after myocardial infarction." N Engl J Med **355**(12): 1222-32.

Assmus, B., V. Schachinger, C. Teupe, M. Britten, R. Lehmann, N. Dobert, F. Grunwald, A. Aicher, C. Urbich, H. Martin, et al. (2002). "Transplantation of Progenitor Cells and Regeneration Enhancement in Acute Myocardial Infarction (TOPCARE-AMI)." Circulation **106**(24): 3009-17.

Balbarini, A., M. C. Barsotti, R. Di Stefano, A. Leone and T. Santoni (2007). "Circulating endothelial progenitor cells characterization, function and relationship with cardiovascular risk factors." Curr Pharm Des **13**(16): 1699-713.

Balsam, L. B., A. J. Wagers, J. L. Christensen, T. Kofidis, I. L. Weissman and R. C. Robbins (2004). "Haematopoietic stem cells adopt mature haematopoietic fates in ischaemic myocardium." Nature **428**(6983): 668-73.

Barile, L., I. Chimenti, R. Gaetani, E. Forte, F. Miraldi, G. Frati, E. Messina and A. Giacomello (2007). "Cardiac stem cells: isolation, expansion and experimental use for myocardial regeneration." Nat Clin Pract Cardiovasc Med **4 Suppl 1**: S9-S14.

Bartunek, J., M. Vanderheyden, B. Vandekerckhove, S. Mansour, B. De Bruyne, P. De Bondt, I. Van Haute, N. Lootens, G. Heyndrickx and W. Wijns (2005). "Intracoronary injection of CD133-positive enriched bone marrow progenitor cells promotes cardiac recovery after recent myocardial infarction: feasibility and safety." Circulation **112**(9 Suppl): I178-83.

Bauer, S. M., R. J. Bauer, Z. J. Liu, H. Chen, L. Goldstein and O. C. Velazquez (2005). "Vascular endothelial growth factor-C promotes vasculogenesis, angiogenesis, and collagen constriction in three-dimensional collagen gels." J Vasc Surg **41**(4): 699-707.

Bax, J. J., F. Fath-Ordoubadi, E. Boersma, W. Wijns and P. G. Camici (2002). "Accuracy of PET in predicting functional recovery after revascularisation in patients with chronic ischaemic dysfunction: head-to-head comparison between blood flow,

glucose utilisation and water-perfusable tissue fraction." Eur J Nucl Med Mol Imaging **29**(6): 721-7.

Beanlands, R. S., T. D. Ruddy, R. A. deKemp, R. M. Iwanochko, G. Coates, M. Freeman, C. Nahmias, P. Hendry, R. J. Burns, A. Lamy, et al. (2002). "Positron emission tomography and recovery following revascularization (PARR-1): the importance of scar and the development of a prediction rule for the degree of recovery of left ventricular function." J Am Coll Cardiol **40**(10): 1735-43.

Beeres, S. L., F. M. Bengel, J. Bartunek, D. E. Atsma, J. M. Hill, M. Vanderheyden, M. Penicka, M. J. Schalij, W. Wijns and J. J. Bax (2007). "Role of imaging in cardiac stem cell therapy." J Am Coll Cardiol **49**(11): 1137-48.

Beltrami, A. P., L. Barlucchi, D. Torella, M. Baker, F. Limana, S. Chimenti, H. Kasahara, M. Rota, E. Musso, K. Urbanek, et al. (2003). "Adult cardiac stem cells are multipotent and support myocardial regeneration." Cell **114**(6): 763-76.

Beltrami, A. P., K. Urbanek, J. Kajstura, S. M. Yan, N. Finato, R. Bussani, B. Nadal-Ginard, F. Silvestri, A. Leri, C. A. Beltrami, et al. (2001). "Evidence that human cardiac myocytes divide after myocardial infarction." N Engl J Med **344**(23): 1750-7.

Bengel, F. M., P. Ueberfuhr, J. Karja, K. Schreiber, S. G. Nekolla, B. Reichart and M. Schwaiger (2004). "Sympathetic reinnervation, exercise performance and effects of beta-adrenergic blockade in cardiac transplant recipients." Eur Heart J **25**(19): 1726-33.

Blasberg, R. G. and J. G. Tjuvajev (2003). "Molecular-genetic imaging: current and future perspectives." J Clin Invest **111**(11): 1620-9.

Blokland, J. A., P. Trindev, M. P. Stokkel and E. K. Pauwels (2002). "Positron emission tomography: a technical introduction for clinicians." Eur J Radiol **44**(1): 70-5.

Boccafoschi, F., J. Habermehl, S. Vesentini and D. Mantovani (2005). "Biological performances of collagen-based scaffolds for vascular tissue engineering." Biomaterials **26**(35): 7410-7.

Bonaros, N., R. Rauf, D. Wolf, E. Margreiter, A. Tzankov, B. Schlechta, A. Kocher, H. Ott, T. Schachner, S. Hering, et al. (2006). "Combined transplantation of skeletal myoblasts and angiopoietic progenitor cells reduces infarct size and apoptosis and improves cardiac function in chronic ischemic heart failure." J Thorac Cardiovasc Surg **132**(6): 1321-8.

Boodhwani, M., N. R. Sodha and F. W. Sellke (2006). "Biologically based myocardial regeneration: is there a role for the surgeon?" Curr Opin Cardiol **21**(6): 589-94.

Botti, C., D. R. Negri, E. Seregni, V. Ramakrishna, F. Arienti, L. Maffioli, C. Lombardo, A. Bogni, C. Pascali, F. Crippa, et al. (1997). "Comparison of three different methods for radiolabelling human activated T lymphocytes." Eur J Nucl Med **24**(5): 497-504.

Brenner, W., A. Aicher, T. Eckey, S. Massoudi, M. Zuhayra, U. Koehl, C. Heeschen, W. U. Kampen, A. M. Zeiher, S. Dimmeler, et al. (2004). "111In-labeled CD34+ hematopoietic progenitor cells in a rat myocardial infarction model." J Nucl Med **45**(3): 512-8.

Bulte, J. W. and D. L. Kraitchman (2004). "Monitoring cell therapy using iron oxide MR contrast agents." Curr Pharm Biotechnol **5**(6): 567-84.

Burst, V. R., M. Gillis, F. Putsch, R. Herzog, J. H. Fischer, P. Heid, J. Muller-Ehmsen, K. Schenk, J. W. Fries, C. A. Baldamus, et al. "Poor cell survival limits the beneficial impact of mesenchymal stem cell transplantation on acute kidney injury." Nephron Exp Nephrol **114**(3): e107-16.

Buursma, A. R., V. Rutgers, G. A. Hospers, N. H. Mulder, W. Vaalburg and E. F. de Vries (2006). "18F-FEAU as a radiotracer for herpes simplex virus thymidine kinase gene expression: in-vitro comparison with other PET tracers." Nucl Med Commun **27**(1): 25-30.

Cao, F., S. Lin, X. Xie, P. Ray, M. Patel, X. Zhang, M. Drukker, S. J. Dylla, A. J. Connolly, X. Chen, et al. (2006). "In vivo visualization of embryonic stem cell survival, proliferation, and migration after cardiac delivery." Circulation **113**(7): 1005-14.

Cao, X. and M. S. Shoichet (2002). "Photoimmobilization of biomolecules within a 3-dimensional hydrogel matrix." J Biomater Sci Polym Ed **13**(6): 623-36.

Cao, X. and M. S. Shoichet (2003). "Investigating the synergistic effect of combined neurotrophic factor concentration gradients to guide axonal growth." Neuroscience **122**(2): 381-9.

Case, J., L. E. Mead, W. K. Bessler, D. Prater, H. A. White, M. R. Saadatzadeh, J. R. Bhavsar, M. C. Yoder, L. S. Haneline and D. A. Ingram (2007). "Human CD34+AC133+VEGFR-2+ cells are not endothelial progenitor cells but distinct, primitive hematopoietic progenitors." Exp Hematol **35**(7): 1109-18.

Chavakis, E., M. Koyanagi and S. Dimmeler "Enhancing the outcome of cell therapy for cardiac repair: progress from bench to bedside and back." Circulation **121**(2): 325-35.

Cho, H. J., J. Lee, A. Wecker and Y. S. Yoon (2006). "Bone marrow-derived stem cell therapy in ischemic heart disease." Regen Med **1**(3): 337-45.

Cho, H. J., N. Lee, J. Y. Lee, Y. J. Choi, M. Ii, A. Wecker, J. O. Jeong, C. Curry, G. Qin and Y. S. Yoon (2007). "Role of host tissues for sustained humoral effects after endothelial progenitor cell transplantation into the ischemic heart." J Exp Med **204**(13): 3257-69.

Christman, K. L., Q. Fang, M. S. Yee, K. R. Johnson, R. E. Sievers and R. J. Lee (2005). "Enhanced neovasculature formation in ischemic myocardium following delivery of pleiotrophin plasmid in a biopolymer." Biomaterials **26**(10): 1139-44.

Christman, K. L., H. H. Fok, R. E. Sievers, Q. Fang and R. J. Lee (2004). "Fibrin glue alone and skeletal myoblasts in a fibrin scaffold preserve cardiac function after myocardial infarction." Tissue Eng **10**(3-4): 403-9.

Christman, K. L., A. J. Vardanian, Q. Fang, R. E. Sievers, H. H. Fok and R. J. Lee (2004). "Injectable fibrin scaffold improves cell transplant survival, reduces infarct expansion, and induces neovasculature formation in ischemic myocardium." J Am Coll Cardiol **44**(3): 654-60.

Colazzo, F., A. H. Chester, P. M. Taylor and M. H. Yacoub (2010). "Induction of mesenchymal to endothelial transformation of adipose-derived stem cells." J Heart Valve Dis **19**(6): 736-44.

Copland, I., K. Sharma, L. Lejeune, N. Eliopoulos, D. Stewart, P. Liu, K. Lachapelle and J. Galipeau (2008). "CD34 expression on murine marrow-derived mesenchymal stromal cells: impact on neovascularization." Exp Hematol **36**(1): 93-103.

de Vries, E. F., A. R. Buursma, G. A. Hospers, N. H. Mulder and W. Vaalburg (2002). "Scintigraphic imaging of HSVtk gene therapy." Curr Pharm Des **8**(16): 1435-50.

deKemp, R. A., T. D. Ruddy, T. Hewitt, M. M. Dalipaj and R. S. Beanlands (2000). "Detection of serial changes in absolute myocardial perfusion with 82Rb PET." J Nucl Med **41**(8): 1426-35.

Dewanjee, M. K., R. P. Robinson, R. L. Hellman, W. I. Ganz, A. N. Serafini and G. N. Sfakianakis (1991). "Technetium-99m-labeled platelets: comparison of labeling with a new lipid-soluble Sn(II)-mercaptopyridine-N-oxide and 99mTc-HMPAO." Int J Rad Appl Instrum B **18**(5): 461-8.

Dimmeler, S., J. Burchfield and A. M. Zeiher (2008). "Cell-based therapy of myocardial infarction." Arterioscler Thromb Vasc Biol **28**(2): 208-16.

Dimmeler, S. and A. Leri (2008). "Aging and disease as modifiers of efficacy of cell therapy." Circ Res **102**(11): 1319-30.

Dimmeler, S., A. M. Zeiher and M. D. Schneider (2005). "Unchain my heart: the scientific foundations of cardiac repair." J Clin Invest **115**(3): 572-83.

Dobert, N., M. Britten, B. Assmus, U. Berner, C. Menzel, R. Lehmann, N. Hamscho, V. Schachinger, S. Dimmeler, A. M. Zeiher, et al. (2004). "Transplantation of progenitor cells after reperfused acute myocardial infarction: evaluation of perfusion and myocardial viability with FDG-PET and thallium SPECT." Eur J Nucl Med Mol Imaging **31**(8): 1146-51.

Doyle, B., B. J. Kemp, P. Chareonthaitawee, C. Reed, J. Schmeckpeper, P. Sorajja, S. Russell, P. Araoz, S. J. Riederer and N. M. Caplice (2007). "Dynamic tracking during intracoronary injection of 18F-FDG-labeled progenitor cell therapy for acute myocardial infarction." J Nucl Med **48**(10): 1708-14.

Drexler, H., G. P. Meyer and K. C. Wollert (2006). "Bone-marrow-derived cell transfer after ST-elevation myocardial infarction: lessons from the BOOST trial." Nat Clin Pract Cardiovasc Med **3 Suppl 1**: S65-8.

Duinsbergen, D., M. Eriksson, P. A. t Hoen, J. Frisen and H. Mikkers (2008). "Induced pluripotency with endogenous and inducible genes." Exp Cell Res **314**(17): 3255-63.

Ecclestone, M., A. Proulx, J. R. Ballinger, B. Gerson, R. H. Reid and K. Y. Gulenchyn (1990). "In vitro comparison of HMPAO and gentisic acid for labelling leukocytes with 99mTc." Eur J Nucl Med **16**(4-6): 299-302.

Edelberg, J. M., L. Tang, K. Hattori, D. Lyden and S. Rafii (2002). "Young adult bone marrow-derived endothelial precursor cells restore aging-impaired cardiac angiogenic function." Circ Res **90**(10): E89-93.

Erbs, S., A. Linke, V. Adams, K. Lenk, H. Thiele, K. W. Diederich, F. Emmrich, R. Kluge, K. Kendziorra, O. Sabri, et al. (2005). "Transplantation of blood-derived progenitor cells after recanalization of chronic coronary artery occlusion: first randomized and placebo-controlled study." Circ Res **97**(8): 756-62.

Erbs, S., A. Linke, V. Schachinger, B. Assmus, H. Thiele, K. W. Diederich, C. Hoffmann, S. Dimmeler, T. Tonn, R. Hambrecht, et al. (2007). "Restoration of microvascular function in the infarct-related artery by intracoronary

transplantation of bone marrow progenitor cells in patients with acute myocardial infarction: the Doppler Substudy of the Reinfusion of Enriched Progenitor Cells and Infarct Remodeling in Acute Myocardial Infarction (REPAIR-AMI) trial." Circulation **116**(4): 366-74.

Etzion, S., A. Battler, I. M. Barbash, E. Cagnano, P. Zarin, Y. Granot, L. H. Kedes, R. A. Kloner and J. Leor (2001). "Influence of embryonic cardiomyocyte transplantation on the progression of heart failure in a rat model of extensive myocardial infarction." J Mol Cell Cardiol **33**(7): 1321-30.

Fazel, S., M. Cimini, L. Chen, S. Li, D. Angoulvant, P. Fedak, S. Verma, R. D. Weisel, A. Keating and R. K. Li (2006). "Cardioprotective c-kit+ cells are from the bone marrow and regulate the myocardial balance of angiogenic cytokines." J Clin Invest **116**(7): 1865-77.

Frangioni, J. V. and R. J. Hajjar (2004). "In vivo tracking of stem cells for clinical trials in cardiovascular disease." Circulation **110**(21): 3378-83.

Furukawa, T., T. G. Lohith, S. Takamatsu, T. Mori, T. Tanaka and Y. Fujibayashi (2006). "Potential of the FES-hERL PET reporter gene system -- basic evaluation for gene therapy monitoring." Nucl Med Biol **33**(1): 145-51.

Gambhir, S. S., H. R. Herschman, S. R. Cherry, J. R. Barrio, N. Satyamurthy, T. Toyokuni, M. E. Phelps, S. M. Larson, J. Balatoni, R. Finn, et al. (2000). "Imaging transgene expression with radionuclide imaging technologies." Neoplasia **2**(1-2): 118-38.

Glowacki, J. and S. Mizuno (2008). "Collagen scaffolds for tissue engineering." Biopolymers **89**(5): 338-44.

Gnecchi, M., Z. Zhang, A. Ni and V. J. Dzau (2008). "Paracrine mechanisms in adult stem cell signaling and therapy." Circ Res **103**(11): 1204-19.

Grabski, E., Z. Waibler, S. Schule, B. P. Kloke, L. Y. Sender, S. Panitz, K. Cichutek, M. Schweizer and U. Kalinke "Comparative analysis of transduced primary human dendritic cells generated by the use of three different lentiviral vector systems." Mol Biotechnol **47**(3): 262-9.

Graf, T. (2002). "Differentiation plasticity of hematopoietic cells." Blood **99**(9): 3089-101.

Hahn, J. Y., H. J. Cho, H. J. Kang, T. S. Kim, M. H. Kim, J. H. Chung, J. W. Bae, B. H. Oh, Y. B. Park and H. S. Kim (2008). "Pre-treatment of mesenchymal stem cells with a combination of growth factors enhances gap junction formation, cytoprotective effect on cardiomyocytes, and therapeutic efficacy for myocardial infarction." J Am Coll Cardiol **51**(9): 933-43.

Hamm, A., N. Krott, I. Breibach, R. Blindt and A. K. Bosserhoff (2002). "Efficient transfection method for primary cells." Tissue Eng **8**(2): 235-45.

Heeschen, C., R. Lehmann, J. Honold, B. Assmus, A. Aicher, D. H. Walter, H. Martin, A. M. Zeiher and S. Dimmeler (2004). "Profoundly reduced neovascularization capacity of bone marrow mononuclear cells derived from patients with chronic ischemic heart disease." Circulation **109**(13): 1615-22.

Hendrikx, M., K. Hensen, C. Clijsters, H. Jongen, R. Koninckx, E. Bijnens, M. Ingels, A. Jacobs, R. Geukens, P. Dendale, et al. (2006). "Recovery of regional but not global contractile function by the direct intramyocardial autologous bone marrow

transplantation: results from a randomized controlled clinical trial." Circulation **114**(1 Suppl): I101-7.

Herreros, J., F. Prosper, A. Perez, J. J. Gavira, M. J. Garcia-Velloso, J. Barba, P. L. Sanchez, C. Canizo, G. Rabago, J. M. Marti-Climent, et al. (2003). "Autologous intramyocardial injection of cultured skeletal muscle-derived stem cells in patients with non-acute myocardial infarction." Eur Heart J **24**(22): 2012-20.

Herschman, H. R. (2004). "PET reporter genes for noninvasive imaging of gene therapy, cell tracking and transgenic analysis." Crit Rev Oncol Hematol **51**(3): 191-204.

Hill, J. M., M. A. Syed, A. E. Arai, T. M. Powell, J. D. Paul, G. Zalos, E. J. Read, H. M. Khuu, S. F. Leitman, M. Horne, et al. (2005). "Outcomes and risks of granulocyte colony-stimulating factor in patients with coronary artery disease." J Am Coll Cardiol **46**(9): 1643-8.

Hill, J. M., G. Zalos, J. P. Halcox, W. H. Schenke, M. A. Waclawiw, A. A. Quyyumi and T. Finkel (2003). "Circulating endothelial progenitor cells, vascular function, and cardiovascular risk." N Engl J Med **348**(7): 593-600.

Hofmann, M., K. C. Wollert, G. P. Meyer, A. Menke, L. Arseniev, B. Hertenstein, A. Ganser, W. H. Knapp and H. Drexler (2005). "Monitoring of bone marrow cell homing into the infarcted human myocardium." Circulation **111**(17): 2198-202.

Honold, J., R. Lehmann, C. Heeschen, D. H. Walter, B. Assmus, K. Sasaki, H. Martin, J. Haendeler, A. M. Zeiher and S. Dimmeler (2006). "Effects of granulocyte colony simulating factor on functional activities of endothelial progenitor cells in patients with chronic ischemic heart disease." Arterioscler Thromb Vasc Biol **26**(10): 2238-43.

Hosoda, T., H. Zheng, M. Cabral-da-Silva, F. Sanada, N. Ide-Iwata, B. Ogorek, J. Ferreira-Martins, C. Arranto, D. D'Amario, F. del Monte, et al. (2011). "Human cardiac stem cell differentiation is regulated by a mircrine mechanism." Circulation **123**(12): 1287-96.

Hou, D., E. A. Youssef, T. J. Brinton, P. Zhang, P. Rogers, E. T. Price, A. C. Yeung, B. H. Johnstone, P. G. Yock and K. L. March (2005). "Radiolabeled cell distribution after intramyocardial, intracoronary, and interstitial retrograde coronary venous delivery: implications for current clinical trials." Circulation **112**(9 Suppl): I150-6.

Hristov, M., W. Erl and P. C. Weber (2003). "Endothelial progenitor cells: isolation and characterization." Trends Cardiovasc Med **13**(5): 201-6.

Islam, M. Q., V. Panduri and K. Islam (2007). "Generation of somatic cell hybrids for the production of biologically active factors that stimulate proliferation of other cells." Cell Prolif **40**(1): 91-105.

Iwaguro, H., J. Yamaguchi, C. Kalka, S. Murasawa, H. Masuda, S. Hayashi, M. Silver, T. Li, J. M. Isner and T. Asahara (2002). "Endothelial progenitor cell vascular endothelial growth factor gene transfer for vascular regeneration." Circulation **105**(6): 732-8.

Jacobs, A., J. Voges, R. Reszka, M. Lercher, A. Gossmann, L. Kracht, C. Kaestle, R. Wagner, K. Wienhard and W. D. Heiss (2001). "Positron-emission tomography of vector-mediated gene expression in gene therapy for gliomas." Lancet **358**(9283): 727-9.

Jaffe, R. and B. H. Strauss (2007). "Late and very late thrombosis of drug-eluting stents: evolving concepts and perspectives." J Am Coll Cardiol **50**(2): 119-27.

Jain, M., H. DerSimonian, D. A. Brenner, S. Ngoy, P. Teller, A. S. Edge, A. Zawadzka, K. Wetzel, D. B. Sawyer, W. S. Colucci, et al. (2001). "Cell therapy attenuates deleterious ventricular remodeling and improves cardiac performance after myocardial infarction." Circulation **103**(14): 1920-7.

Janssens, S., C. Dubois, J. Bogaert, K. Theunissen, C. Deroose, W. Desmet, M. Kalantzi, L. Herbots, P. Sinnaeve, J. Dens, et al. (2006). "Autologous bone marrow-derived stem-cell transfer in patients with ST-segment elevation myocardial infarction: double-blind, randomised controlled trial." Lancet **367**(9505): 113-21.

Jiang, Y., B. N. Jahagirdar, R. L. Reinhardt, R. E. Schwartz, C. D. Keene, X. R. Ortiz-Gonzalez, M. Reyes, T. Lenvik, T. Lund, M. Blackstad, et al. (2002). "Pluripotency of mesenchymal stem cells derived from adult marrow." Nature **418**(6893): 41-9.

Kamihata, H., H. Matsubara, T. Nishiue, S. Fujiyama, Y. Tsutsumi, R. Ozono, H. Masaki, Y. Mori, O. Iba, E. Tateishi, et al. (2001). "Implantation of bone marrow mononuclear cells into ischemic myocardium enhances collateral perfusion and regional function via side supply of angioblasts, angiogenic ligands, and cytokines." Circulation **104**(9): 1046-52.

Kang, W. J., H. J. Kang, H. S. Kim, J. K. Chung, M. C. Lee and D. S. Lee (2006). "Tissue distribution of 18F-FDG-labeled peripheral hematopoietic stem cells after intracoronary administration in patients with myocardial infarction." J Nucl Med **47**(8): 1295-301.

Kattman, S. J., A. D. Witty, M. Gagliardi, N. C. Dubois, M. Niapour, A. Hotta, J. Ellis and G. Keller (2011). "Stage-specific optimization of activin/nodal and BMP signaling promotes cardiac differentiation of mouse and human pluripotent stem cell lines." Cell Stem Cell **8**(2): 228-40.

Kawamoto, A., H. C. Gwon, H. Iwaguro, J. I. Yamaguchi, S. Uchida, H. Masuda, M. Silver, H. Ma, M. Kearney, J. M. Isner, et al. (2001). "Therapeutic potential of ex vivo expanded endothelial progenitor cells for myocardial ischemia." Circulation **103**(5): 634-7.

Kawamoto, A., T. Tkebuchava, J. Yamaguchi, H. Nishimura, Y. S. Yoon, C. Milliken, S. Uchida, O. Masuo, H. Iwaguro, H. Ma, et al. (2003). "Intramyocardial transplantation of autologous endothelial progenitor cells for therapeutic neovascularization of myocardial ischemia." Circulation **107**(3): 461-8.

Kay, M. A., J. C. Glorioso and L. Naldini (2001). "Viral vectors for gene therapy: the art of turning infectious agents into vehicles of therapeutics." Nat Med **7**(1): 33-40.

Kim, S. J., D. J. Doudet, A. R. Studenov, C. Nian, T. J. Ruth, S. S. Gambhir and C. H. McIntosh (2006). "Quantitative micro positron emission tomography (PET) imaging for the in vivo determination of pancreatic islet graft survival." Nat Med **12**(12): 1423-8.

Kinnaird, T., E. Stabile, M. S. Burnett and S. E. Epstein (2004). "Bone-marrow-derived cells for enhancing collateral development: mechanisms, animal data, and initial clinical experiences." Circ Res **95**(4): 354-63.

Kinnaird, T., E. Stabile, M. S. Burnett, C. W. Lee, S. Barr, S. Fuchs and S. E. Epstein (2004). "Marrow-derived stromal cells express genes encoding a broad spectrum

of arteriogenic cytokines and promote in vitro and in vivo arteriogenesis through paracrine mechanisms." Circ Res **94**(5): 678-85.

Kocher, A. A., M. D. Schuster, M. J. Szabolcs, S. Takuma, D. Burkhoff, J. Wang, S. Homma, N. M. Edwards and S. Itescu (2001). "Neovascularization of ischemic myocardium by human bone-marrow-derived angioblasts prevents cardiomyocyte apoptosis, reduces remodeling and improves cardiac function." Nat Med **7**(4): 430-6.

Kofidis, T., P. Akhyari, B. Wachsmann, K. Mueller-Stahl, J. Boublik, A. Ruhparwar, H. Mertsching, L. Balsam, R. Robbins and A. Haverich (2003). "Clinically established hemostatic scaffold (tissue fleece) as biomatrix in tissue- and organ-engineering research." Tissue Eng **9**(3): 517-23.

Kofidis, T., D. R. Lebl, E. C. Martinez, G. Hoyt, M. Tanaka and R. C. Robbins (2005). "Novel injectable bioartificial tissue facilitates targeted, less invasive, large-scale tissue restoration on the beating heart after myocardial injury." Circulation **112**(9 Suppl): I173-7.

Korbling, M. and Z. Estrov (2003). "Adult stem cells for tissue repair - a new therapeutic concept?" N Engl J Med **349**(6): 570-82.

Krause, D. S. (2002). "Plasticity of marrow-derived stem cells." Gene Ther **9**(11): 754-8.

Krause, D. S., N. D. Theise, M. I. Collector, O. Henegariu, S. Hwang, R. Gardner, S. Neutzel and S. J. Sharkis (2001). "Multi-organ, multi-lineage engraftment by a single bone marrow-derived stem cell." Cell **105**(3): 369-77.

Kutschka, I., I. Y. Chen, T. Kofidis, T. Arai, G. von Degenfeld, A. Y. Sheikh, S. L. Hendry, J. Pearl, G. Hoyt, R. Sista, et al. (2006). "Collagen matrices enhance

survival of transplanted cardiomyoblasts and contribute to functional improvement of ischemic rat hearts." Circulation **114**(1 Suppl): I167-73.

Laflamme, M. A., S. Zbinden, S. E. Epstein and C. E. Murry (2007). "Cell-based therapy for myocardial ischemia and infarction: pathophysiological mechanisms." Annu Rev Pathol **2**: 307-39.

Langer, R. and J. P. Vacanti (1993). "Tissue engineering." Science **260**(5110): 920-6.

Lee, J. and C. M. Terracciano "Cell therapy for cardiac repair." Br Med Bull **94**: 65-80.

Leor, J., H. Prentice, V. Sartorelli, M. J. Quinones, M. Patterson, L. K. Kedes and R. A. Kloner (1997). "Gene transfer and cell transplant: an experimental approach to repair a 'broken heart'." Cardiovasc Res **35**(3): 431-41.

Levine, B. L., L. M. Humeau, J. Boyer, R. R. MacGregor, T. Rebello, X. Lu, G. K. Binder, V. Slepushkin, F. Lemiale, J. R. Mascola, et al. (2006). "Gene transfer in humans using a conditionally replicating lentiviral vector." Proc Natl Acad Sci U S A **103**(46): 17372-7.

Leyva, F. J., J. J. Anzinger, J. P. McCoy, Jr. and H. S. Kruth (2011). "Evaluation of transduction efficiency in macrophage colony-stimulating factor differentiated human macrophages using HIV-1 based lentiviral vectors." BMC Biotechnol **11**: 13.

Li, F., D. Carlsson, C. Lohmann, E. Suuronen, S. Vascotto, K. Kobuch, H. Sheardown, R. Munger, M. Nakamura and M. Griffith (2003). "Cellular and nerve regeneration within a biosynthetic extracellular matrix for corneal transplantation." Proc Natl Acad Sci U S A **100**(26): 15346-51.

Lindsey, M. L., D. L. Mann, M. L. Entman and F. G. Spinale (2003). "Extracellular matrix remodeling following myocardial injury." Ann Med **35**(5): 316-26.

Liu, J., Q. Hu, Z. Wang, C. Xu, X. Wang, G. Gong, A. Mansoor, J. Lee, M. Hou, L. Zeng, et al. (2004). "Autologous stem cell transplantation for myocardial repair." Am J Physiol Heart Circ Physiol **287**(2): H501-11.

Liu, J. W., G. Pernod, S. Dunoyer-Geindre, R. J. Fish, H. Yang, H. Bounameaux and E. K. Kruithof (2006). "Promoter dependence of transgene expression by lentivirus-transduced human blood-derived endothelial progenitor cells." Stem Cells **24**(1): 199-208.

Losordo, D. W., R. A. Schatz, C. J. White, J. E. Udelson, V. Veereshwarayya, M. Durgin, K. K. Poh, R. Weinstein, M. Kearney, M. Chaudhry, et al. (2007). "Intramyocardial transplantation of autologous CD34+ stem cells for intractable angina: a phase I/IIa double-blind, randomized controlled trial." Circulation **115**(25): 3165-72.

Lovell, M. J. and A. Mathur (2010). "Cardiac stem cell therapy: progress from the bench to bedside." Heart **96**(19): 1531-7.

Lowry, W. E., L. Richter, R. Yachechko, A. D. Pyle, J. Tchieu, R. Sridharan, A. T. Clark and K. Plath (2008). "Generation of human induced pluripotent stem cells from dermal fibroblasts." Proc Natl Acad Sci U S A **105**(8): 2883-8.

Ma, B., K. D. Hankenson, J. E. Dennis, A. I. Caplan, S. A. Goldstein and M. R. Kilbourn (2005). "A simple method for stem cell labeling with fluorine 18." Nucl Med Biol **32**(7): 701-5.

MacArthur, B. D. and R. O. Oreffo (2005). "Bridging the gap." Nature **433**(7021): 19.

Mai, X. L., Z. L. Ma, J. H. Sun, S. H. Ju, M. Ma and G. J. Teng (2009). "Assessments of proliferation capacity and viability of New Zealand rabbit peripheral blood endothelial progenitor cells labeled with superparamagnetic particles." Cell Transplant **18**(2): 171-81.

Maltais, S., L. P. Perrault and H. Q. Ly (2011). "The bone marrow-cardiac axis: role of endothelial progenitor cells in heart failure." Eur J Cardiothorac Surg **39**(3): 368-74.

Maltais, S., J. P. Tremblay, L. P. Perrault and H. Q. Ly (2010). "The paracrine effect: pivotal mechanism in cell-based cardiac repair." J Cardiovasc Transl Res **3**(6): 652-62.

Mangi, A. A., N. Noiseux, D. Kong, H. He, M. Rezvani, J. S. Ingwall and V. J. Dzau (2003). "Mesenchymal stem cells modified with Akt prevent remodeling and restore performance of infarcted hearts." Nat Med **9**(9): 1195-201.

Massler, J., C. Mento, S. Shodavaram, R. Cason, S. Das, T. S. Wang and R. L. Van Heertum (1997). "Effects of sequential reagent addition on technetium-99m red blood cell labeling efficiency using the UltraTag kit." J Nucl Med Technol **25**(4): 269-71.

Masuda, H. and T. Asahara (2003). "Post-natal endothelial progenitor cells for neovascularization in tissue regeneration." Cardiovasc Res **58**(2): 390-8.

Matsuura, K., A. Honda, T. Nagai, N. Fukushima, K. Iwanaga, M. Tokunaga, T. Shimizu, T. Okano, H. Kasanuki, N. Hagiwara, et al. (2009). "Transplantation of cardiac progenitor cells ameliorates cardiac dysfunction after myocardial infarction in mice." J Clin Invest **119**(8): 2204-17.

Mayer, N. J. and S. A. Rubin (1997). "Molecular and cellular prospects for repair, augmentation, and replacement of the failing heart." Am Heart J **134**(3): 577-86.

Mazo, M., V. Planat-Benard, G. Abizanda, B. Pelacho, B. Leobon, J. J. Gavira, I. Penuelas, A. Cemborain, L. Penicaud, P. Laharrague, et al. (2008). "Transplantation of adipose derived stromal cells is associated with functional improvement in a rat model of chronic myocardial infarction." Eur J Heart Fail **10**(5): 454-62.

McGinley, L., J. McMahon, P. Strappe, F. Barry, M. Murphy, D. O'Toole and T. O'Brien "Lentiviral vector mediated modification of mesenchymal stem cells & enhanced survival in an in vitro model of ischaemia." Stem Cell Res Ther **2**(2): 12.

Meliga, E., B. M. Strem, H. J. Duckers and P. W. Serruys (2007). "Adipose-derived cells." Cell Transplant **16**(9): 963-70.

Menasche, P., A. A. Hagege, M. Scorsin, B. Pouzet, M. Desnos, D. Duboc, K. Schwartz, J. T. Vilquin and J. P. Marolleau (2001). "Myoblast transplantation for heart failure." Lancet **357**(9252): 279-80.

Menasche, P., A. A. Hagege, J. T. Vilquin, M. Desnos, E. Abergel, B. Pouzet, A. Bel, S. Sarateanu, M. Scorsin, K. Schwartz, et al. (2003). "Autologous skeletal myoblast transplantation for severe postinfarction left ventricular dysfunction." J Am Coll Cardiol **41**(7): 1078-83.

Meyer, G. P., K. C. Wollert and H. Drexler (2007). "The role of stem cells in the post-MI patient." Curr Heart Fail Rep **4**(4): 198-203.

Meyer, G. P., K. C. Wollert, J. Lotz, J. Steffens, P. Lippolt, S. Fichtner, H. Hecker, A. Schaefer, L. Arseniev, B. Hertenstein, et al. (2006). "Intracoronary bone marrow

cell transfer after myocardial infarction: eighteen months' follow-up data from the randomized, controlled BOOST (BOne marrOw transfer to enhance ST-elevation infarct regeneration) trial." Circulation **113**(10): 1287-94.

Mi, L., S. Fischer, B. Chung, S. Sundelacruz and J. L. Harden (2006). "Self-assembling protein hydrogels with modular integrin binding domains." Biomacromolecules **7**(1): 38-47.

Min, J. J., M. Iyer and S. S. Gambhir (2003). "Comparison of [18F]FHBG and [14C]FIAU for imaging of HSV1-tk reporter gene expression: adenoviral infection vs stable transfection." Eur J Nucl Med Mol Imaging **30**(11): 1547-60.

Miyahara, Y., N. Nagaya, M. Kataoka, B. Yanagawa, K. Tanaka, H. Hao, K. Ishino, H. Ishida, T. Shimizu, K. Kangawa, et al. (2006). "Monolayered mesenchymal stem cells repair scarred myocardium after myocardial infarction." Nat Med **12**(4): 459-65.

Mizuno, H. (2010). "Adipose-derived stem and stromal cells for cell-based therapy: current status of preclinical studies and clinical trials." Curr Opin Mol Ther **12**(4): 442-9.

Mizuno, T., T. M. Yau, R. D. Weisel, C. G. Kiani and R. K. Li (2005). "Elastin stabilizes an infarct and preserves ventricular function." Circulation **112**(9 Suppl): I81-8.

Moench, C., W. O. Bechstein, V. Hermanutz, G. Hoexter and H. P. Knaebel "Comparison of the collagen haemostat Sangustop(R) versus a carrier-bound fibrin sealant during liver resection; ESSCALIVER-Study." Trials **11**: 109.

Moretti, A., M. Bellin, A. Welling, C. B. Jung, J. T. Lam, L. Bott-Flugel, T. Dorn, A. Goedel, C. Hohnke, F. Hofmann, et al. (2010). "Patient-specific induced

pluripotent stem-cell models for long-QT syndrome." N Engl J Med **363**(15): 1397-409.

Muller-Ehmsen, J., K. L. Peterson, L. Kedes, P. Whittaker, J. S. Dow, T. I. Long, P. W. Laird and R. A. Kloner (2002). "Rebuilding a damaged heart: long-term survival of transplanted neonatal rat cardiomyocytes after myocardial infarction and effect on cardiac function." Circulation **105**(14): 1720-6.

Murry, C. E., M. H. Soonpaa, H. Reinecke, H. Nakajima, H. O. Nakajima, M. Rubart, K. B. Pasumarthi, J. I. Virag, S. H. Bartelmez, V. Poppa, et al. (2004). "Haematopoietic stem cells do not transdifferentiate into cardiac myocytes in myocardial infarcts." Nature **428**(6983): 664-8.

Nahrendorf, M., H. Zhang, S. Hembrador, P. Panizzi, D. E. Sosnovik, E. Aikawa, P. Libby, F. K. Swirski and R. Weissleder (2008). "Nanoparticle PET-CT imaging of macrophages in inflammatory atherosclerosis." Circulation **117**(3): 379-87.

Naldini, L., U. Blomer, P. Gallay, D. Ory, R. Mulligan, F. H. Gage, I. M. Verma and D. Trono (1996). "In vivo gene delivery and stable transduction of nondividing cells by a lentiviral vector." Science **272**(5259): 263-7.

Nelson, T. J., A. Martinez-Fernandez, S. Yamada, C. Perez-Terzic, Y. Ikeda and A. Terzic (2009). "Repair of acute myocardial infarction by human stemness factors induced pluripotent stem cells." Circulation **120**(5): 408-16.

Nohroudi, K., S. Arnhold, T. Berhorn, K. Addicks, M. Hoehn and U. Himmelreich "In vivo MRI stem cell tracking requires balancing of detection limit and cell viability." Cell Transplant **19**(4): 431-41.

Numaguchi, Y., T. Sone, K. Okumura, M. Ishii, Y. Morita, R. Kubota, K. Yokouchi, H. Imai, M. Harada, H. Osanai, et al. (2006). "The impact of the capability of circulating progenitor cell to differentiate on myocardial salvage in patients with primary acute myocardial infarction." Circulation **114**(1 Suppl): I114-9.

Nygren, J. M., S. Jovinge, M. Breitbach, P. Sawen, W. Roll, J. Hescheler, J. Taneera, B. K. Fleischmann and S. E. Jacobsen (2004). "Bone marrow-derived hematopoietic cells generate cardiomyocytes at a low frequency through cell fusion, but not transdifferentiation." Nat Med **10**(5): 494-501.

Oh, H., S. B. Bradfute, T. D. Gallardo, T. Nakamura, V. Gaussin, Y. Mishina, J. Pocius, L. H. Michael, R. R. Behringer, D. J. Garry, et al. (2003). "Cardiac progenitor cells from adult myocardium: homing, differentiation, and fusion after infarction." Proc Natl Acad Sci U S A **100**(21): 12313-8.

Oh, H., X. Chi, S. B. Bradfute, Y. Mishina, J. Pocius, L. H. Michael, R. R. Behringer, R. J. Schwartz, M. L. Entman and M. D. Schneider (2004). "Cardiac muscle plasticity in adult and embryo by heart-derived progenitor cells." Ann N Y Acad Sci **1015**: 182-9.

Ohnishi, S., H. Sumiyoshi, S. Kitamura and N. Nagaya (2007). "Mesenchymal stem cells attenuate cardiac fibroblast proliferation and collagen synthesis through paracrine actions." FEBS Lett **581**(21): 3961-6.

Okita, K., T. Ichisaka and S. Yamanaka (2007). "Generation of germline-competent induced pluripotent stem cells." Nature **448**(7151): 313-7.

Orlic, D., J. M. Hill and A. E. Arai (2002). "Stem cells for myocardial regeneration." Circ Res **91**(12): 1092-102.

Orlic, D., J. Kajstura, S. Chimenti, I. Jakoniuk, S. M. Anderson, B. Li, J. Pickel, R. McKay, B. Nadal-Ginard, D. M. Bodine, et al. (2001). "Bone marrow cells regenerate infarcted myocardium." Nature **410**(6829): 701-5.

Ozawa, T., D. A. Mickle, R. D. Weisel, N. Koyama, S. Ozawa and R. K. Li (2002). "Optimal biomaterial for creation of autologous cardiac grafts." Circulation **106**(12 Suppl 1): I176-82.

Paik, J. Y., K. H. Lee, S. S. Byun, Y. S. Choe and B. T. Kim (2002). "Use of insulin to improve [18 F]fluorodeoxyglucose labelling and retention for in vivo positron emission tomography imaging of monocyte trafficking." Nucl Med Commun **23**(6): 551-7.

Park, I. H., R. Zhao, J. A. West, A. Yabuuchi, H. Huo, T. A. Ince, P. H. Lerou, M. W. Lensch and G. Q. Daley (2008). "Reprogramming of human somatic cells to pluripotency with defined factors." Nature **451**(7175): 141-6.

Patel, A. N., L. Geffner, R. F. Vina, J. Saslavsky, H. C. Urschel, Jr., R. Kormos and F. Benetti (2005). "Surgical treatment for congestive heart failure with autologous adult stem cell transplantation: a prospective randomized study." J Thorac Cardiovasc Surg **130**(6): 1631-8.

Patel, A. N. and J. A. Genovese (2007). "Stem cell therapy for the treatment of heart failure." Curr Opin Cardiol **22**(5): 464-70.

Peichev, M., A. J. Naiyer, D. Pereira, Z. Zhu, W. J. Lane, M. Williams, M. C. Oz, D. J. Hicklin, L. Witte, M. A. Moore, et al. (2000). "Expression of VEGFR-2 and AC133 by circulating human CD34(+) cells identifies a population of functional endothelial precursors." Blood **95**(3): 952-8.

Perin, E. C., H. F. Dohmann, R. Borojevic, S. A. Silva, A. L. Sousa, C. T. Mesquita, M. I. Rossi, A. C. Carvalho, H. S. Dutra, H. J. Dohmann, et al. (2003). "Transendocardial, autologous bone marrow cell transplantation for severe, chronic ischemic heart failure." Circulation **107**(18): 2294-302.

Perin, E. C., Y. J. Geng and J. T. Willerson (2003). "Adult stem cell therapy in perspective." Circulation **107**(7): 935-8.

Pittenger, M. F. and B. J. Martin (2004). "Mesenchymal stem cells and their potential as cardiac therapeutics." Circ Res **95**(1): 9-20.

Plathow, C. and W. A. Weber (2008). "Tumor cell metabolism imaging." J Nucl Med **49 Suppl 2**: 43S-63S.

Ponomarev, V., M. Doubrovin, A. Shavrin, I. Serganova, T. Beresten, L. Ageyeva, C. Cai, J. Balatoni, M. Alauddin and J. Gelovani (2007). "A human-derived reporter gene for noninvasive imaging in humans: mitochondrial thymidine kinase type 2." J Nucl Med **48**(5): 819-26.

Powell, T. M., J. D. Paul, J. M. Hill, M. Thompson, M. Benjamin, M. Rodrigo, J. P. McCoy, E. J. Read, H. M. Khuu, S. F. Leitman, et al. (2005). "Granulocyte colony-stimulating factor mobilizes functional endothelial progenitor cells in patients with coronary artery disease." Arterioscler Thromb Vasc Biol **25**(2): 296-301.

Pozzilli, P., C. Pozzilli, P. Pantano, M. Negri, D. Andreani and A. G. Cudworth (1983). "Tracking of indium-111-oxine labelled lymphocytes in autoimmune thyroid disease." Clin Endocrinol (Oxf) **19**(1): 111-6.

Qian, H., Y. Yang, J. Huang, R. Gao, K. Dou, G. Yang, J. Li, R. Shen, Z. He, M. Lu, et al. (2007). "Intracoronary delivery of autologous bone marrow mononuclear cells radiolabeled by 18F-fluoro-deoxy-glucose: tissue distribution and impact on post-infarct swine hearts." J Cell Biochem **102**(1): 64-74.

Quattrocelli, M., G. Palazzolo, I. Agnolin, S. Martino, M. Bouche, L. Anastasia and M. Sampaolesi (2011). "Synthetic sulfonyl-hydrazone-1 positively regulates cardiomyogenic microRNA expression and cardiomyocyte differentiation of induced pluripotent stem cells." J Cell Biochem.

Rao, S. A. and M. K. Dewanjee (1982). "Comparative evaluation of red cell-labeling parameters of three lipid-soluble- 111In-chelates: effect of lipid solubility on membrane incorporation and stability constant on transchelation." Eur J Nucl Med **7**(6): 282-5.

Ray, P., A. De, J. J. Min, R. Y. Tsien and S. S. Gambhir (2004). "Imaging tri-fusion multimodality reporter gene expression in living subjects." Cancer Res **64**(4): 1323-30.

Rehman, J., J. Li, C. M. Orschell and K. L. March (2003). "Peripheral blood "endothelial progenitor cells" are derived from monocyte/macrophages and secrete angiogenic growth factors." Circulation **107**(8): 1164-9.

Reinecke, H., G. H. MacDonald, S. D. Hauschka and C. E. Murry (2000). "Electromechanical coupling between skeletal and cardiac muscle. Implications for infarct repair." J Cell Biol **149**(3): 731-40.

Reinecke, H., V. Poppa and C. E. Murry (2002). "Skeletal muscle stem cells do not transdifferentiate into cardiomyocytes after cardiac grafting." J Mol Cell Cardiol **34**(2): 241-9.

Reinlib, L. and W. Abraham (2003). "Recovery from heart failure with circulatory assist: a working group of the National, Heart, Lung, and Blood Institute." J Card Fail **9**(6): 459-63.

Rini, J. N., K. K. Bhargava, G. G. Tronco, C. Singer, R. Caprioli, S. E. Marwin, H. L. Richardson, K. J. Nichols, P. V. Pugliese and C. J. Palestro (2006). "PET with FDG-labeled leukocytes versus scintigraphy with 111In-oxine-labeled leukocytes for detection of infection." Radiology **238**(3): 978-87.

Robinson, K. A., J. Li, M. Mathison, A. Redkar, J. Cui, N. A. Chronos, R. G. Matheny and S. F. Badylak (2005). "Extracellular matrix scaffold for cardiac repair." Circulation **112**(9 Suppl): I135-43.

Rodriguez-Porcel, M., O. Gheysens, I. Y. Chen, J. C. Wu and S. S. Gambhir (2005). "Image-guided cardiac cell delivery using high-resolution small-animal ultrasound." Mol Ther **12**(6): 1142-7.

Romano, G., C. Pacilio and A. Giordano (1999). "Gene transfer technology in therapy: current applications and future goals." Stem Cells **17**(4): 191-202.

Ruel, M., R. S. Beanlands, M. Lortie, V. Chan, N. Camack, R. A. deKemp, E. J. Suuronen, F. D. Rubens, J. N. DaSilva, F. W. Sellke, et al. (2008). "Concomitant treatment with oral L-arginine improves the efficacy of surgical angiogenesis in patients with severe diffuse coronary artery disease: the Endothelial Modulation

in Angiogenic Therapy randomized controlled trial." J Thorac Cardiovasc Surg **135**(4): 762-70, 770 e1.

Ruel, M., R. J. Laham, J. A. Parker, M. J. Post, J. A. Ware, M. Simons and F. W. Sellke (2002). "Long-term effects of surgical angiogenic therapy with fibroblast growth factor 2 protein." J Thorac Cardiovasc Surg **124**(1): 28-34.

Ruel, M., J. Song and F. W. Sellke (2004). "Protein-, gene-, and cell-based therapeutic angiogenesis for the treatment of myocardial ischemia." Mol Cell Biochem **264**(1-2): 119-31.

Ruel, M., A. F. Stewart and E. J. Suuronen (2008). "From genes to regenerative medicine: approaches in development." Circ Res **103**(10): 1050-2.

Ruel, M., E. J. Suuronen, J. Song, V. Kapila, D. Gunning, G. Waghray, F. D. Rubens and T. G. Mesana (2005). "Effects of off-pump versus on-pump coronary artery bypass grafting on function and viability of circulating endothelial progenitor cells." J Thorac Cardiovasc Surg **130**(3): 633-9.

Sasaki, K., C. Heeschen, A. Aicher, T. Ziebart, J. Honold, C. Urbich, L. Rossig, U. Koehl, M. Koyanagi, A. Mohamed, et al. (2006). "Ex vivo pretreatment of bone marrow mononuclear cells with endothelial NO synthase enhancer AVE9488 enhances their functional activity for cell therapy." Proc Natl Acad Sci U S A **103**(39): 14537-41.

Schachinger, V., B. Assmus, M. B. Britten, J. Honold, R. Lehmann, C. Teupe, N. D. Abolmaali, T. J. Vogl, W. K. Hofmann, H. Martin, et al. (2004). "Transplantation of progenitor cells and regeneration enhancement in acute myocardial infarction:

final one-year results of the TOPCARE-AMI Trial." J Am Coll Cardiol **44**(8): 1690-9.

Seaberg, R. M. and D. van der Kooy (2003). "Stem and progenitor cells: the premature desertion of rigorous definitions." Trends Neurosci **26**(3): 125-31.

Segers, V. F. and R. T. Lee (2008). "Stem-cell therapy for cardiac disease." Nature **451**(7181): 937-42.

Shantsila, E., T. Watson and G. Y. Lip (2007). "Endothelial progenitor cells in cardiovascular disorders." J Am Coll Cardiol **49**(7): 741-52.

Shao, Y., S. R. Cherry, K. Farahani, K. Meadors, S. Siegel, R. W. Silverman and P. K. Marsden (1997). "Simultaneous PET and MR imaging." Phys Med Biol **42**(10): 1965-70.

Sharma, V., G. D. Luker and D. Piwnica-Worms (2002). "Molecular imaging of gene expression and protein function in vivo with PET and SPECT." J Magn Reson Imaging **16**(4): 336-51.

Sheikh, A. Y. and J. C. Wu (2006). "Molecular imaging of cardiac stem cell transplantation." Curr Cardiol Rep **8**(2): 147-54.

Shintani, S., T. Murohara, H. Ikeda, T. Ueno, T. Honma, A. Katoh, K. Sasaki, T. Shimada, Y. Oike and T. Imaizumi (2001). "Mobilization of endothelial progenitor cells in patients with acute myocardial infarction." Circulation **103**(23): 2776-9.

Siminiak, T., D. Fiszer, O. Jerzykowska, B. Grygielska, N. Rozwadowska, P. Kalmucki and M. Kurpisz (2005). "Percutaneous trans-coronary-venous transplantation of

autologous skeletal myoblasts in the treatment of post-infarction myocardial contractility impairment: the POZNAN trial." Eur Heart J **26**(12): 1188-95.

Smart, N. and P. R. Riley (2008). "The stem cell movement." Circ Res **102**(10): 1155-68.

Smith, R. R., L. Barile, E. Messina and E. Marban (2008). "Stem cells in the heart: what's the buzz all about?--Part 1: preclinical considerations." Heart Rhythm **5**(5): 749-57.

Smith, R. R., L. Barile, E. Messina and E. Marban (2008). "Stem cells in the heart: what's the buzz all about? Part 2: Arrhythmic risks and clinical studies." Heart Rhythm **5**(6): 880-7.

Soonpaa, M. H., G. Y. Koh, M. G. Klug and L. J. Field (1994). "Formation of nascent intercalated disks between grafted fetal cardiomyocytes and host myocardium." Science **264**(5155): 98-101.

Stamm, C., H. D. Kleine, Y. H. Choi, S. Dunkelmann, J. A. Lauffs, B. Lorenzen, A. David, A. Liebold, C. Nienaber, D. Zurakowski, et al. (2007). "Intramyocardial delivery of CD133+ bone marrow cells and coronary artery bypass grafting for chronic ischemic heart disease: safety and efficacy studies." J Thorac Cardiovasc Surg **133**(3): 717-25.

Stamm, C., B. Westphal, H. D. Kleine, M. Petzsch, C. Kittner, H. Klinge, C. Schumichen, C. A. Nienaber, M. Freund and G. Steinhoff (2003). "Autologous bone-marrow stem-cell transplantation for myocardial regeneration." Lancet **361**(9351): 45-6.

Strauer, B. E., M. Brehm, T. Zeus, M. Kostering, A. Hernandez, R. V. Sorg, G. Kogler and P. Wernet (2002). "Repair of infarcted myocardium by autologous

intracoronary mononuclear bone marrow cell transplantation in humans." Circulation **106**(15): 1913-8.

Stripecke, R., M. Carmen Villacres, D. Skelton, N. Satake, S. Halene and D. Kohn (1999). "Immune response to green fluorescent protein: implications for gene therapy." Gene Ther **6**(7): 1305-12.

Sun, N., A. Lee and J. C. Wu (2009). "Long term non-invasive imaging of embryonic stem cells using reporter genes." Nat Protoc **4**(8): 1192-201.

Suuronen, E. J., D. Kuraitis and M. Ruel (2008). "Improving cell engraftment with tissue engineering." Semin Thorac Cardiovasc Surg **20**(2): 110-4.

Suuronen, E. J., L. Muzakare, C. J. Doillon, V. Kapila, F. Li, M. Ruel and M. Griffith (2006). "Promotion of angiogenesis in tissue engineering: developing multicellular matrices with multiple capacities." Int J Artif Organs **29**(12): 1148-57.

Suuronen, E. J., M. Nakamura, M. A. Watsky, P. K. Stys, L. J. Muller, R. Munger, N. Shinozaki and M. Griffith (2004). "Innervated human corneal equivalents as in vitro models for nerve-target cell interactions." Faseb J **18**(1): 170-2.

Suuronen, E. J., J. Price, J. P. Veinot, K. Ascah, V. Kapila, X. W. Guo, S. Wong, T. G. Mesana and M. Ruel (2007). "Comparative effects of mesenchymal progenitor cells, endothelial progenitor cells, or their combination on myocardial infarct regeneration and cardiac function." J Thorac Cardiovasc Surg **134**(5): 1249-58.

Suuronen, E. J., J. P. Veinot, S. Wong, V. Kapila, J. Price, M. Griffith, T. G. Mesana and M. Ruel (2006). "Tissue-engineered injectable collagen-based matrices for improved cell delivery and vascularization of ischemic tissue using CD133+

progenitors expanded from the peripheral blood." Circulation **114**(1 Suppl): I138-44.

Suuronen, E. J., S. Wong, V. Kapila, G. Waghray, S. C. Whitman, T. G. Mesana and M. Ruel (2006). "Generation of CD133+ cells from CD133- peripheral blood mononuclear cells and their properties." Cardiovasc Res **70**(1): 126-35.

Suuronen, E. J., P. Zhang, D. Kuraitis, X. Cao, A. Melhuish, D. McKee, F. Li, T. G. Mesana, J. P. Veinot and M. Ruel (2009). "An acellular matrix-bound ligand enhances the mobilization, recruitment and therapeutic effects of circulating progenitor cells in a hindlimb ischemia model." FASEB J **e-pub**: fj.08-111054v1.

Takahashi, K., K. Tanabe, M. Ohnuki, M. Narita, T. Ichisaka, K. Tomoda and S. Yamanaka (2007). "Induction of pluripotent stem cells from adult human fibroblasts by defined factors." Cell **131**(5): 861-72.

Takahashi, T., C. Kalka, H. Masuda, D. Chen, M. Silver, M. Kearney, M. Magner, J. M. Isner and T. Asahara (1999). "Ischemia- and cytokine-induced mobilization of bone marrow-derived endothelial progenitor cells for neovascularization." Nat Med **5**(4): 434-8.

Takamatsu, S., T. Furukawa, T. Mori, Y. Yonekura and Y. Fujibayashi (2005). "Noninvasive imaging of transplanted living functional cells transfected with a reporter estrogen receptor gene." Nucl Med Biol **32**(8): 821-9.

Takeshita, S., T. Isshiki, M. Ochiai, K. Eto, H. Mori, E. Tanaka, K. Umetani and T. Sato (1998). "Endothelium-dependent relaxation of collateral microvessels after intramuscular gene transfer of vascular endothelial growth factor in a rat model of hindlimb ischemia." Circulation **98**(13): 1261-3.

Taylor, D. A., B. Z. Atkins, P. Hungspreugs, T. R. Jones, M. C. Reedy, K. A. Hutcheson, D. D. Glower and W. E. Kraus (1998). "Regenerating functional myocardium: improved performance after skeletal myoblast transplantation." Nat Med **4**(8): 929-33.

Thackeray, J. T., R. S. Beanlands and J. N. Dasilva (2007). "Presence of specific 11C-meta-Hydroxyephedrine retention in heart, lung, pancreas, and brown adipose tissue." J Nucl Med **48**(10): 1733-40.

Tiscornia, G., O. Singer and I. M. Verma (2006). "Production and purification of lentiviral vectors." Nat Protoc **1**(1): 241-5.

Tjuvajev, J. G., M. Doubrovin, T. Akhurst, S. Cai, J. Balatoni, M. M. Alauddin, R. Finn, W. Bornmann, H. Thaler, P. S. Conti, et al. (2002). "Comparison of radiolabeled nucleoside probes (FIAU, FHBG, and FHPG) for PET imaging of HSV1-tk gene expression." J Nucl Med **43**(8): 1072-83.

Tjuvajev, J. G., G. Stockhammer, R. Desai, H. Uehara, K. Watanabe, B. Gansbacher and R. G. Blasberg (1995). "Imaging the expression of transfected genes in vivo." Cancer Res **55**(24): 6126-32.

Tura, O., J. Crawford, G. R. Barclay, K. Samuel, P. W. Hadoke, H. Roddie, J. Davies and M. L. Turner "Granulocyte colony-stimulating factor (G-CSF) depresses angiogenesis in vivo and in vitro: implications for sourcing cells for vascular regeneration therapy." J Thromb Haemost **8**(7): 1614-23.

Uemura, R., M. Xu, N. Ahmad and M. Ashraf (2006). "Bone marrow stem cells prevent left ventricular remodeling of ischemic heart through paracrine signaling." Circ Res **98**(11): 1414-21.

Urbich, C., A. Aicher, C. Heeschen, E. Dernbach, W. K. Hofmann, A. M. Zeiher and S. Dimmeler (2005). "Soluble factors released by endothelial progenitor cells promote migration of endothelial cells and cardiac resident progenitor cells." J Mol Cell Cardiol **39**(5): 733-42.

Urbich, C. and S. Dimmeler (2004). "Endothelial progenitor cells functional characterization." Trends Cardiovasc Med **14**(8): 318-22.

Urbich, C. and S. Dimmeler (2004). "Endothelial progenitor cells: characterization and role in vascular biology." Circ Res **95**(4): 343-53.

Vassaux, G. and T. Groot-Wassink (2003). "In Vivo Noninvasive Imaging for Gene Therapy." J Biomed Biotechnol **2003**(2): 92-101.

Wagner, W., F. Wein, A. Seckinger, M. Frankhauser, U. Wirkner, U. Krause, J. Blake, C. Schwager, V. Eckstein, W. Ansorge, et al. (2005). "Comparative characteristics of mesenchymal stem cells from human bone marrow, adipose tissue, and umbilical cord blood." Exp Hematol **33**(11): 1402-16.

Wang, D. S., M. D. Dake, J. M. Park and M. D. Kuo (2009). "Molecular imaging: a primer for interventionalists and imagers." J Vasc Interv Radiol **20**(7 Suppl): S505-22.

Welling, M., H. I. Feitsma, D. Blok, W. Calame, G. J. Ensing, W. Goedemans and E. K. Pauwels (1995). "A new 99mTc labelling method for leucocytes: in vitro and in vivo comparison with 99mTc-HMPAO." Q J Nucl Med **39**(2): 89-98.

Welt, F. G. and D. W. Losordo (2006). "Cell therapy for acute myocardial infarction: curb your enthusiasm?" Circulation **113**(10): 1272-4.

Wernig, M., A. Meissner, R. Foreman, T. Brambrink, M. Ku, K. Hochedlinger, B. E. Bernstein and R. Jaenisch (2007). "In vitro reprogramming of fibroblasts into a pluripotent ES-cell-like state." Nature **448**(7151): 318-24.

Wollert, K. C., G. P. Meyer, J. Lotz, S. Ringes-Lichtenberg, P. Lippolt, C. Breidenbach, S. Fichtner, T. Korte, B. Hornig, D. Messinger, et al. (2004). "Intracoronary autologous bone-marrow cell transfer after myocardial infarction: the BOOST randomised controlled clinical trial." Lancet **364**(9429): 141-8.

Wu, J. C., F. Cao, S. Dutta, X. Xie, E. Kim, N. Chungfat, S. Gambhir, S. Mathewson, A. J. Connolly, M. Brown, et al. (2006). "Proteomic analysis of reporter genes for molecular imaging of transplanted embryonic stem cells." Proteomics **6**(23): 6234-49.

Wu, J. C., J. M. Spin, F. Cao, S. Lin, X. Xie, O. Gheysens, I. Y. Chen, A. Y. Sheikh, R. C. Robbins, A. Tsalenko, et al. (2006). "Transcriptional profiling of reporter genes used for molecular imaging of embryonic stem cell transplantation." Physiol Genomics **25**(1): 29-38.

Yaghoubi, S., J. R. Barrio, M. Dahlbom, M. Iyer, M. Namavari, N. Satyamurthy, R. Goldman, H. R. Herschman, M. E. Phelps and S. S. Gambhir (2001). "Human pharmacokinetic and dosimetry studies of [(18)F]FHBG: a reporter probe for imaging herpes simplex virus type-1 thymidine kinase reporter gene expression." J Nucl Med **42**(8): 1225-34.

Yaghoubi, S. S. and S. S. Gambhir (2006). "PET imaging of herpes simplex virus type 1 thymidine kinase (HSV1-tk) or mutant HSV1-sr39tk reporter gene expression in mice and humans using [18F]FHBG." Nat Protoc **1**(6): 3069-75.

Yeghiazarians, Y., Y. Zhang, M. Prasad, H. Shih, S. A. Saini, J. Takagawa, R. E. Sievers, M. L. Wong, N. K. Kapasi, R. Mirsky, et al. (2009). "Injection of bone marrow cell extract into infarcted hearts results in functional improvement comparable to intact cell therapy." Mol Ther **17**(7): 1250-6.

Yin, A. H., S. Miraglia, E. D. Zanjani, G. Almeida-Porada, M. Ogawa, A. G. Leary, J. Olweus, J. Kearney and D. W. Buck (1997). "AC133, a novel marker for human hematopoietic stem and progenitor cells." Blood **90**(12): 5002-12.

Yoon, C. H., J. Hur, K. W. Park, J. H. Kim, C. S. Lee, I. Y. Oh, T. Y. Kim, H. J. Cho, H. J. Kang, I. H. Chae, et al. (2005). "Synergistic neovascularization by mixed transplantation of early endothelial progenitor cells and late outgrowth endothelial cells: the role of angiogenic cytokines and matrix metalloproteinases." Circulation **112**(11): 1618-27.

Yoon, C. H., M. Koyanagi, K. Iekushi, F. Seeger, C. Urbich, A. M. Zeiher and S. Dimmeler "Mechanism of improved cardiac function after bone marrow mononuclear cell therapy: role of cardiovascular lineage commitment." Circulation **121**(18): 2001-11.

Yoshinaga, K., B. J. Chow, R. A. dekemp, S. Thorn, T. D. Ruddy, R. A. Davies, J. N. DaSilva and R. Beanlands (2005). "Application of cardiac molecular imaging using positron emission tomography in evaluation of drug and therapeutics for cardiovascular disorders." Curr Pharm Des **11**(7): 903-32.

Yu, J., M. A. Vodyanik, K. Smuga-Otto, J. Antosiewicz-Bourget, J. L. Frane, S. Tian, J. Nie, G. A. Jonsdottir, V. Ruotti, R. Stewart, et al. (2007). "Induced pluripotent stem cell lines derived from human somatic cells." Science **318**(5858): 1917-20.

Yukawa, H., S. Mizufune, C. Mamori, Y. Kagami, K. Oishi, N. Kaji, Y. Okamoto, M. Takeshi, H. Noguchi, Y. Baba, et al. (2009). "Quantum dots for labeling adipose tissue-derived stem cells." Cell Transplant **18**(5): 591-9.

Zeng, X. and M. S. Rao (2008). "Controlled genetic modification of stem cells for developing drug discovery tools and novel therapeutic applications." Curr Opin Mol Ther **10**(3): 207-13.

Zhang, M., D. Methot, V. Poppa, Y. Fujio, K. Walsh and C. E. Murry (2001). "Cardiomyocyte grafting for cardiac repair: graft cell death and anti-death strategies." J Mol Cell Cardiol **33**(5): 907-21.

Zhang, P., H. Zhang, H. Wang, Y. Wei and S. Hu (2006). "Artificial matrix helps neonatal cardiomyocytes restore injured myocardium in rats." Artif Organs **30**(2): 86-93.

Zhang, Y., M. Ruel, R. S. Beanlands, R. A. deKemp, E. J. Suuronen and J. N. DaSilva (2008). "Tracking stem cell therapy in the myocardium: applications of positron emission tomography." Curr Pharm Des **14**(36): 3835-53.

Zhang, Y., S. Thorn, J. N. DaSilva, M. Lamoureux, R. A. DeKemp, R. S. Beanlands, M. Ruel and E. J. Suuronen (2008). "Collagen-based matrices improve the delivery of transplanted circulating progenitor cells: development and demonstration by ex vivo radionuclide cell labeling and in vivo tracking with positron-emission tomography." Circ Cardiovasc Imaging **1**(3): 197-204.

Zhang, Y., S. Thorn, J. N. DaSilva, M. Lamoureux, R. A. deKemp, R. S. Beanlands, M. Ruel and E. J. Suuronen (2008). "Collagen-Based Matrices Improve the Delivery of Transplanted Circulating Progenitor Cells: Development and Demonstration by

Ex Vivo Radionuclide Cell Labeling and In Vivo Tracking With Positron-Emission Tomography " Circ Cardiovasc Imaging. **1**(3): 197-204.

Zhang, Y., S. Wong, J. Lafleche, S. Crowe, T. G. Mesana, E. J. Suuronen and M. Ruel (2010). "In vitro functional comparison of therapeutically relevant human vasculogenic progenitor cells used for cardiac cell therapy." J Thorac Cardiovasc Surg **140**(1): 216-24, 224 e1-4.

APPENDICES

Structure of Radioisotopes

A

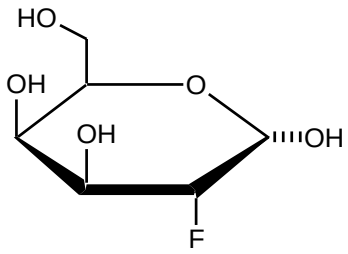

B

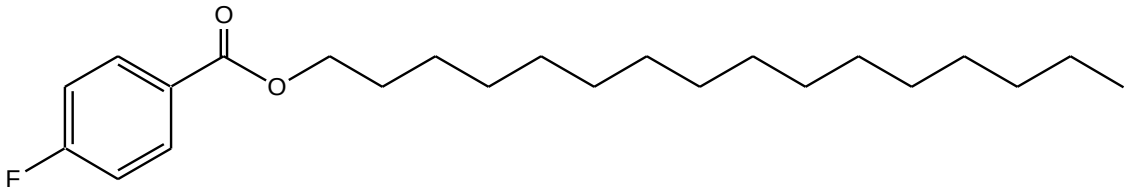

Figure 8-1: Structures of PET radiotracers for direct cell labeling.
A. ^{18}F-FDG; B. ^{18}F-HFB.

Curriculum Vitae
Yan (Mary) Zhang, MD, MSc, PhD Candidate

Education

Ph.D. Candidate in Cellular and Molecular Medicine 2006-Present
University of Ottawa
M.Sc. in Medical Science 1998-2001
China Medical University
M.D. 1988-1993
Shenyang Medical School

Work Experience

Ph.D. Student 2006-Present
Division of Cardiac Surgery, University of Ottawa Heart Institute
Research Assistant 2005-2006
Department of Medicine, Lawson Research Institute, University of Western Ontario
Cardiologist, Assistant Professor 2001-2005
Division of Cardiology, General Hospital of Shenyang Medical School
M.Sc. Student, Clinical Fellow 1998-2001
Division of Cardiology, First Hospital of China Medical University
Chief Resident 1997-1998
Division of Cardiology, General Hospital of Shenyang Medical School
Resident 1993-1997
Division of Cardiology, Department of Internal Medicine, General Hospital of Shenyang Medical School

Awards & Scholarships

SCN-ISSCR Travel Award	2011
CIHR-ICRH Skills Development Travel Award	2011
Heart and Stroke Foundation of Canada Doctoral Research Award	2009-2011
Ontario Graduate Scholarship	2009-2010
University of Ottawa Excellence Scholarship	2009-2011
CIHR Young Investigators Forum Travel Award	2008-2010
Canadian Cardiovascular Society Have a Heart Bursary Program Award	2008
Molecular Function Imaging Program Annual Research Award	2008
Ontario Graduate Scholarship in Science and Technology	2008-2009
University of Ottawa Heart Institute Research Travel Award	2007

Listing of Publications (during PhD. study)

Articles published in refereed journals

1. Kuraitis D, Zhang P, **Zhang Y**, Padavan DT, McEwan K, Sofrenovic T, McKee D, Zhang J, Griffith M, Cao X, Musarò A, Ruel M, Suuronen EJ. (2011) A stromal cell-derived factor-1 releasing matrix enhances the progenitor cell response and blood vessel growth in ischaemic skeletal muscle. Eur Cell Mater. 22:109-123.
2. Kuraitis D, Hou C, **Zhang Y**, Vulesevic B, Sofrenovic T, McKee D, Ruel M, Suuronen EJ. (2011) Collagen matrices for endothelial progenitor cell enrichment and functional enhancement. J Mol Cell Cardiol. 51:187-197.
3. **Zhang Y**, Wong S, Laflèche J, Crowe S, Mesana TG, Suuronen EJ, Ruel M. (2010) In vitro functional comparison of therapeutically relevant human vasculogenic progenitor cells used for cardiac cell therapy. J Thorac Cardiovasc Surg. 140:216-24.
4. Suuronen EJ, Hazra S, Zhang P, Vincent R, Kumarathasan P, **Zhang Y**, Price J, Chan V, Sellke FW, Mesana TG, Veinot JP, Ruel M. (2010) Impairment of human cell-based vasculogenesis in rats by hypercholesterolemia-induced endothelial dysfunction and rescue with L-arginine supplementation. J Thorac Cardiovasc Surg. 139:209-16.
5. **Zhang Y**, Suuronen EJ, Sellke FW, Ruel M. (2010) Regenerative cell-based therapy for the treatment of cardiac disease. In Sellke FW, Del Nido PJ, Swanson SJ (eds): Sabiston and Spencer's Surgery of the Chest, 8th ed. Philadelphia, Elsevier Science, Chap. 102.
6. **Zhang Y**, Thorn S, DaSilva JN, Lamoureux M, DeKemp RA, Beanlands RS, Ruel M, Suuronen EJ. (2008) Collagen-based matrices improve the delivery of transplanted circulating progenitor cells: development and demonstration by ex vivo radionuclide cell labeling and in vivo tracking with positron-emission tomography. Circ Cardiovasc Imaging. 1:197-204
7. **Zhang Y**, Ruel M, Beanlands RS, deKemp RA, Suuronen EJ, DaSilva JN. (2008) Tracking stem cell therapy in the myocardium: applications of positron emission tomography. Curr Pharm Des. 14:3835-53

Articles submitted and prepared to refereed journals

1. **Zhang Y**, DaSilva JN, Hadizad T, Thorn S, Kuraitis D, Renaud JM, Ahmadi A, Kordos M, deKemp R, Beanlands RS, Suuronen EJ, Ruel M. (2011) ^{18}F-FDG cell labeling may underestimate transplanted cell homing: more accurate, efficient and stable cell labeling with hexadecyl-4-[^{18}F]fluorobenzoate for in vivo tracking of intramyocardially injected human progenitor cells by positron emission tomography. Cell Transplantation; accepted with minor revisions.
2. **Zhang Y**, Burgon P, Kuraitis D, Crowe S, Vulesevic B, DaSilva JN, deKemp RA, Beanlands R, Suuronen EJ, Ruel M. (2011) Development of reporter gene PET imaging techniques for long-term assessment of transplanted human progenitor cells. In preparation for Nucl. Med. Biol.

Other refereed contributions (first-authored and presented at national or international conferences)

1. **Zhang Y**, Hadizad T, DaSilva JN, Thorn S, Renaud JM, Kuraitis D, Kordos M, Mesana TG, deKemp R, Beanlands RS, Suuronen EJ, Ruel M. (2010) Improved stem cell tracking after intramyocardial injection by hexadecyl-4-[^{18}F]fluorobenzoate labeling with positron emission tomography. Circulation. 122 (suppl):A18167
2. **Zhang Y**, Hadizad T, DaSilva JN, Thorn S, Renaud JM, Kuraitis D, Kordos M, deKemp R, Beanlands RS, Suuronen EJ, Ruel M. (2010) Dynamic tracking of human progenitor cells after intramyocardial injection: comparison of ^{18}F-HFB versus ^{18}F-FDG in cell labeling for PET imaging. Can J Cardiol. 26(suppl D):A391
3. **Zhang Y**, Hadizad T, DaSilva JN, Thorn S, Kuraitis D, Kordos M, deKemp R, Beanlands RS, Suuronen EJ, Ruel M. (2010) Dynamic tracking of transplanted progenitor cells in infarcted myocardium. Circulation. 122:e95-A480
4. **Zhang Y**, Burgon P, Crowe S, Kuraitis D, Thorn S, DaSilva JN, deKemp RA, Beanlands R, Suuronen EJ, Ruel M. (2010) Development of reporter gene PET imaging techniques for long-term assessment of biopolymer matrices on progenitor cell therapy. Circulation. 122:e84-A426
5. **Zhang Y**, Thorn S, DaSilva JN, Hadizad T, Renaud JM, Kuraitis D, deKemp R, Beanlands RS, Suuronen EJ, Ruel M. (2010) Comparison of ^{18}F-HFB and ^{18}F-FDG cell labeling for tracking transplanted progenitor cells by PET imaging. CIHR's Young Investigators Forum.
6. **Zhang Y**, Burgon P, Crowe S, Kuraitis D, Thorn S, DaSilva JN, deKemp RA, Beanlands R, Suuronen EJ, Ruel M. (2009) Progenitor cells transplantation with biopolymer matrices: development of PET imaging tracking techniques for long-term assessment. Can J Cardiol. 25(suppl B): A856
7. **Zhang Y**, Burgon P, Crowe S, Kuraitis D, Thorn S, DaSilva JN, deKemp RA, Beanlands R, Suuronen EJ, Ruel M. (2009) Development of positron emission tomography imaging for the long-term assessment of progenitor cells transplanted with collagen matrices. CIHR's Young Investigators Forum.
8. **Zhang Y**, Lamoureux M, Thorn S, Chan V, Price J, Beanlands RB, DaSilva JN, deKemp RA, Suuronen EJ, Ruel M. (2008) Early retention and subsequent engraftment of transplanted progenitor cells is improved by delivery with collagen matrix. Circulation. 118 (suppl): S790-A2876.
9. **Zhang Y**, Thorn S, DaSilva JN, Lamoureux M, deKemp RA, Beanlands RB, Chan V, Price J, Suuronen EJ, Ruel M. (2008) Collagen-based matrices improve early retention and subsequent engraftment of transplanted progenitor cells. Can J Cardiol. 24(suppl E): A274
10. **Zhang Y**, Wong S, Crowe S, O'Brien ER, Mesana TG, Suuronen EJ, Ruel M. (2008) Cell-cell interactions regulate the in vitro expansion of CD133^{+} progenitor cells and are involved in improving their function. Can J Cardiol. 24(suppl E): A256
11. **Zhang Y**, Thorn S, DaSilva JN, Lamoureux M, deKemp RA, Beanlands RB, Suuronen EJ, Ruel M. (2008) Assessment of collagen delivery matrices to improve early engraftment of transplanted circulating progenitor cells by positron emission tomography. CIHR's Young Investigators Forum.

12. **Zhang Y**, Suuronen EJ, Thorn S, Lamoureux M, deKemp RA, Beanlands RB, DaSilva JN, Ruel M. (2007) Cell labeling with ^{18}F-FDG for trafficking endothelial progenitor cells delivered by polymer matrices in a rat ischemic model using PET. Can J Cardiol; 23(suppl C): A489

Relevant activities

International Society for Stem Cell Research Member	2011
Graduate Students' Association General Election Scrutineer	2011
CUPE2626 Executive Election Scrutineer	2011
Imaging Network of Ontario Symposium Invited Speaker	2010
Molecular Function & Imaging Symposium Committee Member	2009 –10
The Quintessence Breastfeeding Challenge Volunteer	2009
HOPE Volleyball Summer Fest Volunteer	2009
American Heart Association Member	2008 –11
University of Ottawa Heart Institute Bench-to-Bed Member	2007 –11
Canadian Cardiovascular Society Member	2007 –11
University of Ottawa Heart Institute Works-In-Progress Member	2006 –11
Molecular Function & Imaging Journal Club, Research-In-Progress Member	2006 –11